FRACTURE STUDIES IN GLASSY POLYMERS

Lawrence J. Broutman, et al

Illinois Institute of Technology
Chicago, Illinois

August 1969

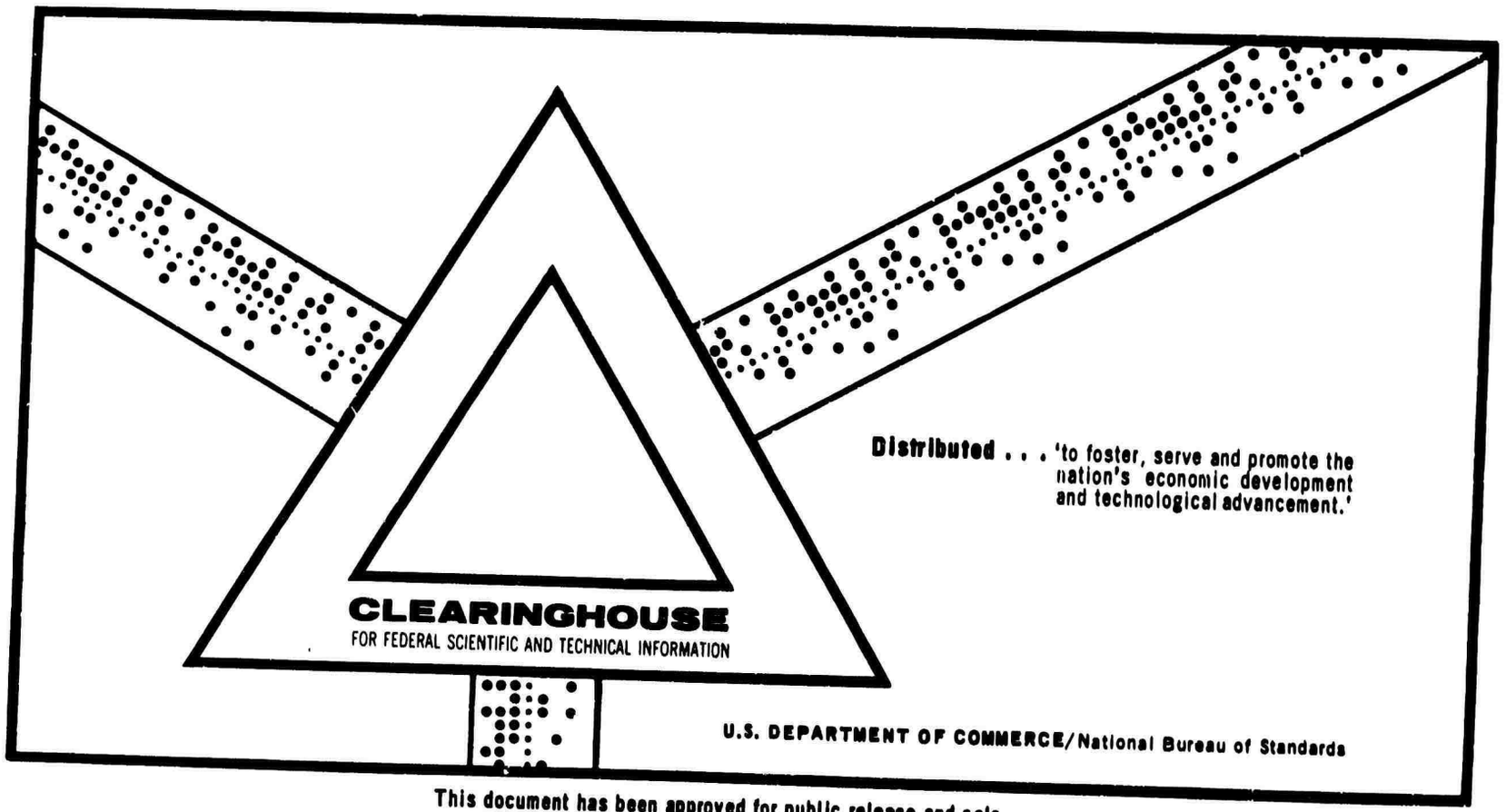

AMMRC CR 69-13

FRACTURE STUDIES IN GLASSY POLYMERS

Final Report

by

LAWRENCE J. BROUTMAN

and

TAKAO KOBAYASHI

August 1969

Illinois Institute of Technology
Chicago, Illinois

Contract DAAG17-67-C-0133

ARMY MATERIALS AND MECHANICS RESEARCH CENTER
WATERTOWN, MASSACHUSETTS 02172

177

Mention of any trade names or manufacturers in this report shall not be construed as advertising nor as an official indorsement or approval of such products or companies by the United States Government.

The findings in this report are not to be construed as an official Department of the Army position, unless so designated by other authorized documents.

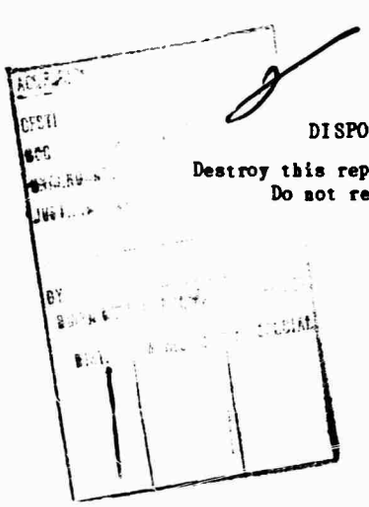

DISPOSITION INSTRUCTIONS

Destroy this report when it is no longer needed.
Do not return it to the originator.

FRACTURE STUDIES IN GLASSY POLYMERS

AMMRC CR 69-13

Final Report

by

Lawrence J. Broutman

and

Takao Kobayashi

August 1969

Illinois Institute of Technology
Chicago, Illinois
Contract DAAG17-67-C-0133

D/A Project 1T062105A329
AMCMS Code 5025.11.295
Organic Materials Research for Army Materiel

ARMY MATERIALS AND MECHANICS RESEARCH CENTER
WATERTOWN, MASSACHUSETTS 02172

FOREWORD

There has been in recent years a growing interest in the use of organic polymers for lightweight armor applications because of the relatively low density and promising performance of these materials. To improve further the degree of ballistic protection afforded by polymeric materials, it is necessary to examine in detail the nature of the failure processes. For example, the occurrence of fracture causes the absorption of much energy and is, therefore, an important mechanism involved in defeating the projectile. Hence, there is great interest in developing more knowledge concerning the detailed energetics of fracture processes and their dependences upon polymer structural features.

The work described in this report was performed at the Illinois Institute of Technology under Contract No. DAAG 17-67-C-0133. This research was originally sponsored by the Materials Research Division, Clothing and Organic Materials Laboratory, U.S. Army Natick Laboratories, Natick, Massachusetts, with Dr. Anthony F. Wilde as Project Officer and Mr. Anthony L. Alesi as Alternate Project Officer. With the transfer of portions of the Materials Research Division and its personnel to the Army Materials and Mechanics Research Center, Watertown, Massachusetts, the sponsorship of the contract was also moved to AMMRC, with the same persons serving as the Project and Alternate Project Officers.

TABLE OF CONTENTS

Page No.

LIST OF FIGURES

APPENDICES

LIST OF TABLES

LIST OF APPENDICES

SUMMARY

The objective of this program was to study the fracture of glassy organic polymers so that a better understanding between the polymer structure and fracture characterics could be gained. Of particular interest was the determination of the fracture surface work or energy required to initiate and propagate a crack through the polymer. Polymer structural features which were studied include 1) chain stiffness, conformation and molar cohesion, 2) degree of crosslinking, 3) tacticity and degree of crystallinity, 4) molecular weight and molecular weight distribution, and 5) polymer molecular orientation.

Equipment was designed and built and test specimens were developed for the measurement of fracture surface work of polymers from room temperature to liquid nitrogen temperatures (-196°C). Uniform height double cantilever cleavage specimens, and a tapered double cantilever cleavage specimen (constant compliance specimen) were used for the measurements. Analyses for each specimen were performed so that the fracture surface work could be accurately determined from experimentally measured forces, deflections and crack lengths. It has been shown that measurements from both types of specimens agree within experimental errors. It has also been shown using a hot stretched polystyrene material that the groove used to confine the crack has very little influence on the measured fracture surface work.

The influence of molecular weight and crosslinking on fracture surface work were investigated. It was shown that decreasing the molecular weight and increasing the molecular weight distribution reduces the value of fracture surface work. Molecular weights were determined by gel permeation chromatography. Crosslinking in polystyrene was achieved by exposures to γ irradiation (Cobalt 60 source) up to 100 megarads. The fracture surface work decreased with increasing degree of crosslinking. In these experiments, the role of crazing in determining fracture surface work becomes evident, and as the crazing increased the fracture surface work increased. The degree of crazing can be controlled by varying the specimen height of the uniform cantilever cleavage specimen.

Isotactic polystyrene was investigated and fracture surface work measurements were made on the amorphous isotactic material as well as annealed specimens having various degrees of crystallinity. Degree of crystallinity was determined by density measurements. The fracture surface work decreases significantly as the degree of crystallinity increases. The isotactic amorphous polymer has a greater fracture surface work than atactic polystyrene but this has been attributed to a higher molecular weight and increased degree of crazing.

Influence of polymer molecular structure was studied by investigating acrylate and methacrylate polymers as well as polyvinyl chloride and polyvinyl acetate. Measurements were made at room temperature and at liquid nitrogen

temperatures. A good correlation between polymer molecular structure or glass transition temperature and fracture surface work could not be established. Although polymethylmethacrylate and polystyrene increase in fracture surface work from room temperature to -196°C (in fact polystyrene could not be cleaved in liquid nitrogen), iso-butylmethacrylate and ethyl methacrylate either have decreasing values or remain nearly constant. For polystyrene, it was observed that the degree of crazing greatly increased at -196°C and accounted for not being able to cleave the polymer. It was easily seen that glass transition temperature of a polymer could not be correlated with fracture behavior.

The influence of polymer molecular orientation was studied by the uniaxial and biaxial cold rolling of polymer sheets of such materials as polycarbonates, ABS polymers, polysulfones and polyphenylene oxides. The orientation by rolling greatly increases the strength and impact resistance of the plastic sheet and causes uniform extension rather than necking and cold drawing of polymers such as polycarbonates. Stress whitening is also eliminated from rubber modified polymers by 40 percent reduction in thickness by cold rolling.

Experiments were also conducted to determine the influence of crack velocity on fracture surface work and to measure the temperature rise occurring at the crack tip. Cracks were propagated in a PMMA polymer at different velocities using the tapered cleavage bar. A modest increase in fracture surface work was measured as the crack velocity increased from approximately .007 to .167 in/sec. Liquid crystal coatings were applied to the surfaces of cleavage and pre-cracked tensile bars to measure temperature increases during crack initiation and propagation. Temperature increases could not be detected for PMMA or polystyrene and a 3°C minimum rise was measured for ABS or polyethylene. These experiments were only brief and are not yet conclusive.

CHAPTER I

INTRODUCTION

1. Objective of Research

Ballistically impacted materials, particularly glassy polymers such as Plexiglas, fail in a complex manner with great amounts of internal crack initiation and propagation contributing to the total failure process. Crack initiation and propagation require or absorb large amounts of energy and so offer a means of dissipating projectile energy. Providing one understands the failure process, new materials or simply new combinations of existing materials can be rationally designed to better resist impact and fracture. This requires knowledge of the material structure and its influence on the fracture process, particularly the energy required to initiate and propagate a crack. The purpose of this research study is to answer this question. A complete solution to the above problem must eventually include dynamic effects such as the influence of crack velocity on crack propagation energy and mode of crack propagation.

Thus, the objective of this program was to study the fracture of glassy organic polymers so that a better understanding between the polymer structure and fracture properties could be gained. The fracture surface work and fracture surface characteristics were studied. Polymer structural features which were studied included 1) chain stiffness, conformation and intermolecular bonding through homologous series of acrylates and methacrylates; 2) degree of crystallinity; 3) crosslinking; 4) prior molecular orientation. The ambient temperature was varied so comparisons of polymers could be made in nearly equivalent thermodynamic states.

2. Background

In this chapter, it is our intent to summarize previous results of investigators studying fracture in glassy polymers and to include only those results pertinent to this research study. The influence of polymer structure, temperature and crack velocity on fracture surface work, and the mechanism of molecular deformation at the crack tip will be reviewed.

A. Measure of Fracture Surface Work of Glassy Polymers

The measurement of the tensile strength of a material, although a simple enough quantity to determine in the laboratory, is not sufficient to yield relations between material structure and fracture mechanisms in the material. The tensile strength of a brittle or glassy material was first shown by Griffith to be related to other more basic material parameters, such as elastic modulus,

fracture surface energy, and flaw size. This relation is expressed by

$$\sigma_{ult} = \sqrt{\frac{2E\gamma}{\pi c}} \qquad (1)$$

where σ_{ult}= ultimate tensile strength, E=Young's modulus of elasticity, γ=fracture energy (defined as energy required to produce fresh unit surface area and as such is a reversible thermodynamic quantity) and c=critical flaw size in material. Orowan (1) later modified this expression to account for irreversible work which also may occur during the fracture process at the tip of the propagating crack. This irreversible work is primarily attributed to local plastic deformation or viscous deformation of the material at the highly stressed crack tip. The modified Griffith equation is then represented by

$$\sigma_{ult} = \sqrt{\frac{2E(\gamma+p)}{\pi c}} \qquad (2)$$

where p represents the irreversible work. It appears that even the most macroscopically brittle materials such as inorganic glasses possess some ability to deform plastically at a crack tip and the surface energy calculated from the original Griffith equation does not agree with theoretical values of solid surface energies. This is true for inorganic glasses and metals as well as for glassy polymers (2-4). Griffith (5) originally was able to demonstrate that σ_{ult} was proportional to 1/c for inorganic glasses and Berry (2) showed that this was also true for glassy polymers. However, the relative position of the curve for σ_{ult} vs. $1/c^{\frac{1}{2}}$ is dependent upon the term $(\gamma+p)$ and of course the experimental curve does not agree with the position of the theoretical curve since $\gamma+p$ is greater than γ. For polymers such as polystyrene and poly(methyl methacrylate) it has been found that the fracture surface work term $(\gamma+p)$ is nearly 10^3 times as great as the calculated fracture surface energy, γ(2-4).

The fracture surface work is a measure not only of the theoretical surface energy of the solid but also includes the contributions due to irreversible work, environmental influences on surface energy and specific effects such as crazing or molecular orientation. It is therefore a valuable material property which can be measured experimentally and used to relate changes in a material's molecular structure to the fracture toughness or resistance of the material. The first method used to experimentally determine this fracture surface work quantity was by measurement of the tensile strength of a material using an edge crack or a centrally notched tensile specimen. The tensile strength is measured for several manufactured crack lengths so that a sufficient relation can be established and from eq. (2) the fracture surface work is determined.

A more accurate measurement of fracture surface work can be obtained using a cleavage technique to propagate a crack. The cleavage specimen developed by Broutman (3, 4) is placed in loading grips as shown in Fig. 1. Berry (2,6-8) used a similar specimen and Benbow and Roesler (9) had a similar specimen but modified loading technique. In order to determine the fracture surface work it is necessary to measure the force of separation at the specimen ends, the resulting end deflection and the crack length. The procedure is described by Broutman (3). Ripling and Mostovoy (10) have recently described another type of cleavage specimen which is a tapered double cantilever cleavage specimen. The purpose of this tapered specimen is to eliminate the need for measuring the crack length as a function of the applied force and deflection. Another benefit of this specimen is that the crack may propagate with a constant velocity for a constant rate of separation of the specimen ends. For the uniformly shaped cleavage specimen the crack propagation rate decreases as the crack is driven or as its length increases. Thus, the tapered specimen simplifies the calculation and the experiment but is more difficult to machine. The design of this specimen will be discussed in a later section.

B. Fracture Surface Characteristics

The appearance of a polymer fracture surface has been a valuable tool thus far in interpreting fracture mechanisms near a propagating crack. Careful inspection of a fracture surface is a necessary part of an investigation and cannot be divorced from other more quantitative measurements such as tensile strength or fracture surface work. It was the observation of colors on fresh fracture surfaces of PMMA* that led investigators (11, 12) to conclude that a thin layer of oriented material existed at the fracture surfaces. This conclusion was further justified by the much greater than theoretical value for the fracture surface work which implied a great amount of viscous or plastic flow had to occur.

The roughness of the fracture surface is also a valuable asset in evaluating the energy absorbing capability of the material in front of the crack. Broutman (3, 4) and Wolock and Newman (13) have discovered that the surface roughness is proportional to the fracture surface work exhibited by the polymer. Increasing surface roughness corresponds to increasing fracture toughness or fracture surface work. The fine details on the fracture surface have been studied (6-8, 13) but much still remains to be learned of the surface topography.

It has recently been established that crazing plays an important role in the fracture process. Kambour (14) has observed that for several polymers such as PMMA and polystyrene the fracture surface has more of a craze like structure than a purely oriented structure. By measurement of the critical angle of reflection of the fracture surface layer and thus its index of refraction it was established that voids existed on this surface layer (perhaps up to 40% of

*Poly methyl methacrylate

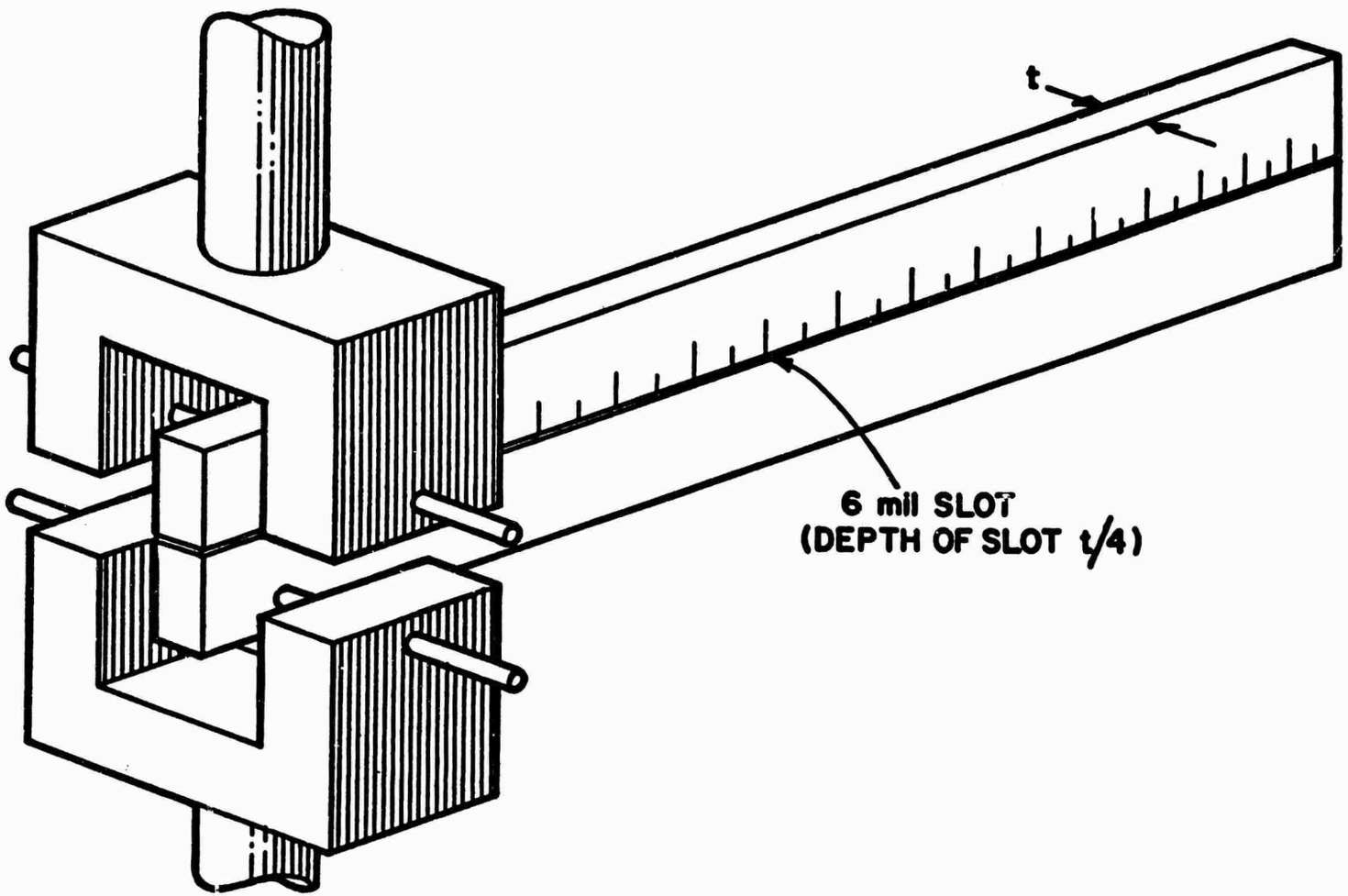

Figure 1. Uniform Cleavage Specimen

layer) but that their dimensions were less than the wave length of light. Kambour has estimated that the fracture surface layer for PMMA (Plexiglas II) has an average thickness of 6800A for zero crack velocity. Polystyrene with a viscosity average molecular weight of 130,000 had surface layer thicknesses ranging from 9300 to 21,000A. This layer thickness is a function of crack velocity and temperature. It is known that crazes in materials such as polycarbonates, PMMA and polystyrenes consist of highly oriented materials and interspersed voids. Therefore, there is not a great deal of difference whether one considers the fracture surface layer to be a crazed region or a highly oriented region. Both of these structures result in large amounts of energy absorption. The polymers investigated by Kambour are shown in Table 1. Because of the nature of Kambour's measurements they are limited to areas of the fracture surface which are relatively smooth. Broutman (3) has visually observed the formation of crazes in polystyrene during cleavage crack propagation. The craze marks were visible above and below the front of the propagating crack and as a result this polymer had a fracture surface work which was four times as great as that measured for PMMA. It appears therefore that the induction of crazing in the material is an important energy dissipating mechanism during the fracture process.

C. Molecular Parameters Influencing Fracture and Fracture Work

Those polymer molecular parameters whose influence on the fracture process have been studied include molecular weight (15, 16), crosslinking (3, 7, 17), and pre-orientation (4). The effects of temperature (3, 15, 16, 18) and crack velocity have also been studied. It was observed for PMMA that increasing the molecular weight (viscosity average molecular weight) caused an increase in fracture surface work but for molecular weights greater than 400,000 there was not a strong dependence upon molecular weight. The appearance of the fracture surface and the mode of crack propagation is also dependent upon molecular weight. At low molecular weights the crack propagation changes from a continuous propagation to a stick-slip discontinuous propagation. The results for the above studies are presented in Table 2. Irregularities in the data can be caused by differences in molecular weight distribution but unfortunately this data was not determined. Benbow (16) has studied the effect of number average molecular weight on the fracture surface work of polystyrene and also observed an increase with increasing molecular weight. The fracture work was measured in two different regions of the specimen since the crack propagation changed from fast to slow in the same specimen and for all molecular weights except the lowest studied, 60,000. At 60,000 the crack propagation was of a continuous nature similar to high molecular weight PMMA. Molecular weight distributions were not reported for the materials sutdied by Benbow.

Broutman has also studied the influence of molecular weight and molecular weight distribution on specially prepared polystyrenes (Table 3). The materials were obtained through the Dow Chemical Co. and narrow distribution polymers were obtained by anionic polymerization while broad distribution polymers were prepared by isothermal polymerization. The measurements were made by uniform

TABLE 1

Summary of Evidence of Craze Formation
in Crack Propagation in Glassy Polymers (Ref. 14)

Polymer	Tg (°C)	Fracture Temp. range where positive evidence found (°C)	Method of Fracture	Type of Evidence
Poly(methylmethacrylate)	105	0-60	Tensile, Cleavage	Color, X-ray
Poly(ethylmethracylate)	50-60	0-25	Cleavage	Color
Polystyrene	78	25-89	Cleavage	Color
Polymethylstyrene	108	100-119	Cleavage	Color
Acrylonitrile-styrene copolymer	96	90-100	Cleavage	Color
Poly(vinylacetate)	30	0-25	Cleavage	Color
Polyhydroxy ether	105	25-104	Cleavage	Color
Polycarbonate	140	-195 to +25	Cleavage impact	Color, X-rays
Poly(vinyl chloride)	-80	-	Tensile, Cleavage	None

TABLE 2

Effect of Molecular Weight on Fracture Surface Work of Polystryene and Poly(methylmethacrylate) (Refs. 15, 16)

Polymer	Molecular Weight	Nature of Surface	Fracture Surface Work 10^5 erg/cm^2
Poly (methylmethacrylate)	$\bar{M}_v$=0.98x10^5*	-	1.14
	1.1x10^5	-	1.24
	1.8x10^5	-	1.33
	4.2x10^5	-	1.45
	12.5x10^5	-	1.50
	30x10^5	-	1.35
	60x10^5	-	1.56
Polystyrene	$\bar{M}_n$=260,000**	Rough Laminated	3.00 19
	130,000	Rough Laminated	1.5 6.1
	80,000	Rough Laminated	1.5 1.7
	60,000	Smooth, Mirror-like	0.3

* viscosity average molecular weights
**molecular weights determined by osmometry

TABLE 3

Fracture Surface Work of Various Molecular Weight Polystyrenes

Material*	Polymerization Method	$\bar{M}_w$	$\bar{M}_w/\bar{M}_n$	Fracture Surface Work (10^5 erg/cm^2)
S103	Anionic	124,700	1.05	3.15
S109	"	193,000	1.06	5.73
S108	"	267,000	1.08	7.69
B8	Isothermal	279,000	2.47	2.71

* Dow Chemical Co. designation

cleavage specimens. These results further reinforce previous observations that increasing molecular weight increases the fracture surface work. For polystyrene above a molecular weight of 200,000 there is little dependence upon the molecular weight providing the distribution remains similar. However, if a wide distribution of molecular weight occurs ($\bar{M}_w/\bar{M}_n$=2.47) the fracture surface work of the polymer with $\bar{M}_w$=279,000 is less than the fracture surface work of the polymer with $\bar{M}_w$=125,000. This demonstrates the importance of molecular weight distribution and of carefully characterizing the polymer in order to properly interpret the results.

Berry (15) has proposed an explanation for the influence of molecular weight on fracture surface work. This work, from the way in which it is defined, is directly proportional to the amount of yielded or crazed region that lies immediately ahead of the crack tip. Consequently the contribution which any particular molecule makes to the surface work will be determined by the length that is contained within this region. A sufficiently long molecule will start in the unyielded region, pass through the yielded region, and terminate once again in the unyielded region. Under these conditions the contribution made by the molecule will be independent of its length. Thus, as indicated by the results, the fracture work will tend to a limiting value at high molecular weights. If one or both ends of a polymer molecule are found within the yielded or crazed region, that molecule will not make a full contribution to the fracture surface work. The polymer chains are believed to be in an extended conformation within the yielded region, and hence the smallest molecule that can contribute fully to the surface work will have its ends on the boundaries of the yielded region, on opposite sides of the fracture plane, and will be fully extended between these points. Assuming that the total thickness of the yielded region is 6 to 7 x 10^3 A, a fully extended molecule of poly(methyl methacrylate) would have a molecular weight of 2.5 - 3x10^5; consequently the fracture surface work must decrease for polymers of lower molecular weight. This is in good agreement with Berry's results considering that it is unlikely for the molecule to become fully extended and that there is really a distribution of molecular lengths in the polymer.

The nature of the dependence of fracture surface work is similar to that observed for other mechanical properties including tensile strength (23):

$$P = A - (B/\bar{M}_n)$$

where P is the measured property, $\bar{M}_n$ is the number-average molecular weight and A and B are constants. For Berry's results A and B are 1.55x10^5 ergs/cm^2 and 3.9x10^9 ergs/cm^2/ mass unit and the molecular weight is viscosity average molecular weight rather than the number average.

Crosslinking

Brief studies have been made on the effect of crosslinking in poly (methyl methacrylate) by Berry (7) and Broutman (3). The results for the change in fracture surface work and inherent flaw size are shown in Fig. 2. In order to produce network polymers from the linear PMMA, Berry copolymerized methyl methacrylate (I) with 10% of ethylene

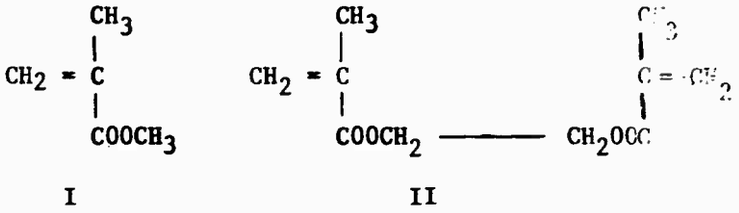

I II

glycol dimethacrylate (II). The fracture surface work of this network polymer was one-third that of the linear PMMA and the fracture surface was smooth and colorless. The concentration of crosslinks was such as to give an average of one crosslink for every ten linear chain segments, assuming complete reaction. However, the crosslinks will be distributed at random and the nature of this (number-average) distribution is such as to have a maximum at the shortest chain lengths. Correspondingly there will be a significant fraction of relatively long chains and hence a capacity for energy dissipation by pronounced intersegmental motion and thus, only a 60 percent reduction in fracture surface work.

Broutman (3) utilized a crosslinked PMMA polymer specially prepared by Rohm and Haas (Polymer K) and also obtained similar results, i.e., a decrease in fracture surface work. The inherent flaw size of the material also decreases. It is thought that this polymer was prepared in a manner similar to that used by Berry. Plexiglas 55 which is also shown in Fig. 2 is described as being lightly crosslinked compared to Plexiglas II.

The influence of cross-link density on the fracture surface work of unsaturated polyester-styrene blends has also been investigated (3,17, 24). The work of Mills et al (17) was the most well defined as far as knowledge of the polymer structure. An unsaturated polyester was formed using maleic anhydride and propylene glycol.

Maleic Anhydride Propylene Glycol

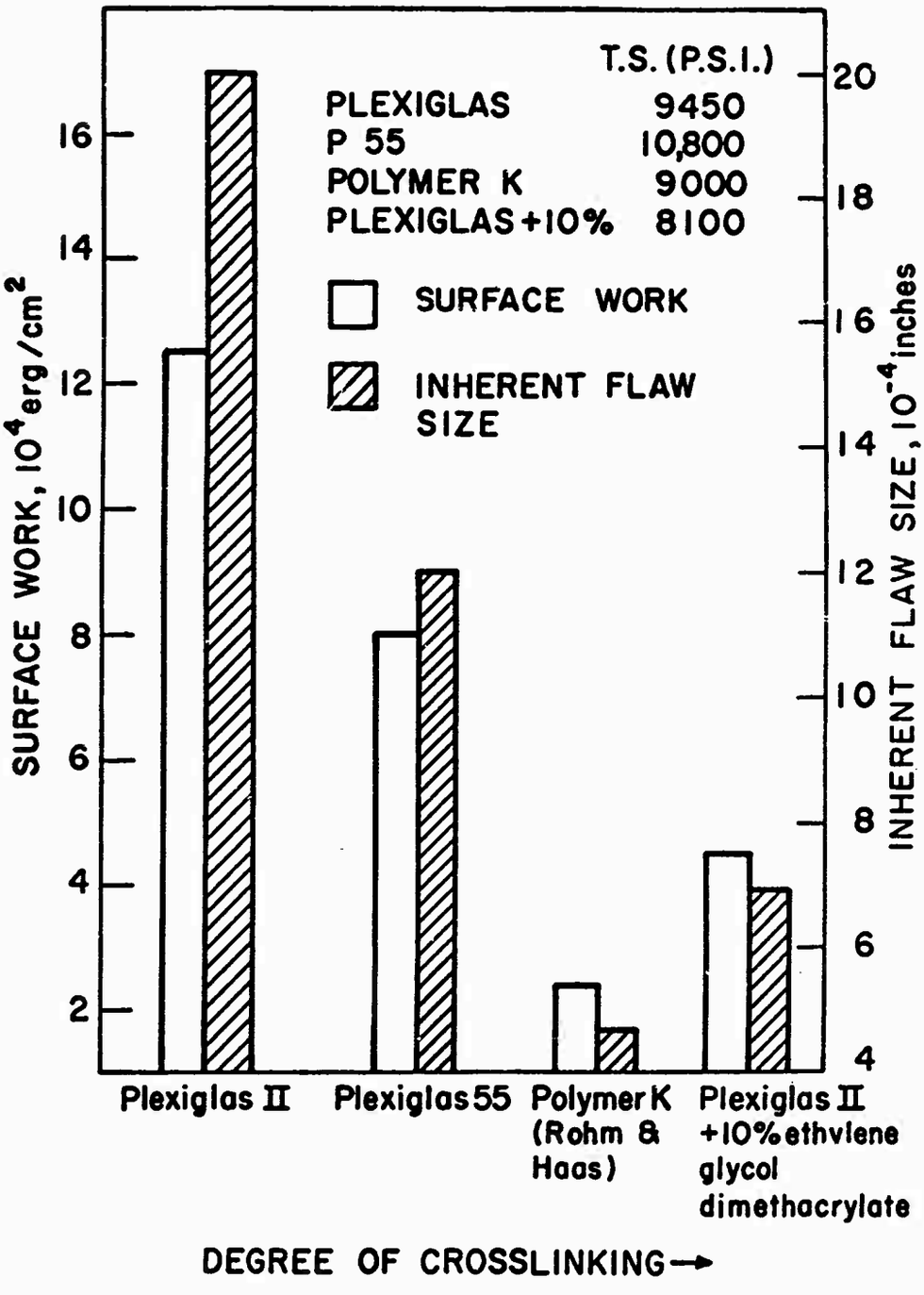

Figure 2. Fracture Surface Work and Flaw Size for Crosslinked Plexiglas

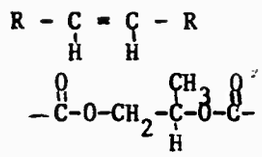

This unsaturated polyester can be crosslinked by adding styrene monomer and a peroxide to initiate a free radical reaction:

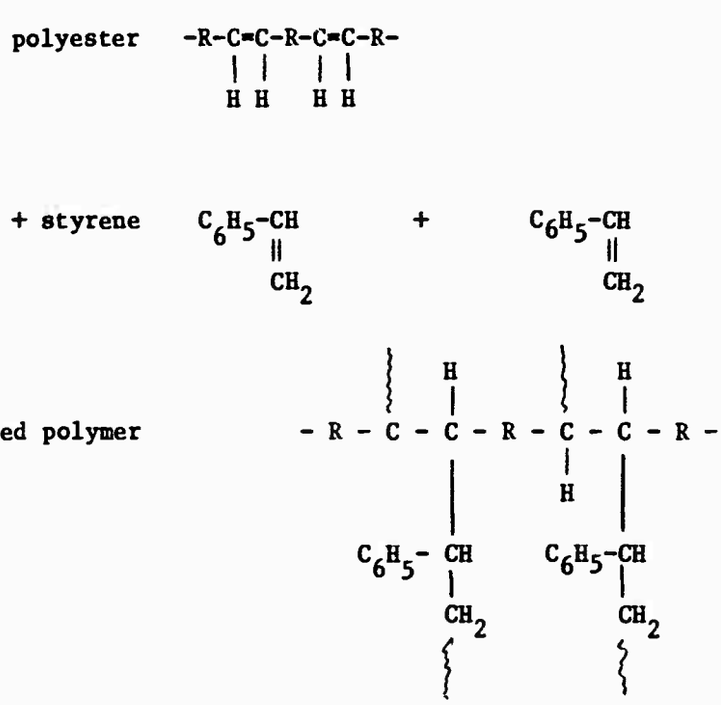

The characteristics of this system can be easily changed. For example, by copolymerizing phthalic anhydride with the maleic anhydride the R group above can be increased in length, and since these phthalic groups do not crosslink with the styrene the crosslink density is reduced. Also, since more than one styrene molecule can be linked together in creating the crosslinks between polyester chains, the average length of crosslinks can be varied to some extent by changing the ratio of moles of styrene to moles of polyester double bonds. Several polyesters were prepared and some of their properties are shown in table 4.

TABLE 4

Properties of Unsaturated Polyesters (Ref. 17)

Polyester	Molar % Maleic Anhydride Unsaturation in Initial Reaction Mixture	Ave. M.W. Between Double Bonds	No. Avg. Double Bonds/Polyester Molecule
A	16	594	1.4
B	14	686	1.2
C	12	808	1.1
D	8	1238	.7
E	4.5	2240	.4

Through analysis of hydrolysis degradation products and also by infrared analysis they determined that 2.6 to 3.0 molecules of styrene enter into reaction with the polyster double bond to form the link between chains. Also, through infrared analysis they were able to determine that all bonds had reacted for less than 12 mole percent maleic anhydride. Above this value, some molecules are trapped in the rigid structure without having reacted. For example, at 16 mole percent unsaturation, 97 percent of the styrene double bonds and 92 percent of the polyester double bonds had reacted.

The fracture surface work of these polyester blends was determined by using a centrally notched tension specimen similar to the one developed by Irwin and Kies (25). Their results are shown in Fig. 3 plotted as stress intensity factor, K_c (psi$\sqrt{\text{in.}}$), and energy release rate, G_c (lb/in). The energy release rate is related to K_c and the fracture surface work by the following:

$$G_c = K_c^2/E \qquad (2\text{-}3)$$

$$G_c = 2\gamma \qquad (2\text{-}4)$$

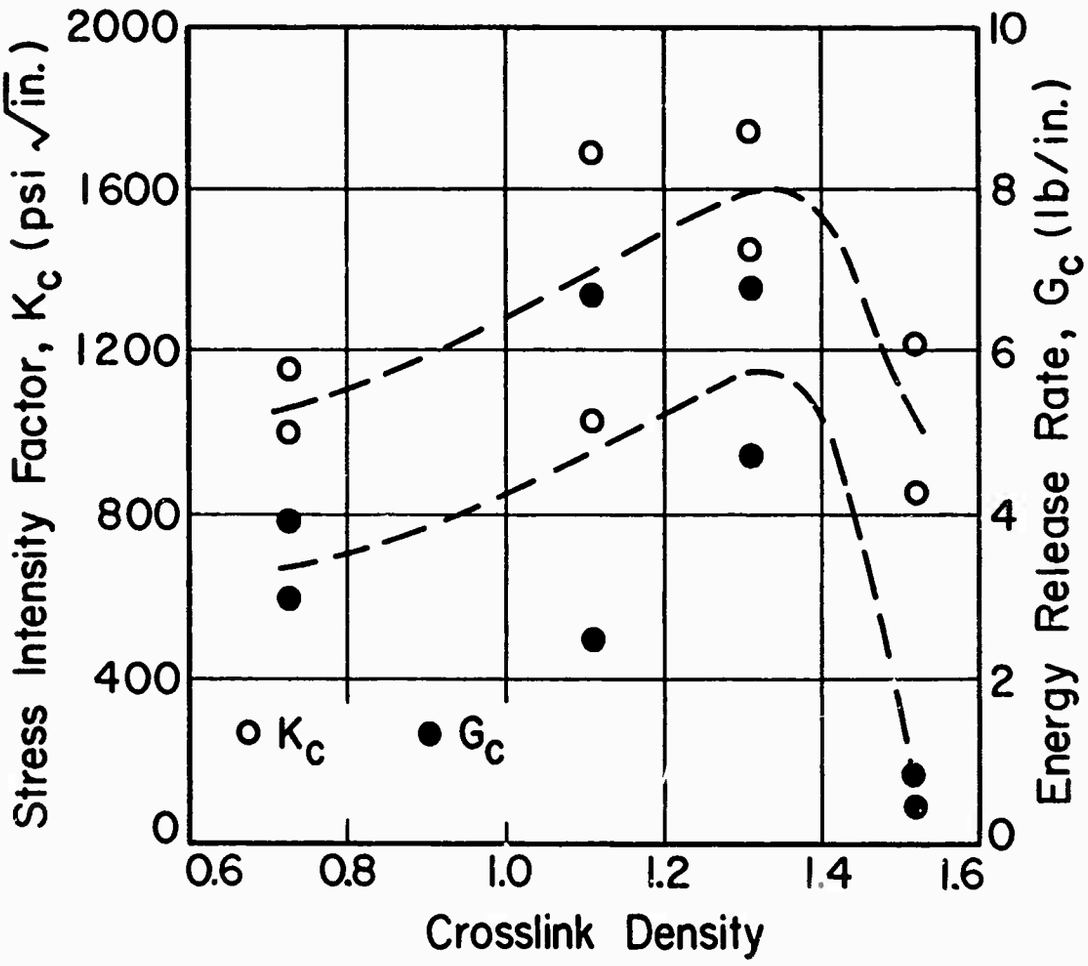

Figure 3. Crack Propagation Parameters for Polystyrene-styrene copolymers as a function of Crosslink Density (Ref. 17)

where E = Young's modulus of elasticity and γ = fracture surface work. As can be seen from Fig. 3 there is a considerable amount of scatter in the results and any real variation is subject to question.

Broutman (3) studied polyester-styrene blends by simply changing the weight percent of styrene in the blend and measured an increase in fracture surface work as the amount of styrene was increased. McGarry (24) used a similar polyester-styrene blend and only changed the post-cure temperature in an attempt to vary the degree of crosslinking by controlling the reaction. His results showed very little change in fracture surface work although the post-cure temperature was altered from 70°F to 300°F. The increase in fracture surface work measured by Broutman can be explained since the addition of the styrene only served to lengthen the link between polyester chains rather than increase the degree of crosslinking. Also, any unreacted styrene may serve to cause an apparent increase in fracture surface work. The results shown in Fig. 3 tend to also show an increase in fracture work with increased degree of crosslinking. This is in contradiction to the results obtained by Berry and Broutman on the crosslinked PMMA.

The fracture toughness of epoxy network polymers has also been studied, but characterization of the molecular structure in these studies is lacking (10,24). The type of epoxy resin studied can be represented as follows:

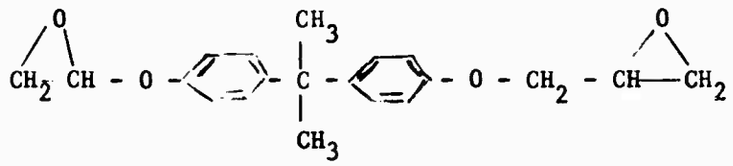

This resin is crosslinked through the reactive epoxy sites

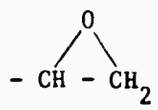

and the cross-linking reaction for the curing agent diethylene triamine (DTA) is shown below,

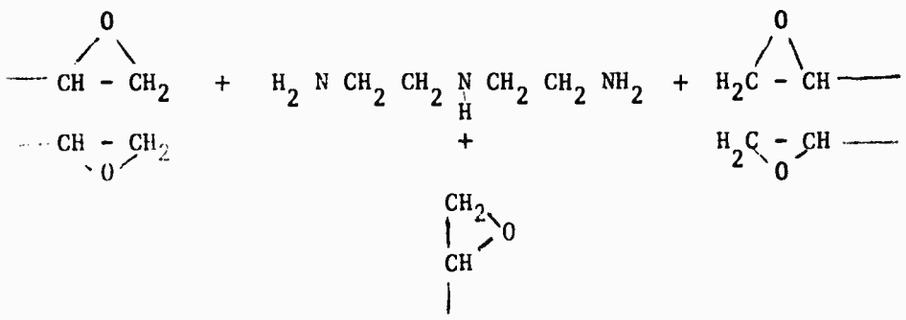

and the final network structure is as follows:

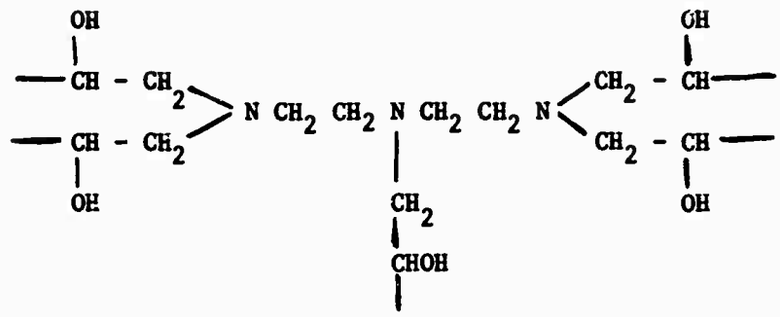

It can be observed that in this polymer the amine curing agent becomes a part of the polymer chain as opposed to the function of the styrene molecule in polyester resins. McGarry (24) has investigated the fracture surface work of this type of polymer by varying the post-cure temperature while maintaining a fixed concentration of curing agent. He has found that increasing the post cure temperature from 70°F to 300°F increases the heat distortion temperature as well as the fracture surface work. The fracture surface work appears to increase by at least a factor of two. Mostovoy and Ripling (10) have also reported an increase in fracture surface work when the amount of curing agent is increased for epoxy resins with the structure shown above. These results also contradict the studies on the crosslinking of the linear polymer, PMMA. A possible explanation exists in the mechanism of the network forming process. For example, with the epoxy resins, if the cure reaction is not complete low molecular weight epoxy molecules and amine molecules are trapped in the structure and these can reduce the fracture surface work of the resin as found in the related molecular weight studies. As the reaction is completed the fracture surface work increases due to the loss of the low molecular weight molecules. This clearly represents a different mechanism than the crosslinking of a linear high molecular weight polymer.

Molecular Orientation

The effects of molecular pre-orientation in thermoplastic polymers are significant especially on physical properties such as strength and toughness. Studies first conducted by the Rohm and Haas Co. for the U. S. Air Force on stretched Plexiglas for aircraft canopies indicated that the fracture toughness

of this material (as measured by a center notched tensile specimen) was increased by the hot stretching. More recently Broutman (4) has investigated the fracture surface work relations for oriented Plexiglas and polystyrene sheets. A commercial multiaxially stretched Plexiglas sheet illustrated in Fig. 4 was used to determine the fracture surface work by a cleavage test in various directions. Of course, the fracture work parallel to the oriented molecules, as shown, is almost two order of magnitude less than the work normal to the direction of orientation. Uniaxially hot stretched sheets of polystyrene and PMMA were also investigated and the fracture surface work was measured parallel to the orientation. In Fig. 5 the large reductions in surface work can be seen as the percent hot stretch was increased. The temperatures shown in the figure represent the stretching temperatures. The fracture surfaces of these specimens were observed in great detail and from the surface topography and from other details such as the color appearance on the surface conclusions concerning the nature of the molecular motions at the tip of the propagating crack were reached.

Another means of achieving molecular orientation in polymers is by metalworking techniques such as strip or sheet rolling. For crystalline polymers and ductile glassy state polymers or polymer blends this rolling process can be performed at room temperature. Polymers such as polyethylene, polypropylene, and polycarbonate have already been cold rolled and properties' changes reported in the literature (27-30). The rolling can be done so that uniaxial orientation, biaxial orientation, or orientation in any combination of directions can be achieved. Cold rolling has many advantages over hot stretching to produce molecular orientation. One obvious advantage is that in cold rolling sufficiently below the glass transition temperature thermal relaxations cannot occur. Therefore, for the same degree of stretch greater molecular orientation can be produced by the rolling process. Although it has been shown that the impact strength of a polymer can be greatly increased by 50 percent roll reduction, there has never been a study of fracture toughness of these materials (27, 29).

Effects of Temperature and Crack Velocity

The effects of temperature on the fracture surface work have been studied by several investigators (3,6,7,16,17,18). The effect most commonly observed for the thermoplastic polymers is shown in Fig. 6 (3) for Plexiglas. Decreasing the temperature from the glass transition temperature of the polymer causes an increase in the fracture surface work. This has been demonstrated for polystyrene as well as for PMMA. Berry has made measurements on tensile specimens down to liquid nitrogen temperatures (-196°C) and observed that the fracture surface work continued to increase even down to this temperature. It should be noted that above the glass transition temperature of a polymer when the polymer is in a rubbery state the previously described experimental techniques for measuring fracture surface work are not valid. However, techniques have been developed for measurement of the tearing energy for rubbery materials and this quantity has the same significance as the fracture surface work for glassy polymers.

STRETCHED P55	SURFACE WORK (erg/cm^2)
0°	6.5×10^5
45°	5.8×10^5
90°	7.8×10^5
11	1.65×10^4

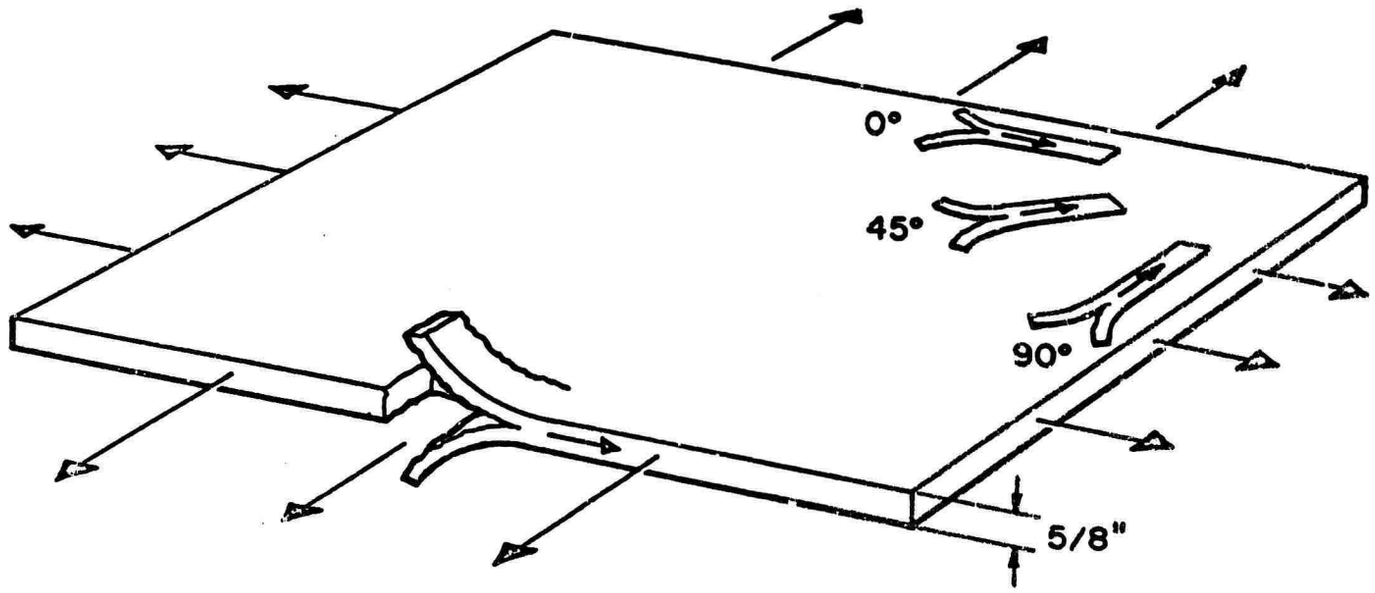

Figure 4. Multiaxially Stretched (65%) Plexiglas

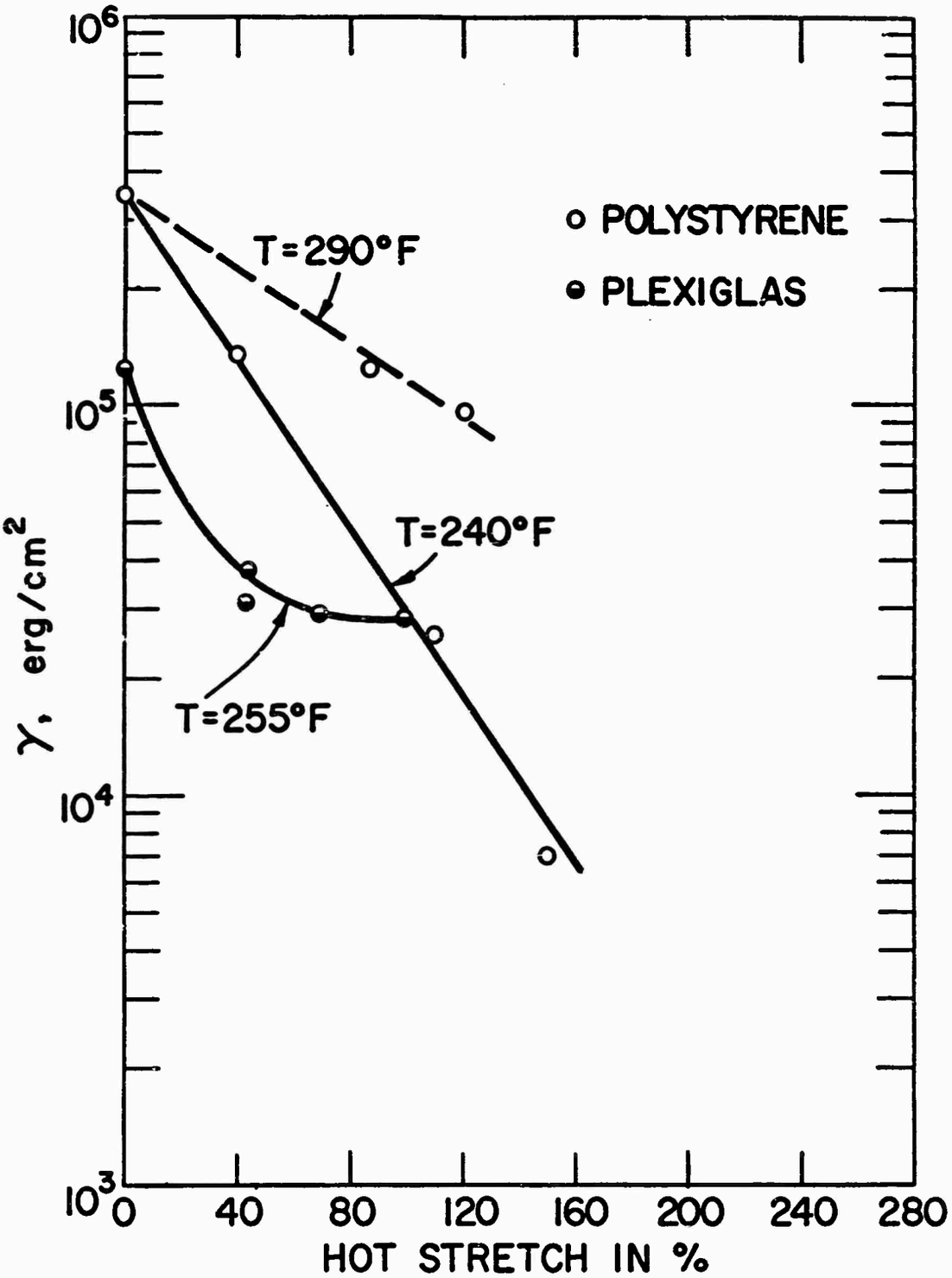

Figure 5. Fracture Surface Work for Oriented Polymers

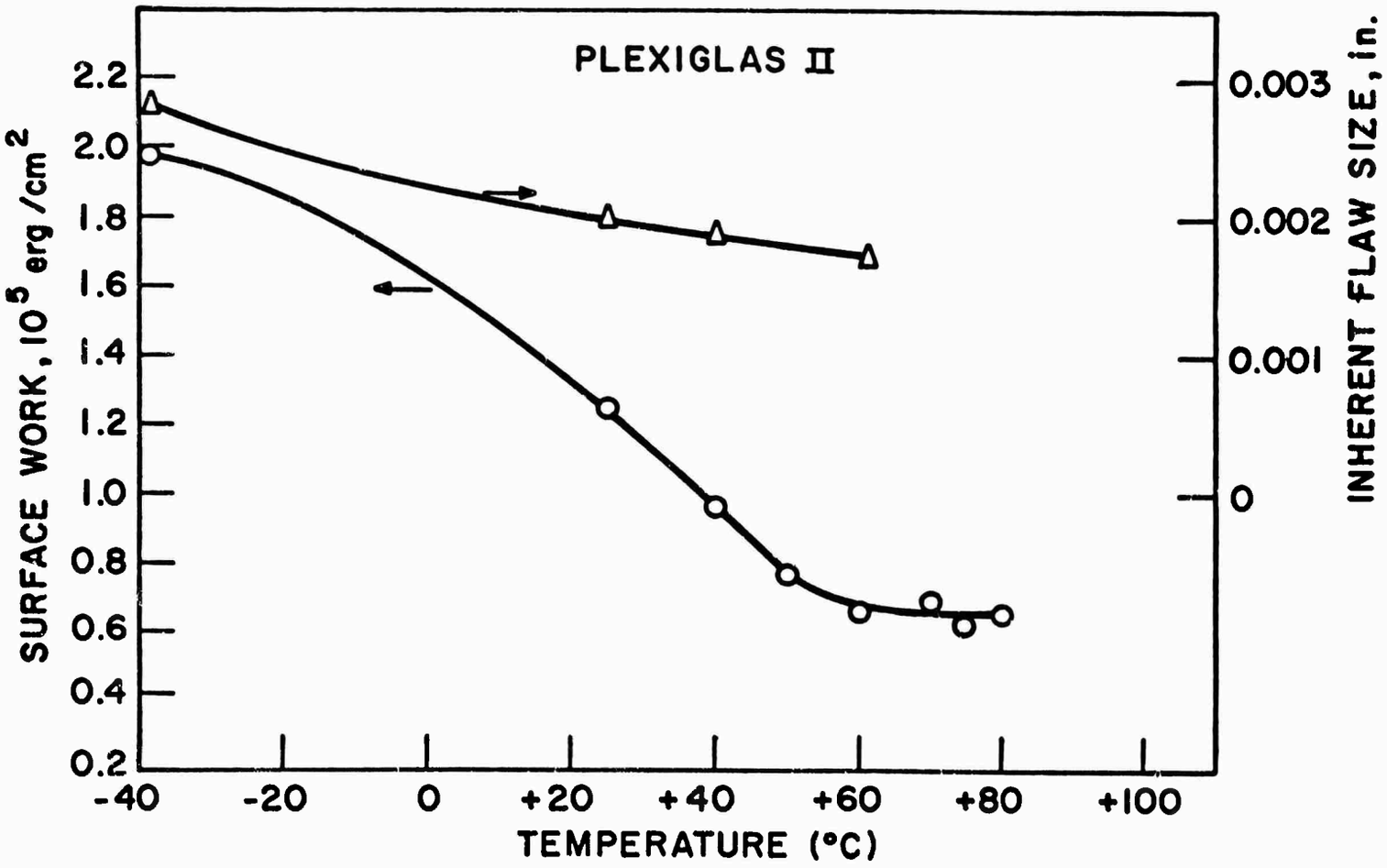

Figure 6. Fracture Surface Work for PMMA as a Function of Temperature

Studies of the influence of crack propagation rates on fracture mechanisms or fracture surface work are not as common as studies on temperature effects, but nevertheless there is some information on this subject (10,19,20,21). Measurements by Cotterell (20) on PMMA indicate that the fracture toughness increases with increasing crack velocity from 0 to 2500 ft/sec. Increases in surface roughness are also readily observed and this can account for a large fraction of the measured increase in fracture surface work. Vincent and Gotham also have reported an increase in fracture surface work with increase in crack propagation velocity for a high molecular weight PMMA sheet (19). However, the measurement methods used to obtain various crack propagation rates varied from tensile methods to cleavage methods to Charpy impact tests and the results are difficult to interpret. Mostovoy and Ripling (22) have studied the effect of crack propagation rate on fracture surface work for an epoxy adhesive. A cleavage specimen is used and the crack is propagated through the thin adhesive layer which bonds aluminum adherends in the shape of the cleavage specimen. Their results also indicate an increase in fracture surface work as the crack propagation rate increases. Investigators from the U. S. Naval Research Laboratory have also studied crack propagation velocity effects in PMMA (21). They designed servo-actuated loading equipment to maintain a constant crack velocity in a uniform cleavage bar and determined a small increase in fracture surface work as the crack velocity was varied from .01 to 100 in/sec. It appears that these increases in fracture surface work can be correlated with increased surface roughness or area as the crack velocity increases. Decreasing temperature and increasing crack velocity or strain rate both cause increases in fracture surface work which correspond to the time-temperature equivalence found in viscoelastic properties of polymers.

CHAPTER II

EQUIPMENT DEVELOPED FOR FRACTURE STUDIES

1. Loading Machine

A loading machine was designed to be compact, simple, and to provide a high degree of accuracy; the loading machine is used for the determination of crack propagation energies over a wide range of temperatures and with the capability of varying rates of deflection.

Four Thompson hardened shafts (3/4"x30") are set parallel between two channels (12"x3"x1/4") and rigidly bolted to the channels as shown in Fig. 7a. These four shafts support the two channels on which the load is actually applied. The upper two shafts are also used to guide the load carriage.

The load carriage consists of two steel bars (14"x2"x1¼"), and three aluminum plates which hold the two bars parallel and rigid. Four Thompson ball bushings are set in the two steel bars of the load carriage which are seated on the upper two shafts. The friction force between the load carriage and shafts is thus reduced. The load carriage moves smoothly on the parallel shafts. A Saginaw ball screw is fixed on the channel with a Boston self-aligning precision ball bearing so that axial movement of the screw is prevented.

A ZERO MAX drive motor, ZERO MAX power block and gear reducer with digital speed control (800 digits, 0 to 20 rpm) are placed behind the channel and connected to the Saginaw ball screw. A Tork-O-Stat overload protecter (± 100 pound-in) is placed between the gear reducer shaft and screw.

The specimen is held between two grips, one of which is bolted to the load cell which is bolted to the channel. The other grip is bolted on the bar of the load carriage. This is shown in Fig. 7a. For low temperature tests conducted in liquid nitrogen, an "L" shaped grip was designed so that the specimen along with the lower portion of the grip was immersed in the liquid nitrogen bath. These grips must be guided so that any vertical deflection of the grips due to the moment caused by the eccentric loading is prevented. The guide was a ball bearing which produced low friction force and allowed only horizontal movement. A liquid nitrogen dewar was placed under the grips through a hole in the table. The dewar can be raised vertically by a laboratory jack when the specimen is to be immersed. This assembly can be seen in Fig. 7b.

The test machine can accomplish the following:

1. linear strain rate range = .01 to 2 inches/minute
2. fully reversible drive system

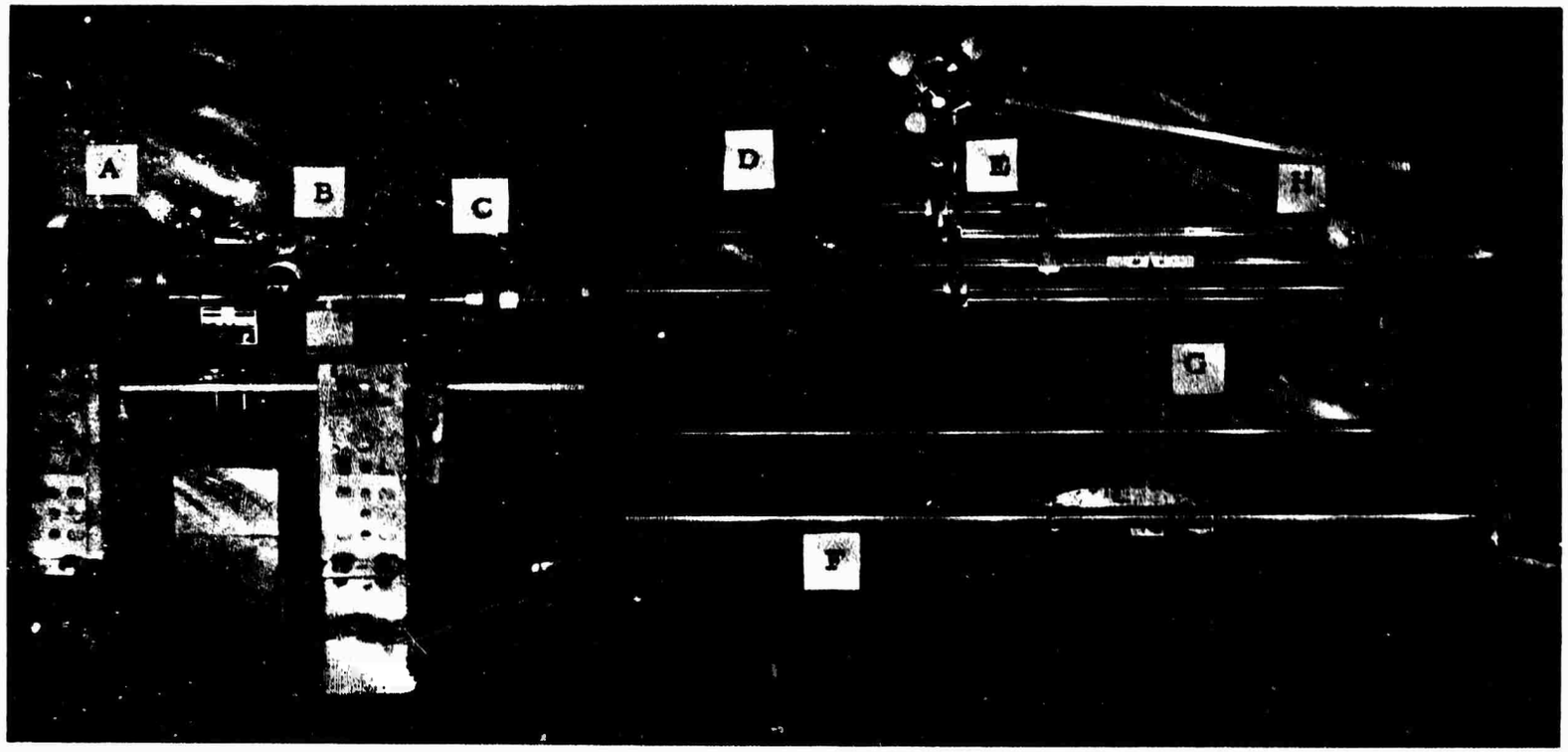

Figure 7A Loading Machine for Crack Propagation Studies

A: Zero -Max Drive Motor B: Zero-Max Power Block and Gear Reducer with Digital (800 digits) Speed Control (0 to 20 rpm) C: Tork-O-Stat Overload Projector D: Loading Carriage (guided by 4 Thompson ball bushings and driven by Saginaw ball screw) E: Sanborn DCDT (+1 inch) F: Thompson Hardened Shafts G: Plexiglas Crack Propagation Specimen H: Daytronic ±100 pound Load Cell

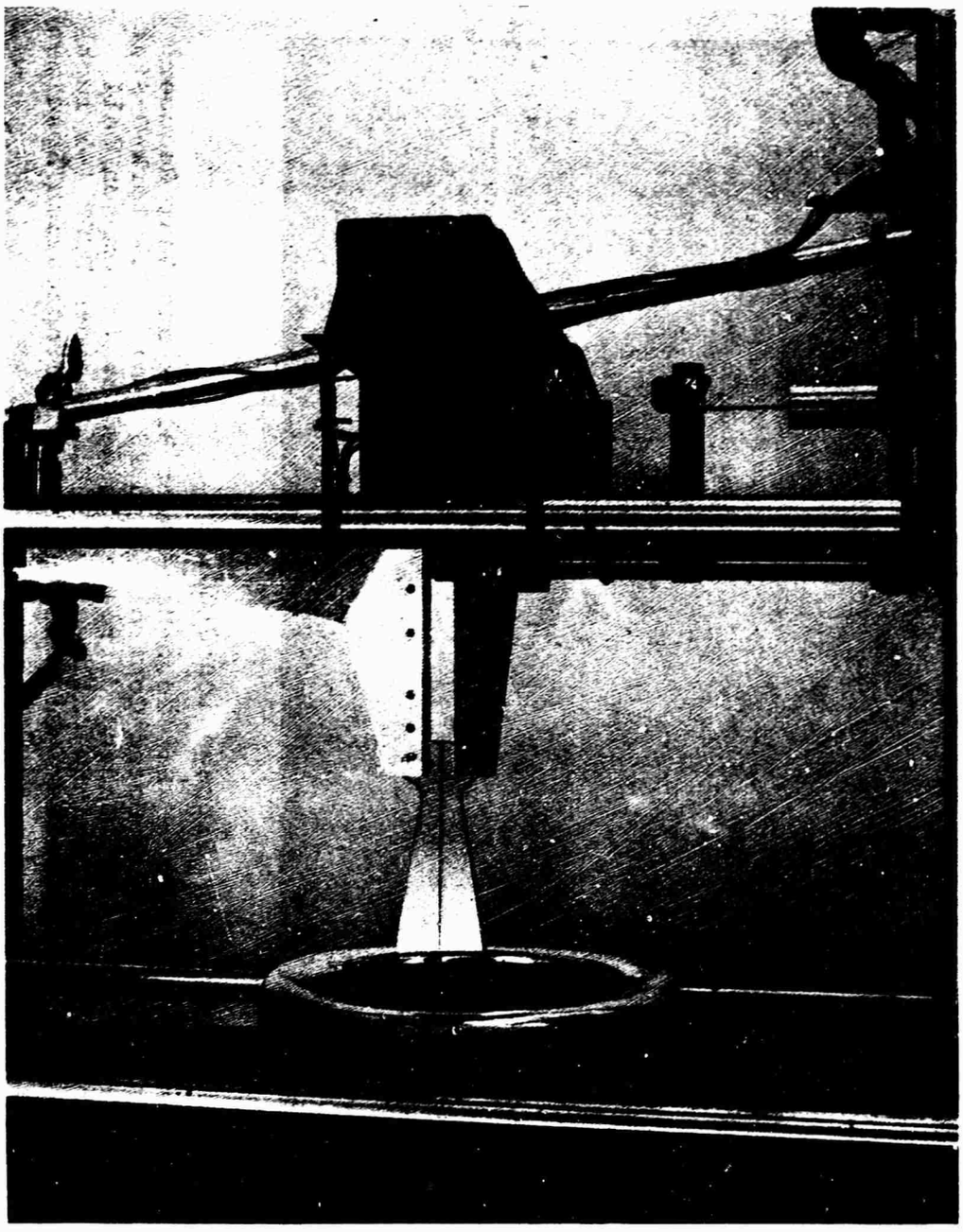

Figure 7B View of Tapered Double Cantilever Cleavage Specimen, Loading Grips and Liquid Nitrogen Dewar

3. load range = ± 100 pounds (load cell capacity)

4. temperature range = - 196°C to +105°C

5. load-displacement recording system (Moseley X-Y recorder)

Daytronic ± 100 pound and ± 25 pound load cells were used with a Daytronic transducer amplifier-indicater (Model 300D) to convert the AC signal from the load-cell to a convenient DC signal which is then recorded on the X-axis of a Moseley(Model 7030A) X-Y recorder. The load cell is an LVDT type which is a high stiffness load cell. The deflection of the ± 100 pound cell is 0.001" at 100 pounds and that of the ± 25 pound cell is 0.001" at 25 pounds.

A Sanborn DC displacement transducer (± 1 inch) is attached on the grip bolted to the load carriage and measures the specimen deflection. A Harrison DC power supply provides 6 volts to the transducer and the signal from the DCDT is recorded on the Y-axis of the recorder.

CHAPTER III

PREPARATION OF MATERIALS AND CLEAVAGE SPECIMENS

1. Material Preparation

Several types of polymers were prepared by compression molding of polymer pellets or powders to form 1/8 or 1/4 inch thick sheets. Techniques had to be developed to eliminate all air voids which could easily be detected since most of the polymers were transparent. The preparation method is reviewed in table 5. Any pertinent comments will be reserved for later sections in which the results will be discussed.

2. Preparation of Cleavage Specimens

A. Uniform Double Cantilever Cleavage Specimens

The first step in preparing a specimen is to prepare a rough blank. The blanks are strips approximately 2 inches wide and 12 inches long cut from molded or cast sheets usually of 1/8 or 1/4 inch thickness. These blanks are then milled so that both sides are parallel. The specimen is next carefully placed in a vise of a Bridgeport milling machine. A groove whose depth is 1/4 of the plate thickness is machined on each side along a parallel line 0.6 inches from the top edge of the specimen with a 0.006 inch thick screw slotting saw (2½ inch diameter, 60 teeth) at 660 rpm and 15/16 inches per minute feed. Lubrite Motor Oil or a soap solution is applied to the blade to reduce frictional heating of the blade and specimen. After machining the side grooves, an initial crack, approximately 2 inches long, is made on one end of the specimen by increasing the depth of the saw cut to half of the plate thickness on each side. The specimen is then rotated 180 degrees in the vertical plane and milled to the final height of 1.2 inches. Using a combination square, a line is drawn 0.2 inches from the end of the specimen. On this line two loading pin holes are drilled with a #29 drill, 0.4 inch from either side of the center groove.

B. Tapered Double Cantilever Cleavage Specimen

Strips which are four inches wide and 14.5 inches long are first cut from molded or cast polymer sheets, and one long edge is machined straight with a router. In order to cut the straight edge, the specimen is fed along a flat edged steel bar which is clamped on the bed of the router. The contour of the tapered cleavage specimen, given by the cubic equation (eq. 24), is difficult to machine without a template. A template was designed and machined from aluminum as shown in Fig. 8. Using the template, a right angle

TABLE 5

Compression Molding Conditions for Preparation of Molded Polymer Sheets*

Material	Temp. °C	Time for heating without pressure	Time under pressure	Remarks
1. Polystyrene M.W. 230,000	155-160	1½-2½ mts.	3 - 5 mts.	Cooled (in air) very slowly in order to avoid dimples on surface.
2. Polystyrene M. W. 35,000	145±5	2-3 mts.	4 - 5 mts.	Cool under platens or air cool (very brittle)
3. Methyl Acrylate Polymer	190-195	5-6 mts.	5-10 mts.	Cool under pressure to 150°C
4. Ethyl Methacrylate	150-155	5-6 mts.	8-10 mts.	Water-cool platens
5. Isobutyl Methacrylate	130-135	8-10 mts.	5-6 mts.	Water-cool platens
6. n-Butyl Methacrylate	90-95	8-10 mts.	5-8 mts.	Water-cool platens
7. Polyvinylchloride +3 pph tin stabilizer	165-170	5-6 mts.	5-6 mts.	Water-cool platens
8. Isotactic Polystyrene	430-445°F	2 mts.	5-6 mts.	Water-cool to below 100°C

* Mold pressure was 110 psi

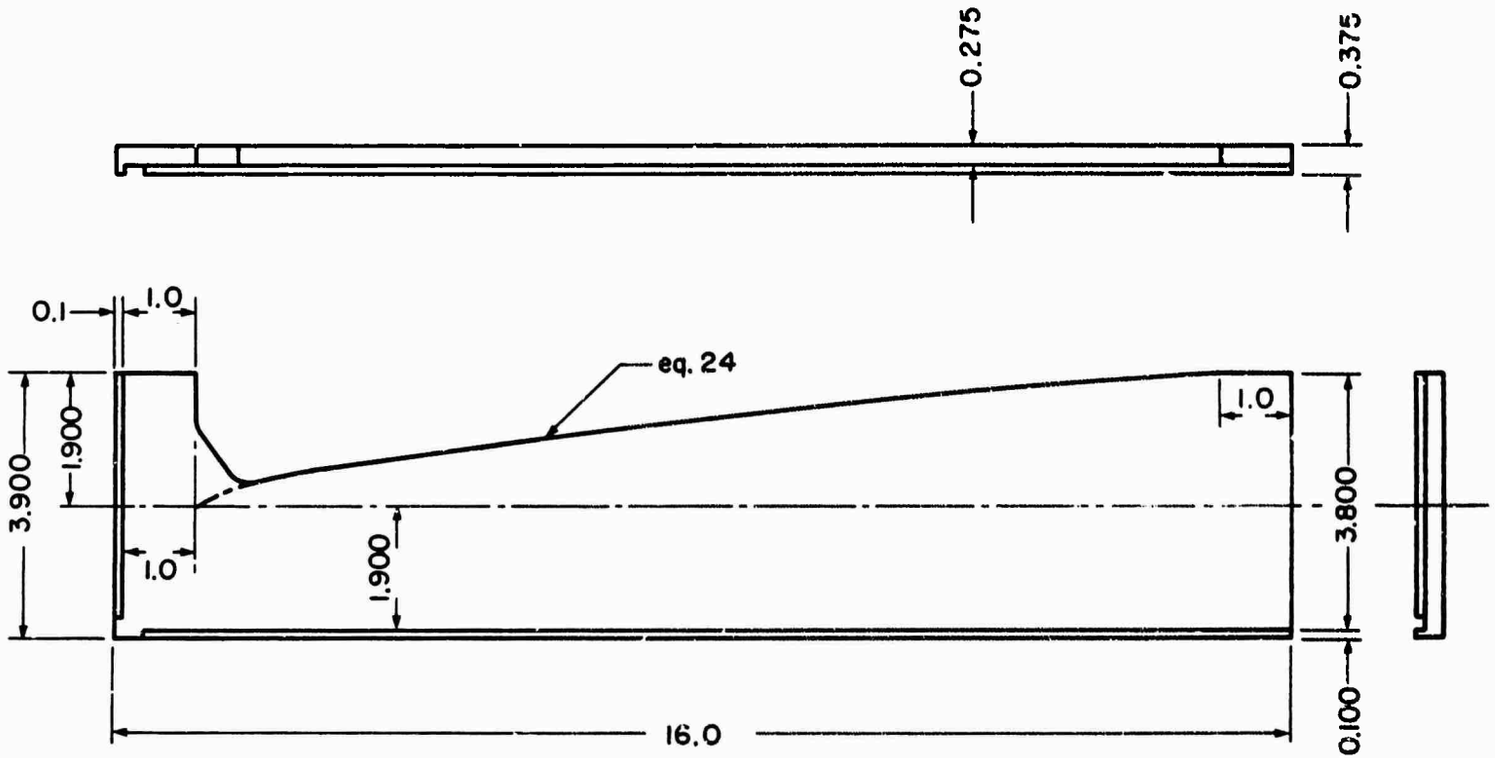

Figure 8. Template Used for Routing Cleavage Specimens

to the straight edge is made on one end of the plastic strip. After this, the specimen is placed with the straight edge down in the vise of a Bridgeport milling machine. A groove (1/4 of the plate thickness) is cut on both sides of the specimen along a line 1.900 inches from the straight machined edge with a 0.006 inch thick screw slotting saw at 600 rpm and 15/16 inches per minute feed. A three inch initial crack is made on the side that has been machined to a right angle by the same procedure described for the uniform cleavage specimen.

After machining the grooves and the initial crack, the specimen is affixed to the template with double coated tape such that the machined edges are set against the rim of the template. By hand feeding the template whose edge is pressed against a pin of the router, one side of the specimen is machined into the final contour. Then the specimen is turned over and affixed to the template, and the other side of the specimen is machined in the same manner. An origin line perpendicular to the groove is drawn 1.000 inch from the machined end where the initial crack was made. On this line two loading pin holes are drilled with a #29 drill, 0.45 inches from either side of the center groove. After this, the specimen head is cut along the line 0.65 inches from the groove on either side and 0.8 inch from the machined end. Thus the specimen is completed.

Materials which are rubbery at room temperature cannot be machined by the methods described in the previous section. For machining of a uniform double cantilever cleavage specimen, a three inch by nine inch strip is first cut from a sample sheet and placed in an aluminum plate holder shown in figure 9. The rubbery sheet is pressed lightly in the plate holder by bolts which also fasten the holder on the bed of an Atlas Horizontal Milling machine. A straight edge is first machined with a screw slotting saw blade (0.006 inch thickness, 2-3/4 inch diameter, and 72 teeth) at 450 rpm and 1.35 inches per minute feed. The plate is then removed and repositioned in the holder with the position setter shown in Fig. 9b. With this position setter the plate is positioned so that a groove can be made 0.6 inches from the machined straight edge. The groove, 1/4 of the plate thickness, is cut in one pass with the screw slotting saw on the upper side of the rubbery sheet. A similar groove is machined on the other side of the sheet by the same method. The initial crack (about 2 inches long) is made by increasing the depth of the groove machined on both sides of the plate. Finally, the plate is positioned in the holder with the position setter to cut the other straight edge which is 1.2 inches from the first straight edge. Two loading pin holes are drilled in the same way as described in the previous section. Thus a specimen is completed.

In the case of tapered cleavage specimens, a 5 inch wide and 10 inch long strip was used for the starting blank. First, one edge is cut straight in the same manner described above, and a groove which is 1.9 inches from the straight machined edge is made in the same manner. An initial crack

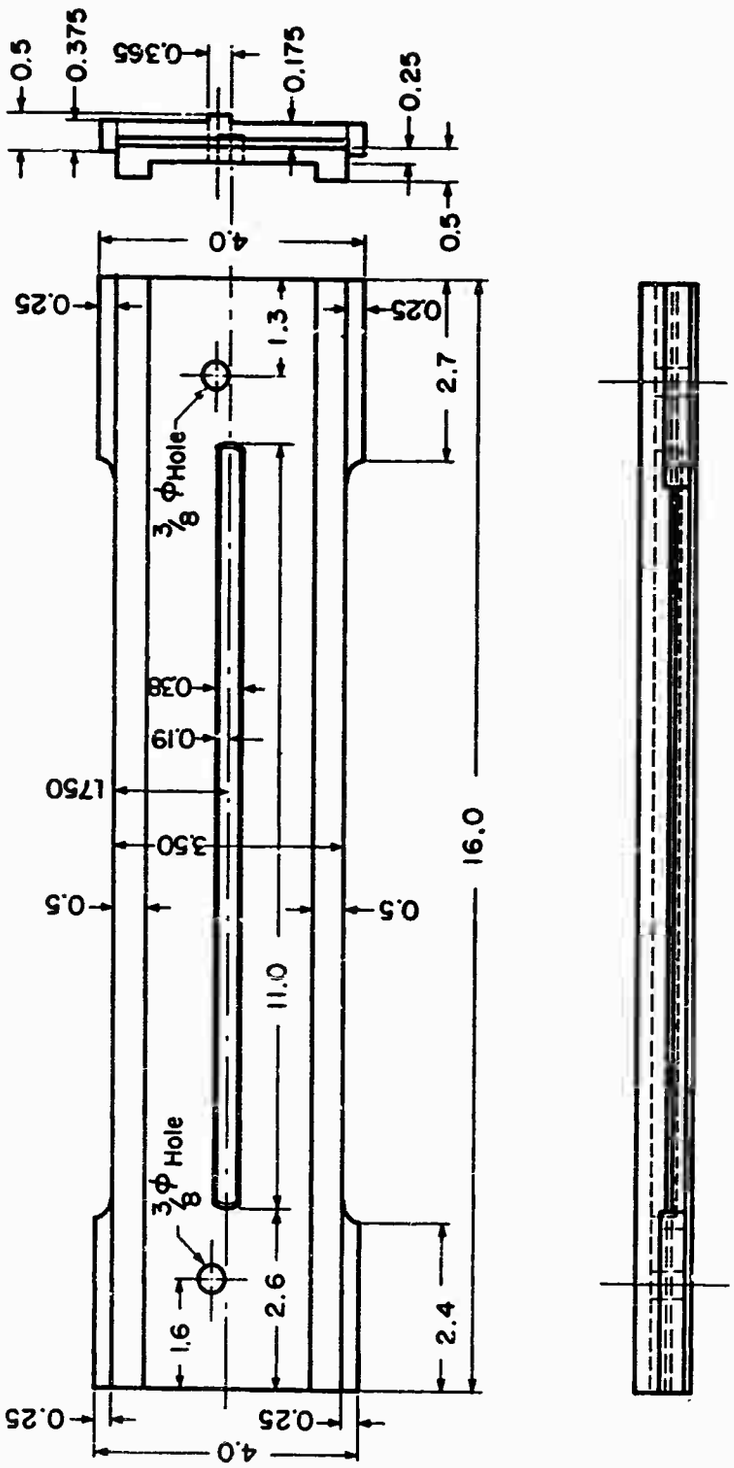

Figure 9(a). Plate Holder for Machining Rubbery Materials

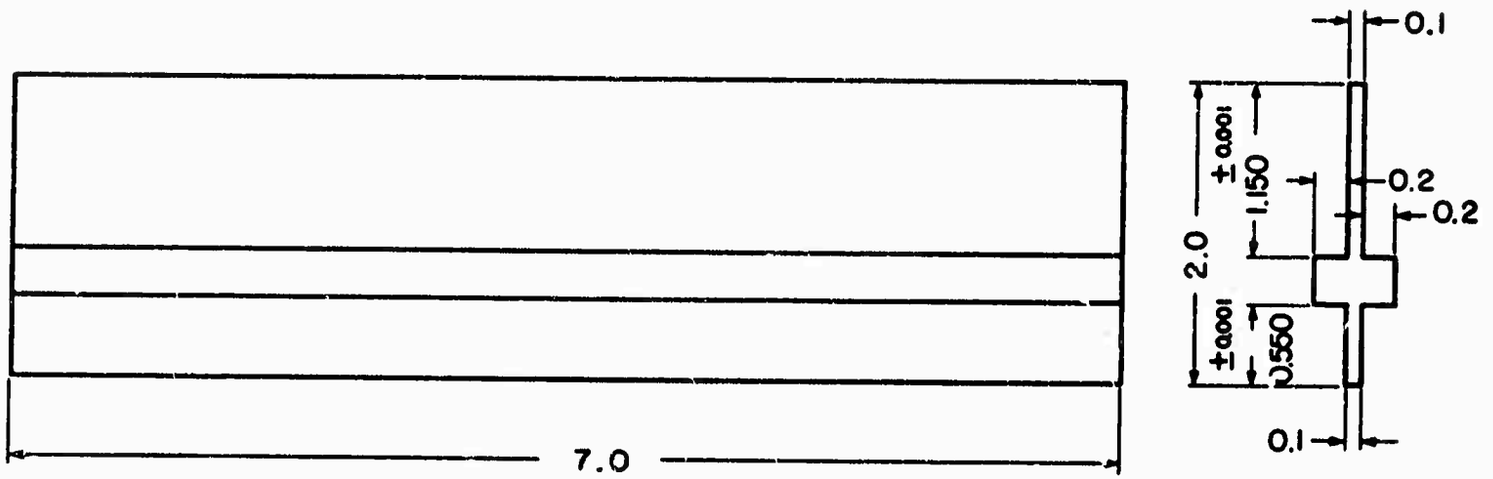

Figure 9(b). Position Setter for Locating Specimen in Plate Holder

approximately 3 inches long is machined. Then the plate is taken out of the holder and affixed to the template with double coated tape. The rest of the machining procedure follows as in the previous section.

CHAPTER IV

ANALYSIS AND DESIGN OF CLEAVAGE SPECIMENS

1. Background

According to the Griffith fracture criterion, brittle fracture occurs by the unstable propagation of a crack initiating from a flaw in a material (5). Griffith calculated the fracture strength using an energy method and proposed the criterion that a system would become unstable and a crack would increase in size if

$$-\frac{dU}{d\ell} = \frac{dS}{d\ell} \qquad (3)$$

where U is equal to the strain energy and S is equal to the surface free energy. The solution of this equation for a uniformly loaded bar in uniaxial tension resulted in the previously discussed equation

$$\sigma_{ult} = \sqrt{\frac{2E\gamma}{\pi c}} \qquad (1)$$

defined in a previous section of this report. Berry (2) was one of the first to apply this criterion to polymers and he showed that polystyrene and PMMA obeyed the criterion $\sigma_{ult}=kc^{-\frac{1}{2}}$. This was accomplished by measuring the tensile strength of bars which had cracks of various lengths introduced into their edges. Berry also determined that the experimentally determined value of the surface energy was much greater than the theoretically predicted value. Thus irreversible work also occurs at the crack tip and the surface energy is best termed fracture surface work.

In the investigations described in this report, fracture surface work values of polymers were measured by a cleavage technique rather than by uniaxial tensile loading of a pre-cracked bar. The cleavage experiment has been utilized to measure fracture surface energies of metallic and ionic single crystals as well as inorganic glasses (31-33). In fact, Gilman's method (31) as applied to crystals was later adopted for use in polymers.

The cleavage technique has some advantages over using tensile stress fields for crack initiation and propagation. For example, the value of the fracture surface work can be obtained from a few experiments on one specimen, the crack propagation rate can be better controlled and the calculation of the surface work is based on simple beam theory. However, the cleavage technique has theoretical and experimental shortcomings. For example, the cleavage technique can not be simply applied to isotropic materials, such as polymers in the glassy state, since the gradient of the maximum tensile stress in the vicinity of the crack tip is such that the crack tends to run out of its plane of propagation towards the edge of the specimen. This stress field at the crack tip in a cleavage specimen has been shown photoelastically (34). In calculating the value of surface work, it cannot be assumed that the cantilever beams forming the specimen are built into the uncracked region with perfect rigidity so that the elastic strain energy is stored only in the cantilever beams whose lengths are that of the central crack. This is not satisfied because the uncracked region also is deformed and stores part of the elastic strain energy.

Berry modified the configuration of cleavage specimens formerly used for single crystals with definite cleavage planes (8) by machining fine slots along each face of the specimen, so that the thickness in the median plane is reduced and a crack is directed in the median plane (see Fig. 1).

2. Uniform Double Cantilever Cleavage Specimen

As shown in Fig. 10 the specimen described here is symmetrical about the median plane and each side can be represented as a cantilever beam of constant height when the specimen is loaded at its ends. The length of the cantilevers is essentially that of the crack length along the grooved median plane.

If it is assumed that f is the force applied to its extremities, δ is the deflection of one beam and ℓ is the crack length as shown in Fig. 10, the stored elastic strain energy U of the total system is given by

$$U = 2 \times \frac{1}{2} f\delta \tag{4}$$

If ω is the width of the cross section at the fracture plane and γ is the surface work, $\frac{\partial S}{\partial \ell} = 2\gamma\omega$ (5)

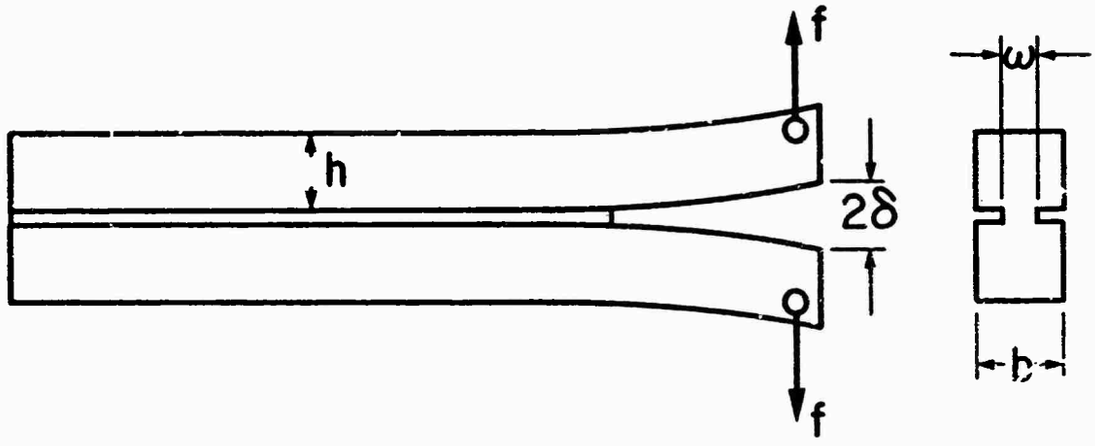

Figure 10. Uniform Double Cantilever Cleavage Specimen

In order to calculate the stored elastic energy, U, Berry and Broutman (3) used an empirical expression for the relationship between the applied force, f, and the deflection δ of the cantilever beams. This empirical relation was proposed to account for shear deflection effects and built-in end rigidity effects.

The empirical expression for the relationship between f and δ is given by

$$f = \frac{a\delta}{\ell^n} \tag{6}$$

where $a = \Phi(EI)$ and n is an experimentally measured constant. E is Young's modulus of elasticity for the material and I is the moment of inertia about the neutral axis of the beam cross-section. Then

$$U = 2.\tfrac{1}{2}f\delta = a\delta^2\ell^{-n} \tag{7}$$

and

$$\frac{\partial U}{\partial \ell} = -n\, a\, \delta^2\, \ell^{-(n+1)} = -\frac{nf\delta}{\ell} \tag{8}$$

Applying the Griffith criterion $\left(-\frac{\partial S}{\partial \ell} = \frac{\partial U}{\partial \ell}\right)$ yields

$$\frac{nf\delta}{\ell} = 2\gamma\omega \tag{9}$$

Therefore

$$\gamma = \frac{f\delta n}{2\ell\omega} \tag{10}$$

In equation (10), f, δ, ω. and ℓ are all measurable quantities as the crack propagates and lengthens and the constant n is obtained from the slope of the line if one plots the $\log_{10} f/\delta$ against $\log_{10}\ell$. This method is described completely by Berry (8) and Broutman (3).

This analysis has here been treated in a more analytical manner. Three contributions to the deflection of the cantilever beam are considered; namely, the bending, shear and end rotation deflections. The end rotation deflection is due to the condition of end support of the cantilever beams since the cantilever beam specimen does not have fixed rigid ends but is more closely approximated by an elastic support. The bending deflection δ_b is given by

$$\delta_b = \frac{f\ell^3}{3EI} \tag{11}$$

The shear deflection, δ_s, assuming the beam ends do not warp is calculated from (35):

$$\delta_s = \frac{1}{10}\ \frac{f\ell h^2}{GI} \tag{12}$$

where G is the shear modulus of the material and h is the height of the beam.

The end rotation deflection of cantilever beams with built-in elastic supports has been studied both analytically and experimentally by O'Donnell (36). He found that the following expression can accurately represent the deflection due to the end support effect:

$$\delta_r = \frac{16.67f\ell^2}{\pi Eh^2} + \frac{(1-\nu)f\ell}{Eh} \tag{13}$$

where ν is Poisson's ratio. Now the deflection measured in an experiment using the double cantilever cleavage specimen can be made equal to the sum of the bending, shear, and end rotation deflections as follows:

$$\delta_{exp} = \delta_b + \delta_s + \delta_r \tag{14}$$

$$\delta_{exp} = \frac{f\ell^3}{3EI} + \frac{1}{10}\frac{f\ell h^2}{GI} + \frac{16.67f\ell^2}{\pi h^2 E} + \frac{(1-\nu)f\ell}{Eh} \qquad (15)$$

and the percent of shear and end rotation deflections for a cantilever beam on an elastic support is shown in Figs. 11 and 12 for two different beam thicknesses and various beam heights. The use of these expressions in the analysis of data will be discussed in a later section.

3. Tapered Double Cantilever Cleavage Specimen

In determination of fracture surface work from a uniform double cantilever cleavage specimen, one has to measure force, deflection, and crack width at each crack length. In some instances it is difficult to measure crack length; for example, when the material is not transparent, or is in liquid environments. A tapered cleavage specimen or constant compliance specimen has the advantage that the load required for crack propagation is independent of the crack length. The use of this type of specimen has been reported by Mostovoy, Crosley, and Ripling (37), and stress intensity factors have been calculated by Srawley and Gross (38). The crack extension force or critical strain energy release rate, G_c, which is twice the value of fracture surface work and frequently referred to in fracture toughness investigations, is defined as

$$G_c = 2\gamma = \frac{f_c^2}{2\omega}\frac{\partial c}{\partial \ell} \qquad (16)$$

where γ = fracture surface work

f_c = applied load at fracture

ω = crack width

ℓ = crack length

c = specimen compliance at crack length ℓ.

The derivation of this equation is shown in Appendix I.

If the specimen is designed so that the compliance changes linearly with crack length ($\frac{\partial c}{\partial \ell}$ is constant), then G_c or γ is only dependent upon the failure load f_c providing that the crack width remains constant.

Since the cleavage specimen is treated as a pair of identical cantilever beams, design of a tapered cleavage specimen is determined through the terms representing bending, shear and end rotation deflections. The compliance of the

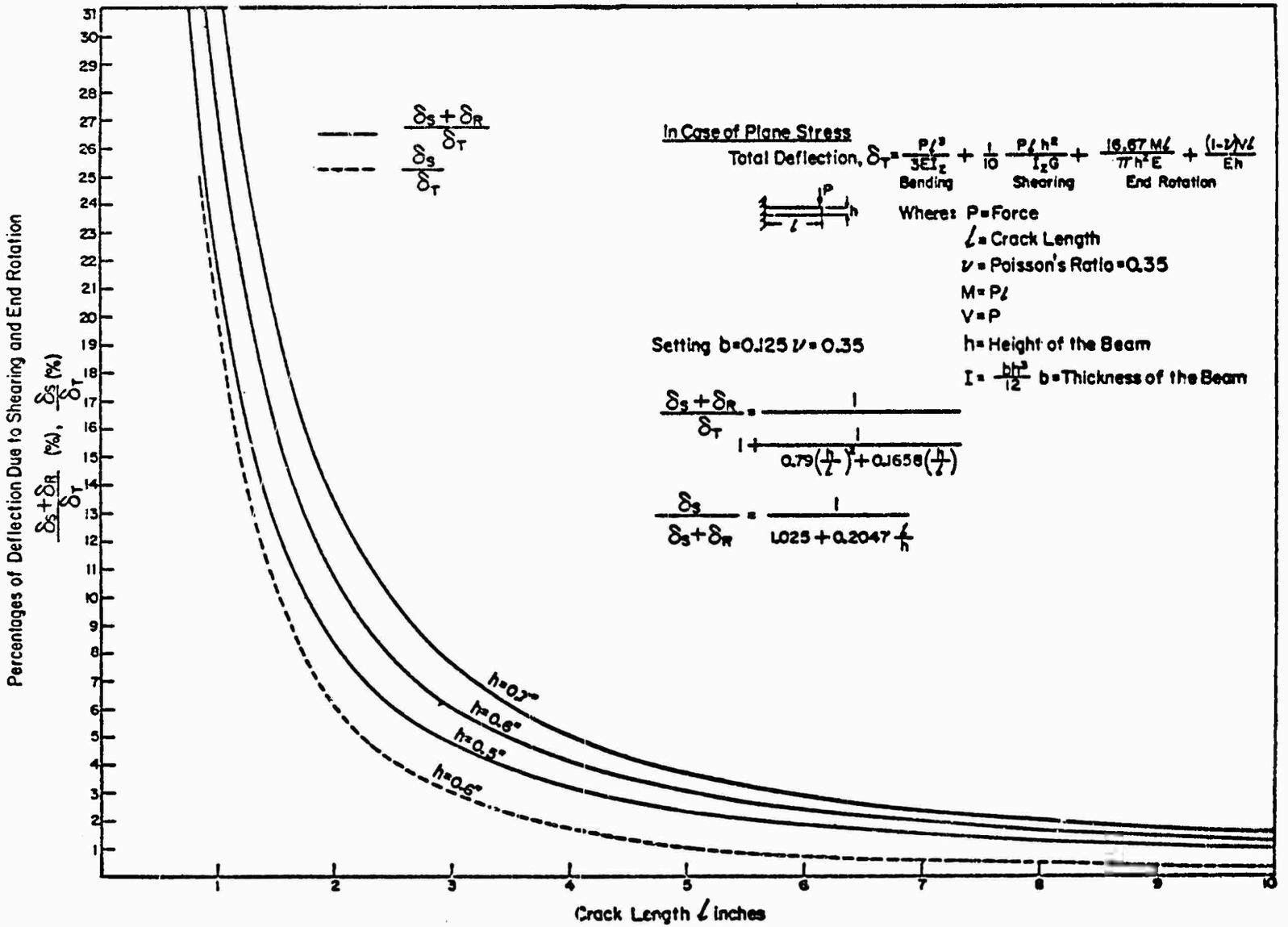

Figure 11 Shear and End Rotation Deflections for a Cantilever Beam

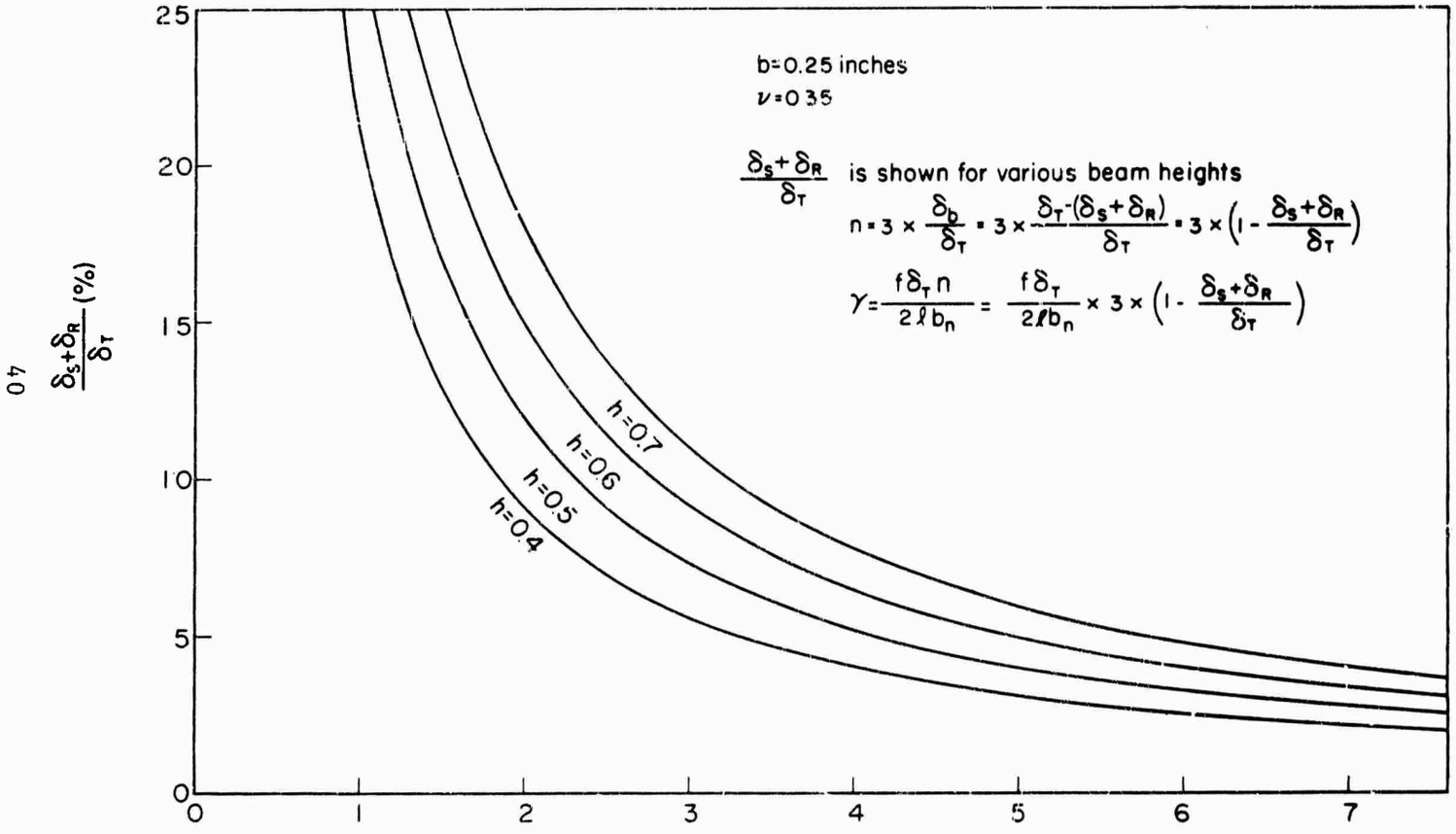

Figure 12. Shear and End Rotation Deflections for a Cantilever Beam

specimen, c, can be expressed as $c = \frac{2\delta}{f}$ where 2δ = total separation of cantilever beams at the point of loading and f= force applied to the specimen ends Therefore

$$c = \frac{24}{Eb}\int_0^{\ell} \frac{x^2}{h^3}\,dx + \frac{6(1+\nu)}{Eb}\int_0^{\ell} \frac{1}{h}\,dx \qquad (17)$$

where E = Young's modulus

ν = Poisson's ratio

b = specimen width

x = distance along the crack plane measured from the loading point

h = beam height at the distance x.

The first term on the right hand side of the equation represents the bending components while the second term is the shear component. Now

$$\frac{\partial c}{\partial \ell} = \frac{6}{Eb}\left[\frac{4\ell^2}{h^3} + \frac{1+\nu}{h}\right] \qquad (18)$$

and setting $\frac{\partial c}{\partial \ell}$ = constant k

$$\frac{6}{Eb}\left[\frac{4\ell^2}{h^3} + \frac{1+\nu}{h}\right] = k \qquad (19)$$

$$\frac{4\ell^2}{h^3} + \frac{1+\nu}{h} = \frac{Eb}{6} = M \qquad (20)$$

therefore

$$Mh^3 - (1+\nu)h^2 - 4\ell^2 = 0 \qquad (21)$$

The specimen used by Mostovoy et al was designed using Eq. (21) by selecting a value of M and then determining h as a function of beam length ℓ.

Therefore

$$G_c = 2\gamma = \frac{f_c^2}{2\omega} k = \frac{f_c^2}{2\omega} \frac{6}{Eb} M \qquad (22)$$

The specimen designed in this study not only included the compliance components of bending and shear but also the end rotation effect. The end rotation results from elastic distortions in the support allowing the cantilever to rotate at the assumed built-in end of the beams. Mostovoy et al have shown empirically that the end rotation effects can be included in the compliance equation by using an effective crack length $\ell+\ell_o$ where $\ell_o=0.6h$ in the bending term of compliance. The compliance is therefore modified so that

$$c = \frac{6}{Eb} \left[\frac{4(\ell+\ell_o)^3}{3h^3} + \frac{(1+\nu)}{h} \ell\right]$$

This factor was determined experimentally by the use of calibration bars. Eq. (21) can then be modified so

$$Mh^3 - (1+\nu)h^2 - 4(\ell+0.6h)^2 = 0 \qquad (23)$$

or

$$\ell = \left[\sqrt{Mh - (1+\nu)} - 1.2\right] \frac{h}{2} \qquad (24)$$

From Eq. (24), for any given value of the constant M a relation between h and ℓ can be established. The specimens used in this experiment have been designed for an M of $\frac{400}{3}$ assuming $\nu=0.35$.

Fig. 13 shows the plots of Eq. (24) or therefore the specimen shapes for M equal to 100 and $\frac{400}{3}$. In addition to using the empirical approach above, one could use an analytical expression for end rotation effects. The compliance of the cantilever specimen can then be expressed as

$$c = \frac{24}{Eb}\int_0^{\ell} \frac{x^2}{h^3}\,dx + \frac{6(1+\nu)}{Eb}\int_0^{\ell} \frac{1}{h}\,dx + 2\left(\frac{16.67\ell^2}{\pi Eh^2} + \frac{(1-\nu)\ell}{Eh}\right) \tag{25}$$

where the last two terms represent the deflection due to the elastic support. Then

$$\frac{\partial c}{\partial \ell} = \frac{24}{Eb}\frac{\ell^2}{h^3} + \frac{6(1+\nu)}{Eb}\frac{1}{h} + \frac{4x16.67\ell}{\pi Eh^2} + \frac{2(1-\nu)}{Eh}$$

$$= \frac{6}{Eb}\left[\frac{4\ell^2}{h^3} + \frac{(1+\nu)}{h} + \frac{33.34b\ell}{3\pi h^2} + \frac{(1-\nu)b}{3h}\right] = \frac{6M}{Eb} \tag{26}$$

where

$$M = \frac{4\ell^2}{h^3} + \frac{1+\nu}{h} + \frac{33.34b\ell}{3\pi h^2} + \frac{(1-\nu)b}{3h} \tag{27}$$

If $M = \frac{400}{3}$, then

$$\ell^2 + \frac{33.34b}{12\pi}h\ell + \left[\frac{(1-\nu)b}{12} + \frac{1+\nu}{4}\right]h^2 - \frac{100h^2}{3} = 0 \tag{28}$$

thus

$$\ell = \left[-\frac{16.67b}{12\pi} + \sqrt{\left(\frac{16.67b}{12\pi}\right)^2 + \frac{100h}{3} - \frac{(1-\nu)b}{12} - \frac{1+\nu}{4}}\right]h \tag{29}$$

Assuming that b=0.25" and ν=0.35, one obtains an equation:

$$\ell = \{-0.1105 + \sqrt{33.33h - 0.3388}\}h \tag{30}$$

This curve has been plotted and compared to the curves for Eq. (24) in Fig. 13. The specimen contour is similar to that predicted by the empirical approach.

CHAPTER V

TESTING PROCEDURE

All of the cleavage testing was carried out in an Instron testing machine and in a loading machine described in a previous section. In the IIT machine a specimen is held in grips with two pins as shown in Fig. 7. In the Instron the specimen is placed in a horizontal position. A constant cross head rate (0.2 in/min) was used to cleave the specimens. The applied force and the deflection were recorded on x and y axes of a recorder. In the experiments at room temperature two types of crack propagation modes were observed. The first type of crack propagation can be considered as "continuous tearing." The crack moves continuously through the specimen as the ends of the specimen are separated. For the materials which show continuous crack propagation, calibration marks are engraved on the uniform cantilever specimen so that the crack length can be conveniently recorded on the load deflection curve during the test. The calibration marks are placed every 1/2" with an accuracy of $\pm$.001". This is not necessary if the tapered type of specimen is used.

The second type of crack propagation is considered as "discontinuous propagation" or stick slip propagation. The crack jumps from one crack length to a new length and the crack velocity is very high. The specimen is unloaded as the crack jumps. The length of the crack jump varies depending on the material being tested and it also varies from point to point in the same material. For the materials which show the discontinuous propagation, the new crack length was measured on the specimen before each succeeding crack jump.

For the experiments at liquid nitrogen temperature temperature, cracks were introduced by separation of the specimen ends at room temperature until desired crack lengths were obtained. The samples were then slowly pre-cooled to the liquid nitrogen temperature with nitrogen gas which was a mixture of liquid nitrogen and air. This pre-cooling of the specimens is necessary to avoid any thermal shock to the specimens. The samples were then immersed in the liquid nitrogen and remained in the dewar for at least two hours. One of the samples would then be placed in the loading grips and the force-deflection curve was measured while the other samples were kept in the dewar. The crack propagation at liquid nitrogen temperature is drastic and generally it is only possible to make one measurement per sample since the specimen does not arrest the crack growth.

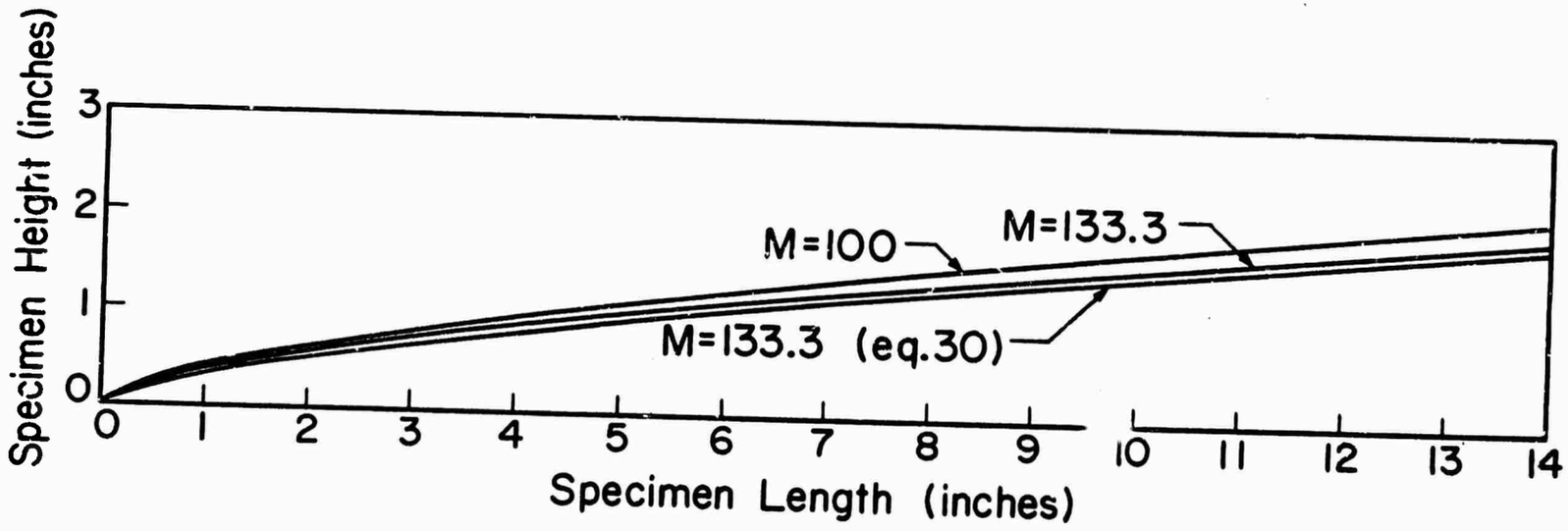

Figure 13. Specimen Contours for Constant Compliance Change Double Cantilever Cleavage Specimen

CHAPTER VI

ANALYSIS OF DATA

1. Uniform Double Cantilever Beam Specimen

The force, deflection, and crack width at each crack length must be obtained by experimental measurements in order to determine the surface work, γ. One method of calculation has been shown by Eq. (10) and requires the determination of the constant n. The ability to properly analyze the data depends on an accurate relationship for the compliance of the cantilever cleavage specimen or for predicting the deflection for a given force and crack or beam length. Two analyses have been compared for this purpose. An analytical expression for the cantilever beam deflection (Eq. 15) and the compliance expression obtained from the use of calibration bars (Eq. 22) have been used to predict the deflections of a Plexiglas uniform double cantilever beam specimen. Eq. 15 can be simplified to

$$\delta = \frac{f\ell}{Ebh^3} \left[4\ell^2 + 5.306bh\ell + (.65b + 3.24)h^2\right] \tag{31}$$

if $\nu = 0.35$.

The compliance expression suggested by Mostovoy and discussed in a previous section can be expressed as

$$\delta = \frac{1}{3EI} \left[(\ell+\ell_o)^3 + h^2\ell\right] \tag{32}$$

where $\ell_o = 0.6h$

This expression can be written as

$$\delta = \frac{4f}{Ebh^3} \left(\ell^3 + 1.8h\ell^2 + 2.08h^2\ell + 0.216h^3\right) \tag{33}$$

A Flexiglas cleavage specimen having b=0.240 inches and h=0.6 inches was fractured and the force and deflection recorded for several crack lengths. The modulus of elasticity was measured in flexure for a Plexiglas bar and a value of 4.6×10^5 psi was determined. A comparison of the predicted deflections is shown in table 6. It can be observed that the empirical equation (Fq. 33) predicts the deflections more closely than the analytically derived equation (Eq. 31). This latter equation underestimates the deflection, and we believe this is due to an underestimate of the end rotation deflection. O'Donnell's (36) theoretical prediction for end rotation deflection is based on a cantilever beam fixed at an elastic support. However, the cleavage specimen is really two cantilever beams bending from the same elastic support and the interaction must produce greater deflections than those originally predicted by O'Donnell.

The data from the uniform cleavage specimens has thus been analyzed using the compliance Eq. 33. The derivation of the fracture surface work is presented in Appendix II and can be expressed as follows:

$$\gamma = \frac{3f\delta_{exp}}{2\omega\ell} \left[\frac{\ell^3 + 1.2h\ell^2 + 0.693h^2\ell}{\ell^3 + 1.8h\ell^2 + 2.08h^2\ell + 0.216h^3}\right] \tag{34}$$

or $$\gamma = \frac{3f\delta_{exp}}{2\omega\ell} K \tag{35}$$

where $$K = \left[\frac{\ell^3 + 1.2h\ell^2 + 0.693h^2\ell}{\ell^3 + 1.8h\ell^2 + 2.08h^2\ell + 0.216h^3}\right]$$

and δ_{exp} = deflection of one beam

The quantity K has been plotted for three different beam heights and for crack lengths from 1 to 11 inches in Fig. 14. Thus, for data analysis one can use Eq. 35 knowing the measured force, f, the crack length, ℓ, the deflection, δ_{exp}, crack width, ω, and the correction factor, K.

The two methods of data analysis, using Eqs. 6 and 9, and using Eq. 35 are compared for a PMMA cleavage specimen in Appendix III. It can be seen that a small difference in the value of fracture surface work is calculated using these two different analysis methods. For example, the calculated surface work using Eq. 9 is 2.05×10^5 erg/cm^2 and is 2.38×10^5 erg/cm^2 using the method developed in this study.

TABLE 6

Comparison of Predicted and Measured Deflections for a Plexiglas Uniform Cantilever Cleavage Specimen

Load (f) lbs.	Crack Length (ℓ) inches	Measured* Deflection (inches)	Predicted Deflection (inches)	
			Eq. 31	Eq. 33
10.8	2.0	0.026	0.017	0.025
9.6	2.5	0.039	0.028	0.039
8.1	3.0	0.054	0.040	0.053
7.2	3.5	0.073	0.056	0.071
6.15	4.0	0.089	0.070	0.087
5.70	4.5	0.113	0.092	0.111
4.70	5.0	0.126	0.104	0.123
4.20	5.5	0.148	.123	0.143
3.95	6.0	0.177	0.149	0.172
3.75	6.5	0.208	0.179	0.205
4.00	7.0	0.269	0.238	0.269

*This is individual beam deflection or one-half of specimen deflection.

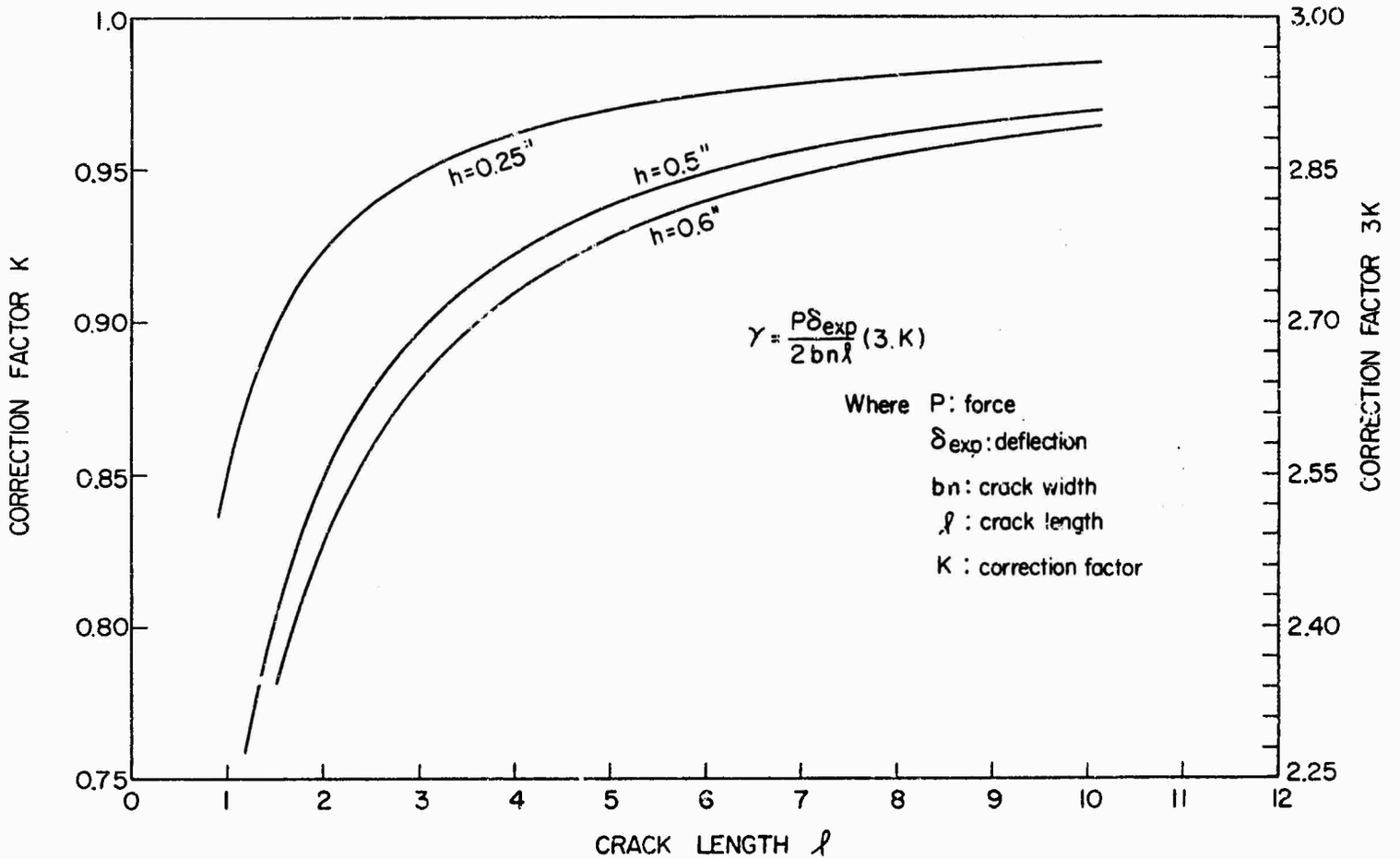

Figure 14. Correction Factor to Predict Fracture Surface Work of Uniform Cleavage Specimen

2. Tapered Double Cantilever Beam Specimen

The calculation of G_c or γ is accomplished by using the equation given in a previous section

$$G_c = 2\gamma = \frac{f_c^2}{2\omega} \frac{\partial c}{\partial \ell} = \frac{f_c^2}{2\omega} \frac{6M}{Eb} \tag{22}$$

where M is constant and taken as $\frac{400}{3}$ for the specimen contour used in this study. The critical load f_c, crack width ω and plate thickness b are obtained during the experiment; therefore, if one knows the value of the Young's modulus E of the material one can calculate G_c or γ. The value of Young's modulus E, however, is a function of loading rate and temperature and the proper value must be used. Also, $\frac{\partial c}{\partial \ell}$ can be determined experimentally from the load-deflection curves since the compliance $\frac{\delta}{f}$ at several crack lengths can be determined. By determining $\frac{\partial c}{\partial \ell}$ experimentally, one can calculate G_c or γ without measurement of Young's modulus under the test conditions.

The calculation of G_c or γ in this study was made using the experimental value of $\frac{\partial c}{\partial \ell}$.

In order to demonstrate the method of calculation of fracture surface work, the data for a cast sheet of polymethyl methacrylate (Plexiglas) will be reviewed. The test specimen is from a 1/4 inch thick plate and was designed such that M=133.3 and the contour of the specimen is therefore shown in Figure 13. The load versus deflection curve for the specimen is shown in Figure 15 and the measurement was made on an Instron testing machine using a separation rate of 0.2 inch per minute. Since the crack propagates in a continuous fashion, a continuous plot results with a nearly constant crack propagation load of 9.45 pounds, local variations of load being due to changes in crack width or area. Points are also shown on this plot representing various crack lengths determined visually from calibration lines on the sample. It can be observed that the crack propagated at nearly constant velocity. The calculation of G_c or γ is accomplished by using Eq. 22. Now, $\frac{\partial c}{\partial \ell}$ can be determined experimentally since from Fig. 15 the compliance (δ/f) at several crack lengths can be determined. This is shown plotted in Fig. 16 and $dc/d\ell$ for a 1/4 inch thick PMMA specimen is $5.98 \times 10^{-3} \frac{\text{inches}}{\text{in.-lb}}$. Although the specimen design was based on M=133.3, the experimental value of M can be determined from

$$M = \left(\frac{dc}{d\ell}\right)_{exp} \frac{Eb}{6}$$

where $E \simeq 4.75 \times 10^5$ psi as determined from a single point flexural test at .2 inch/minute. This gives a value of M=115 which is not identical to the

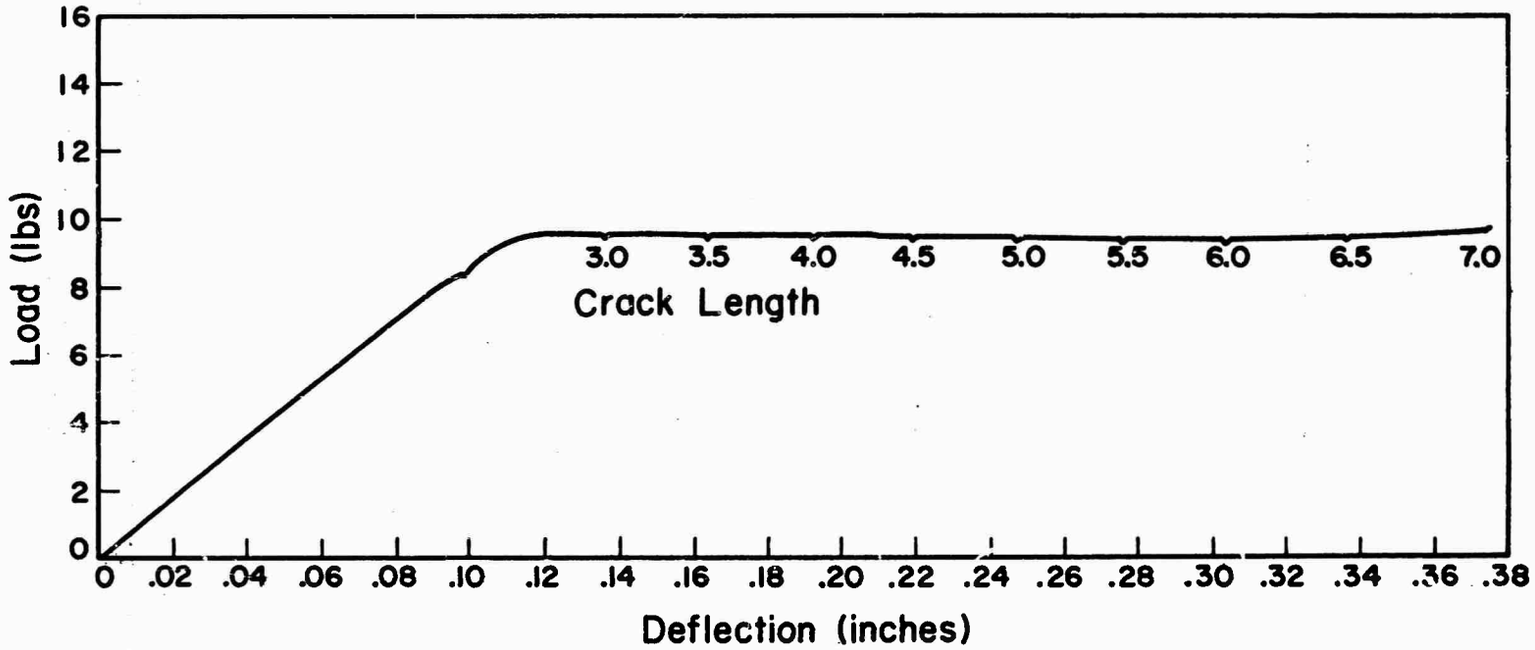

Figure 15. Load-Deflection Curve for 1/4 inch PMMA Tapered Cleavage Bar

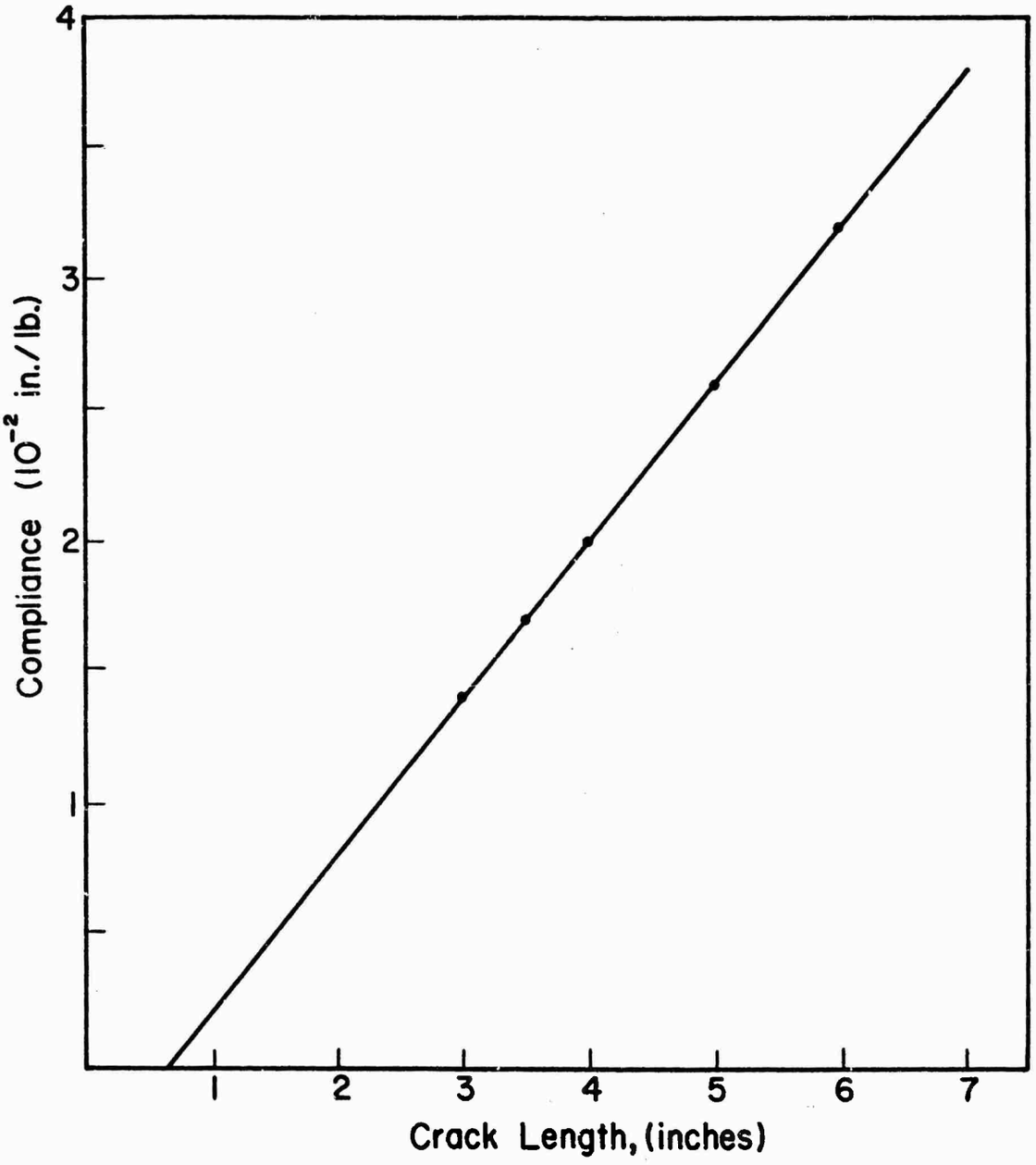

Figure 16. Compliance Change for 1/4 inch PMMA Tapered Cleavage Bar

theoretical value of 133.3. The difference is probably a result of simplifications in the analysis, experimental errors and time dependent effects in the material.

The calculation of G_c or γ can be made using the experimental value of $\frac{dc}{d\ell}$ which should be determined for each type of material since it depends upon the modulus of elasticity. If this is inconvenient, one can use the value of M=115 and the correct modulus of elasticity for the material. The data evaluated thus far has been based on an experimental determination of $\frac{dc}{d\ell}$. For the data shown in Fig. 15, f_c = 9.45 lb. and ω = .105 inches so that $\gamma = 2.22 \times 10^5$ erg/cm^2.

The critical strain energy release rate, G_c, or fracture surface work γ can be calculated directly from the force-deflection curve of Fig. 15. This is accomplished by measuring the energy released as the crack changes length or

$$U = \frac{f(\delta_2 - \delta_1)}{2} \tag{36}$$

and equating this to the work done

$$W = 2 (\ell_2 - \ell_1)\omega\gamma$$

as the crack increases in length from ℓ_1 to ℓ_2. Thus

$$\gamma = \frac{f(\delta_2 - \delta_1)}{4\omega(\ell_2 - \ell_1)} \tag{37}$$

and choosing a crack length increase (Fig. 15) from 3.5 inches to 4 inches the energy release is

$$U = \frac{9.5}{2} \quad (.192 - .164) = 0.133 \text{ lb.-in.}$$

The work done is

$$W = 2 \times 0.5 \times 0.105 \times \gamma$$

so that

$$\gamma = 1.26 \text{ in.-lb.} \quad \text{or} \quad 2.24 \times 10^5 \text{ erg/cm}^2$$

The value of γ calculated from the energy release agrees very well with the value obtained by the other calculation method.

3. Comparison of Instron and IIT Designed Machine for Measuring Fracture Surface Work

One PMMA tapered cleavage specimen was used to determine whether the Instron testing machine and the IIT designed machine would yield the same results for fracture surface work. The specimen was first placed in the Instron and the crack propagated to a length of 6.25 inches. The average fracture surface work was measured to be 2.77×10^5 erg/cm^2. The specimen was removed from the Instron, placed in the IIT machine and the crack propagation completed. The measured value was 2.76×10^5 erg/cm^2.

4. Effect of Cleavage Specimen Groove on Fracture Surface Work

As previously discussed, a cleavage crack propagating in an isotropic material will not do so in a straight continuous line normal to the loading direction because of the nature of the stress field at the crack tip. A groove is typically utilized to keep the crack confined to a given plane. In order to determine the influence of this groove on the measured value of fracture surface work, an anisotropic polymer was prepared to obviate the need for the groove. Thus, a grooved sample could be compared to a sample without the groove.

To provide the anisotropy, a polystyrene sheet or strip was hot-stretched in an Instron testing machine using a heated environmental chamber. Strips which had been hot stretched 100% were utilized for this purpose. A crack propagating parallel to the orientation or in the weak direction should be able to maintain itself in its original plane. It was found that even with 100% hot stretch the crack wandered from the initial plane and the crack could only be maintained for approximately 1/4 inch. However, this was enough to obtain data on fracture surface work at two crack lengths. Uniform cantilever cleavage specimens were machined and cracks were initiated. The depth of the groove on the grooved sample was similar to all other specimens (depth=b/4). The data is shown in table 7 and was analyzed using Eq. 34 and Fig. 14. It can be seen that the results are almost identical for the grooved and ungrooved specimen. It might be expected that the ungrooved specimen would produce a greater value of fracture surface work since the groove confines the crack and produces a flatter fracture surface without the shear lips at the specimen edges. Mostovoy and Ripling (37) determined

for a rolled aluminum alloy that the groove in the cleavage specimen reduced the value of fracture toughness to the plane strain fracture toughness value. The fracture surfaces for the grooved and ungrooved specimens are shown in Fig. 17 and they appear identical.

5. Crack Propagation Mode Related to Cleavage Specimen Force-Deflection Curves

The mode of crack propagation, whether continuous or stick-slip, influences the nature of the force-deflection curve recorded during the loading of the cleavage specimen. It is important to be able to interpret the measured force-deflection curve and to relate the appearance of the fracture surface to specific points on the force-deflection curve. Several examples have been included in Appendix IV to show this relationship and also to show certain irregular behavior displayed by some polymers.

TABLE 7

Data for Grooved and Ungrooved Hot Stretched Polystyrene Cleavage Specimens

Ungrooved Specimen

f (lbs)	δ (inches)	ℓ (inches)	ω (inches)	γ (erg/cm^2)
12.39	.0258	2.015	0.275	1.255×10^5
12.13	.0285	2.125	0.275	1.300×10^5
			Ave.	1.278×10^5

Grooved Specimen

f (lbs)	δ (inches)	ℓ (inches)	ω (inches)	γ (erg/cm^2)
7.93	.0187	2.090	.1321	1.179×10^5
8.15	.0200	2.146	.1324	1.265
7.82	.0209	2.200	.1332	1.236
7.33	.0204	2.245	.1333	1.111
7.17	.0208	2.280	.1339	1.086
7.56	.0227	2.316	.1340	1.233
7.12	.0222	2.370	.1338	1.117
7.85	.0249	2.430	.1338	1.351
7.33	.0243	2.470	.1350	1.205
7.26	.0255	2.500	.1376	1.214
			Ave.	1.200×10^5

a) With Notch (Mag. 35x)

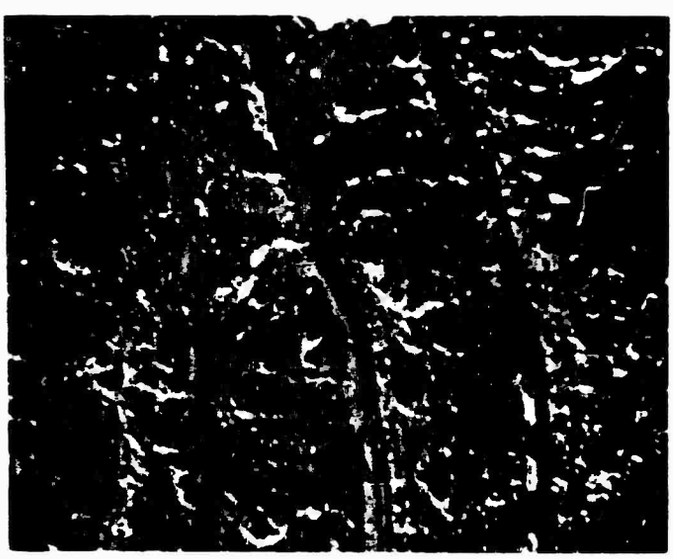

b) Without Notch (Mag. 35x)

Figure 17 Fracture Surfaces for 100% Hot Stretched Polystyrene Cleavage Specimens. Crack propagated from left to right.

CHAPTER VII

INFLUENCE OF MOLECULAR WEIGHT AND CROSSLINKING ON FRACTURE SURFACE WORK OF POLYSTYRENE

1. Background

The purpose of this study was to determine the influence of crosslinking on crack propagation energy or fracture surface work. As indicated in the introduction of this report there is a conflict in the results obtained from the chemically linked linear polymers such as PMMA and the network polymers such as the epoxies and unsaturated polyesters. If the large measured value of fracture surface work in linear polymers is a result of molecular orientation or crazing at the crack front then crosslinking should restrict this flow and reduce the value of surface work.

The method and material chosen to study the effect of crosslinking was through the gamma irradiation of polystyrene. Although polystyrene can be chemically crosslinked by adding various concentrations of divinyl benzene [$H_2C{=}CH{-}\langle\bigcirc\rangle{-}CH = CH_2$] it was thought that this might make interpretation more difficult because of the addition of a second chemical structure which by itself might change the fracture surface work. In order to study the influence of crosslinking on polystyrene, the uncrosslinked material should be well characterized. The polystyrene utilized for the crosslinking studies was purchased both from the Borden Monomer-Polymer Laboratory and a commercial supply house. The Borden material was reported to have a weight average molecular weight of 230,000. The polymer was supplied in pellet form and sheets were compression molded as described in table 5. The commercially available material was supplied in sheet form. Another polystyrene was purchased from Borden in order to consider the influence of molecular weight since it was reported to have an average molecular weight ($\bar{M}_w$) of 35,000.

The irradiation of the polystyrene samples was conducted at the IIT Research Institute using a Cobalt 60 source. Uniform double cantilever cleavage specimens were first completely machined and then exposed to the radiation. Two specimen sizes were utilized. The first batch of specimens subjected to 5, 10 and 25 megarads had b=.125 inches, h=0.5 inches, and ℓ=6 inches. A second batch exposed to 10, 25, 50 and 100 megarads had b=.125 inches, h=1.2 inches and ℓ=6 inches. The length of the specimens had to be limited because uniform radiation could only be achieved in the central 4 inches of the specimen. The necessity for increasing the height of the specimens will be discussed later. Two specimens were exposed to each radiation level. Wall and Brown (39) have shown that a dose of 6 to 8 megarads is sufficient to induce crosslinking in polystyrene and it was anticipated that the selected dosages would be sufficient to produce the desired effect.

2. Molecular Weight

In order to determine the effect of crosslinking on the fracture surface work of polystyrene, a proper value for the uncrosslinked material must first be established. Three materials were investigated as discussed previously. The molecular weight distributions of these materials were characterized by gel permeation chromatography. The molecular weight determinations are shown in table 8 for the polystyrenes studied. The quantities referred to in the table are the following:

$$\bar{M}_n = \frac{W}{\sum_{i=1}^{\infty} N_i} = \frac{\sum_{i=1}^{\infty} M_i N_i}{\sum_{i=1}^{\infty} N_i} \tag{38}$$

$$\bar{M}_w = \sum_{i=1}^{\infty} W_i M_i \tag{39}$$

where W = total weight of polymer

W_i = weight fraction of a given species, i

N_i = number of moles of each species, i

M_i = molecular weight of each species, i

Also, other important relations include

$$M_i = A_i Q$$

$$\bar{M}_n = \bar{A}_n Q$$

$$\bar{M}_w = \bar{A}_w Q$$

where A_i = average angstrom size of the segment

Q = molecular weight units per angstrom

$\bar{A}_n$ = number average molecular size

$\bar{A}_w$ = weight average molecular size

TABLE 3

Molecular Weight Determination by Gel Permeation Chromatography for Polystrenes

Sample	$\bar{A}_n$ angstroms	$\bar{A}_w$ angstroms	$\bar{M}_n$ *	$\bar{M}_w$ *	MWD **
Polystyrene A (Bordon Monomer-Polymer Lab)	1167.5	5594.3	48,217	231,045	4.79
Polystyrene C (Borden Monomer-Polymer Lab)	185.1	1288.4	7,644	53,211	6.96
Polystyrene B (commercial sheet)	511.5	5960	21,125	246,148	11.6
Polystyrene A-25***	739.6	7066.3	30,545	291,838	9.55
Polystyrene B-10	1004.9	5623.9	41,502	232,267	5.60
Polystyrene B-50	790.4	8892.8	32,643	367,272	11.25

*Assuming Q=41.3 (molecular weight units per angstrom)

**MWD = $\frac{\bar{A}_w}{\bar{A}_n} = \frac{\bar{M}_w}{\bar{M}_n}$ = molecular weight distribution

*** 25 megarads

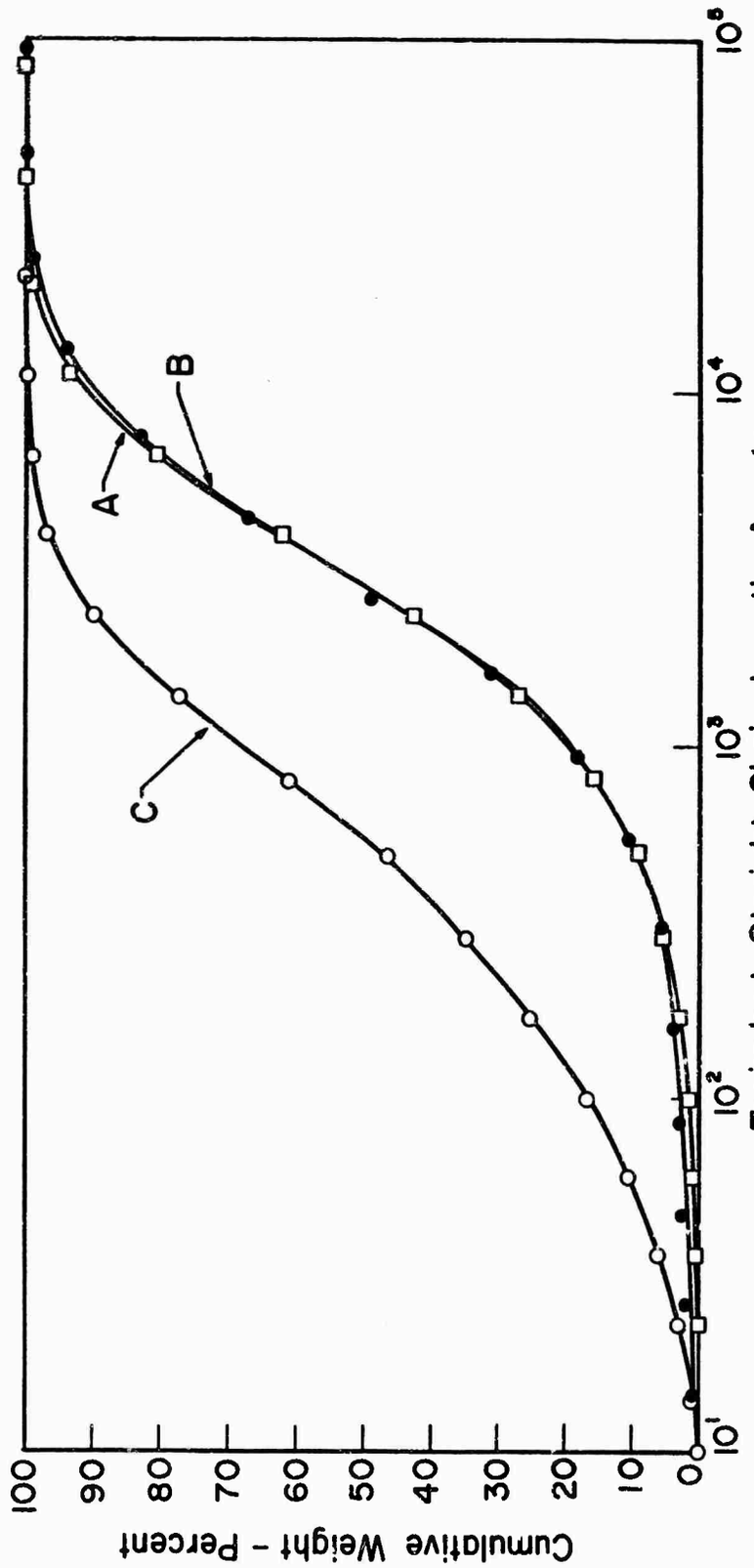

Figure 18. GPC Cummulative Distribution Curves for Various Molecular Weight Polystyrenes

The value of Q for polystyrene has been established by specific calibration techniques and is believed to be accurate so that molecular weights as well as molecular sizes are indicated in table 8. In addition, Fig. 18 is included to show the actual molecular chain length distributions of the polystyrenes studied.

The lowest molecular weight polystyrene, $\bar{M}_w$ = 53,211, was very brittle and therefore difficult to mold and machine without fracturing the plates. However, two tapered cleavage bars (b=.25 inches) having the contour shown in Fig. 13 and expressed by Eq. 24 were prepared and the fracture surface work was evaluated. The results are presented in table 9 and the average value of fracture surface work was 3.52×10^3 erg/cm^2. The crack propagated in a discontinuous manner (stick-slip) and the fracture surface was very smooth and colorless as shown in Fig. 19. The crack arrest position can be seen clearly and the crack propagation direction is also shown. The very small value of fracture surface work is attributable to the very short equivalent straight chain length of this polymer which has 70 wt. percent of the molecules less than 1000 angstroms in length. The fracture surface is colorless since these molecules cannot form a layer thick enough to produce optical interference effects.

The higher molecular weight polystyrenes used for the crosslinking study and obtained in sheet form from a local vendor and in pellet form from Borden Monomer-Polymer Laboratories were quite similar in molecular weight. The polystyrene B had a greater molecular weight distribution as indicated in table 8 and Fig. 18. This can be seen in Fig. 18 by the tail at the lower molecular weight end of the distribution curve.

Several measurements of the fracture surface work of these higher molecular weight polystyrenes have been made using the tapered cleavage bar and the results are indicated in table 9. It can be seen that differences exist between lots of material and even within the same specimen. In fact, in two of the specimens shown in the table the fracture surface appearance and value of fracture surface work differ considerably within the specimens. For this reason the results in table 9 have been divided according to the batch of material used in the experiments. For example, the materials designated by superscripts a and b were purchased at two different times. Because of the difference in behavior noted for these materials, molecular weight distributions were determined for two of the specimens indicated by the superscripts aa and bb in table 8. The molecular weight distributions are shown in Fig. 20 and the following was established.

	$\bar{A}_n$	$\bar{A}_w$	$\bar{M}_n$	$\bar{M}_w$	MWD	γ(erg/cm^2)
aa	443	6227	18,300	257,000	14.4	3.61×10^5
bb	562	6610	23,200	273,000	11.8	4.49×10^5, 2.84×10^5

TABLE 9

Fracture Surface Work of Various Molecular Weight Polystyrenes*

Material	Specimen Type	Crack Propagation Mode	Fracture Surface Work ergs/cm^2	Fracture Surface
$\bar{M}_w$ = 53,211**	Tapered Cleavage	Stick-slip	3.34×10^3	mirror smooth
	Tapered Cleavage	Stick-slip	3.70×10^3	no colors
$\bar{M}_w$ = 231,000**	Tapered Cleavage (b=1/8")	Stick-slip	4.20×10^5	very rough
	Tapered Cleavage (b=1/8")	Stick-slip	4.38×10^5	
$\bar{M}_w$ = 246,148***	Tapered Cleavage (b=1/4")[a]	Stick-slip	3.60×10^5	very rough
	Tapered Cleavage (b=1/4")[aa]	Stick-slip	3.61×10^5	very rough
	Tapered Cleavage (b=1/4")[a]	Stick-slip	3.92×10^5	very rough
	Tapered Cleavage (b=1/4")[a]	Stick-slip	4.62×10^5	very rough
	Tapered Cleavage (b=1/4")[b]	Stick-slip	5.15×10^5	very rough
		continuous	2.97×10^5	smooth, color is observed
	Tapered Cleavage (b=1/4")[bb]	Stick-slip	4.49×10^5	very rough
		continuous	2.84×10^5	smooth, color is observed
	Tapered Cleavage (b=1/4")[b]	Stick-slip	6.10×10^5	very rough

*Fracture Surface Work, $\gamma = \frac{f_c^2}{4w} \left(\frac{dc}{d\ell}\right)_{exp} \times 1.75 \times 10^5$ (erg/cm^2)

**Borden Monomer-Polymer Labs

***Commercial Source: a and b are materials purchased at different times

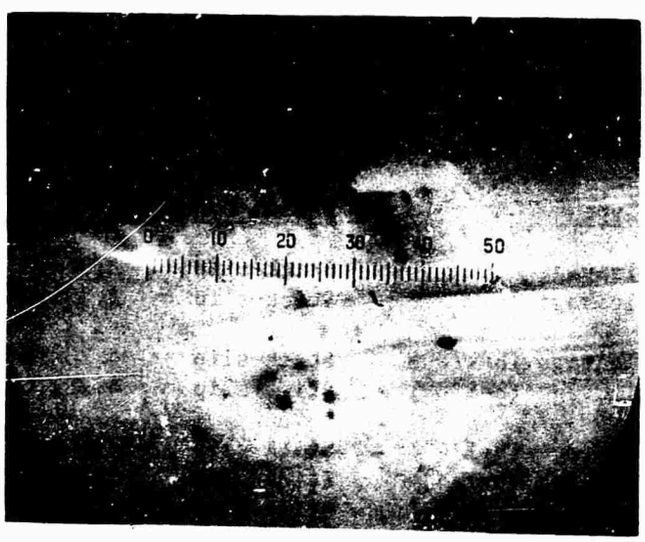

Figure 19 Cleavage Fracture Surface of Polystyrene ($\bar{M}_w$ = 53,211). Crack arrest position can be seen. Crack propagated from left to right. (Mag. 50x)

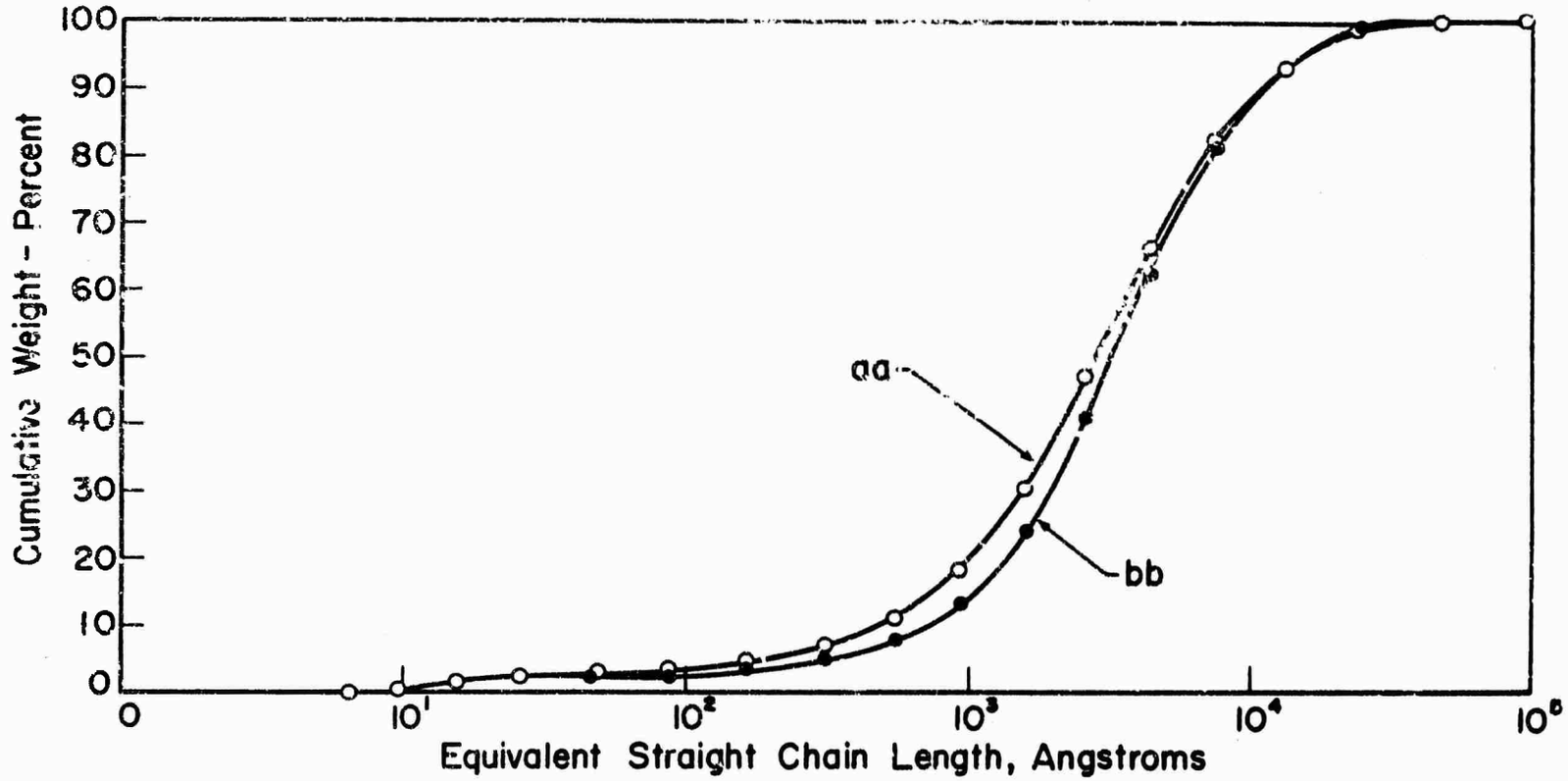

Figure 20. GPC Cummulative Distribution Curves for Polystyrene

It is possible that the higher molecular weight and narrower distribution of the b material could account for increased values of fracture surface work which were generally measured in the specimens. However, the low value encountered within certain regions of two of the specimens and the smooth, colored fracture surfaces produced can only be explained by local differences in the material composition or structure. The two types of fracture surfaces produced are shown in Fig. 21. The smooth colored surface shown in Fig. 21b has characteristic markings due to initiation of secondary fractures ahead of the main crack front. The broad molecular weight distributions are generally undesirable because of greater nonuniformity in the material and the possibility of reducing the fracture surface work.

3. Crosslinking Studies

The first crosslinking studies were conducted on the Borden polystyrene material which was compression molded in our laboratory from pellets. Test specimens were prepared from 1/8 inch thickness sheets and a uniform cleavage specimen having a total height of 0.5 inches (h=0.25") and a length of 6 inches was selected. The machined specimens were irradiated and tested shortly after having been irradiated. For comparison purposes, unirradiated specimens of the same dimensions were also prepared and tested. In order to judge the effectiveness of irradiation in crosslinking the polystyrene, intrinsic viscosities of these materials were determined using tetrahydrofuran (THF) for the solvent.* The results for the fracture surface work and intrinsic viscosity measurements are presented in table 10 and Fig. 22.

As can be seen by the results, considerable scatter exists although there appears to be a trend of decreasing crack propagation energy with increased exposure and an increase in intrinsic viscosity due to the existence of a gel structure in the solutions used for the viscosity measurements. The reduction in fracture surface work is particularly evident when comparing the 25 megarad specimen to the unirradiated specimens. Also, it should be noted that some of the unirradiated samples have much greater measured values of fracture surface work than the similar material previously reported on in table 9. The only obvious difference is in the specimen size. The fact that the specimens used here have a height of only 0.25" produced more crazing at the crack tip than in the previous specimens where h=0.6". This crazing can be observed during the experiment and is nearly perpendicular to the crack front. Care must be exercised in choosing the dimensions of a double cleavage specimen particularly in choosing the height of the beam. This is important since the maximum flexural stress in the beam will be dependent upon the beam height, h, as follows:

$$\sigma = \frac{6f\ell}{bh^2} \qquad (38)$$

---

* Measurements made by Arro Laboratories, Joliet, Illinois.

a) Surface Representation of Stick-Slip Crack Propagation and High Value of Surface Work (Mag. 50x)

b) Surface Representation of Continuous Crack Propagation (Mag. 600x)

Figure 21 Fracture Surfaces for Polystyrene Cleavage Specimen (Specimen bb in table 9)

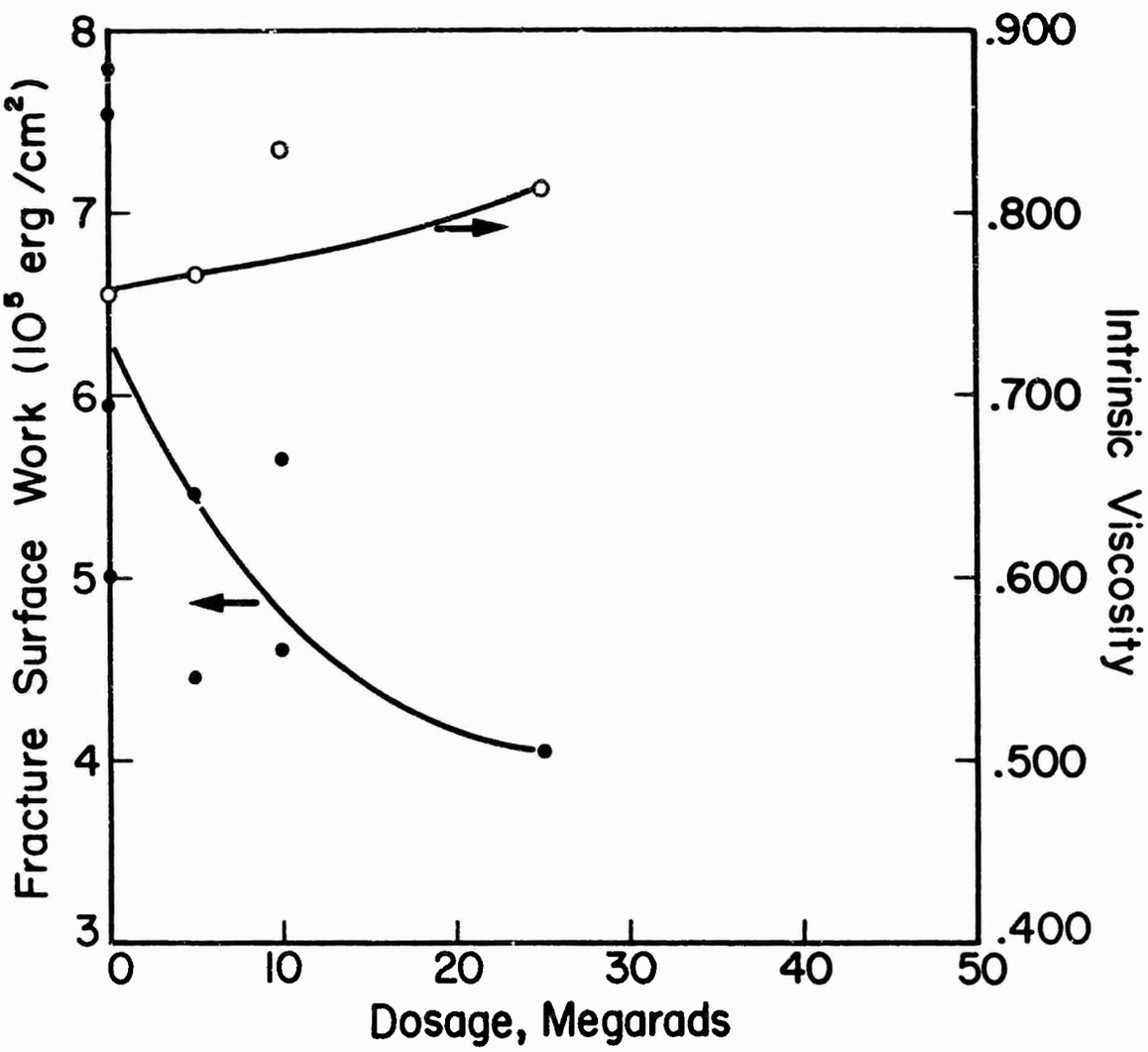

Figure 22. Intrinsic Viscosity and Fracture Surface Work Measurements for Irradiated Polystyrene

TABLE 10

Effect of γ Irradiation on Fracture Surface

Work of Polystyrenes*

Dosage (Megarads)	Intrinsic Viscosity	Molecular Wt. Data $\bar{A}_n$	$\bar{A}_w$	MWD	Average Fracture Surface Work (10^5 erg/cm^2)
0	0.755	1167.5	5594.3	4.79	6.27**
5	0.765				4.45 (6)*** 5.49 (4)
10	0.835				5.68 (5) 4.61 (8)
25	0.812	739.6	7066.3	9.55	4.04 (8)

*Cleavage Specimen Dimensions: b=1/8", h=.25", ℓ=6"

**Ave. of 4 specimens

***1 specimen. Numbers in parenthesis refer to number of data points per specimen.

If the flexural stress becomes too great then the stress-strain relation for the particular polymer may become non-linear which will invalidate the use of our simple elastic bending equations. Even more important, if the polymer tends to craze when subjected to a critical stress (as does polystyrene), a high flexural stress will cause crazing of the beam which will accompany the growth of the crack. However, if one can control the crazing by appropriate choice of beam height then one can also calculate the energy absorbed in the crazing process. Figure 23 indicates the limiting loads which can be applied to uniform double cantilever cleavage specimens for various geometry specimens assuming that maximum bending stresses are not to exceed 2500 psi. These curves can then be an aid in judging the suitability of the test specimen.

It has thus been determined that crazing can raise the fracture surface work of polystyrene and that crosslinking induced by irradiation can inhibit crazing or lower the fracture surface work.

A second series of samples were prepared from commercially available polystyrene sheet and were irradiated with the Cobalt 60 source to dosage levels of 10, 25, 50 and 100 megarads. The height of the specimens was increased to 1.2 inches in order to reduce the amount of crazing which can occur. The fracture surface work of these samples has been measured to establish the influence of crosslinking on crack propagation energy. In addition, intrinsic viscosity, $[\eta]$, measurements were performed on material removed from the center of each cleavage sample (tetrahydrofuran solvent used for viscosity measurements) and molecular weight determinations were made on some of the samples by gel permeation chromatography. The molecular weight distribution curves are shown in Fig. 24 for the commercial sheet exposed to 10 and 50 megarads and the IIT molded sheet exposed to 25 megarads. This data is also presented in tables 10 and 11.

As the radiation exposure increases the weight average molecular size or molecular weight increases and the distribution becomes more broad. The increase in high molecular weight material is due to the crosslinking process. The low molecular weight profiles are similar so that the low ends are not changed much.

It was reported by Arro Laboratories that the sample with 100 megarads of γ irradiation could not be analyzed due to clogging of the pores in the GPC columns which has been attributed to the gel structure formed from the polymer when trying to dissolve it in the THF solvent. An increase in intrinsic viscosity is also reported for the increasing radiation dosages particularly for 100 megarads and this value may also be attributed to gel particles in the solution.

The fracture surface work values are reported in table 11 and Fig. 25. At 50 megarads the fracture surface work has decreased by a factor of two. The total amount of crazing is reduced by using these larger specimens. Using maximum load and deflection values obtained at various crack lengths,

maximum flexural stresses of approximately 2500 psi can be calculated. The calculated flexural stresses for the smaller height cleavage specimens were approximately 5000 psi which would be near the crazing stress for these materials. These stresses also do not include the stresses produced by the crack tip and thus are only nominal values. Typical cleavage fracture surfaces are shown in Fig. 26 for the corsslinked polystyrenes. It can be observed that there is a mirror smooth region very evident for the 100 megarad and 50 megarad material which is the area in which the crack initiates. This very smooth region is a result of the restricted molecular motion caused by the crosslinking of the polymer molecular chains. It has thus been demonstrated that crosslinking will reduce the amount of crazing and therefore also reduces the fracture surface work of polystyrene.

TABLE 11

Effect of γ Irradiation on Fracture Surface Work of Commercially Available Polystyrene Sheets

Dosage (megarads)	Intrinsic Viscosity	Molecular Wt. Data $\bar{A}_n$	$\bar{A}_w$	MWD	Average Fracture Surface Work (10^5 erg/cm^2)
0	0.738	511.5	5960	11.6	4.30
10	0.700	1004.9	5623.9	5.60	4.00 (5)*
10					3.31 (6)
25	0.770				3.54 (5)
25					3.67 (8)
50	0.790	790.4	8892.8	11.25	1.87 (16)
50					2.25 (14)
100	0.965				2.37 (6)
100					2.52 (4)

*Numbers in parentheses refer to number of data pts. obtained per specimen.

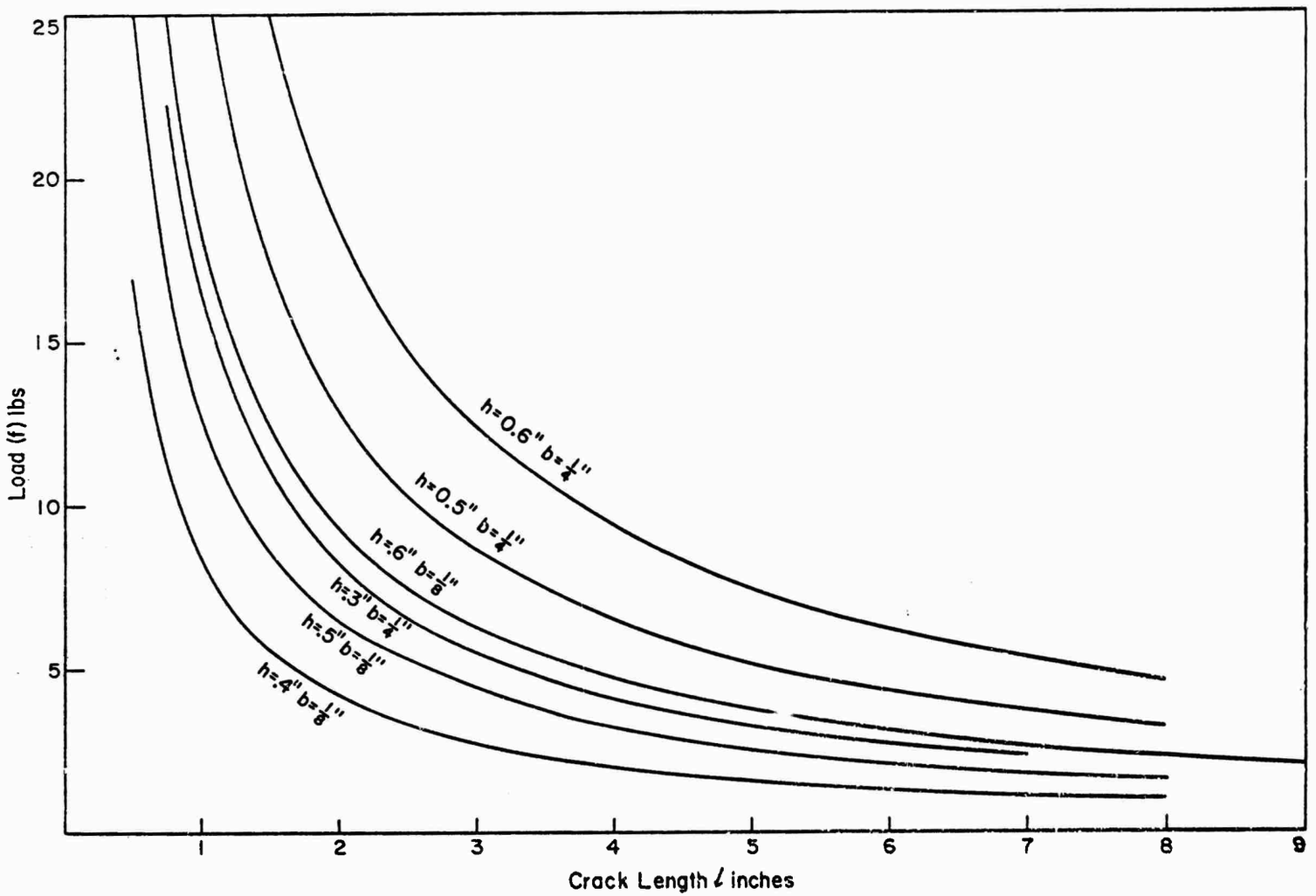

Figure 23. Design Curves for Uniform Cantilever Cleavage Specimens

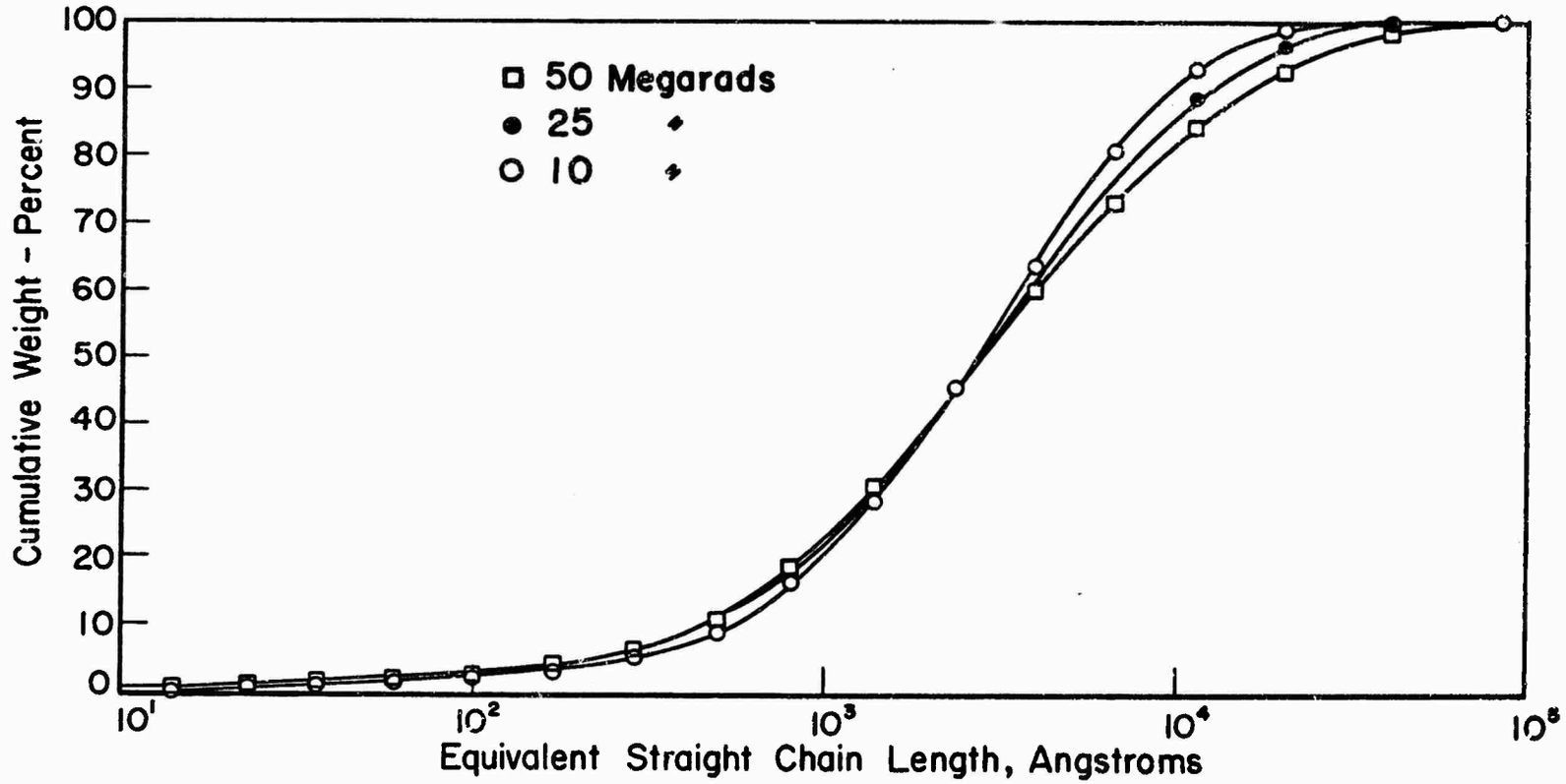

Figure 24. GPC Cummulative Distribution Curves for Irradiated Polystyrenes

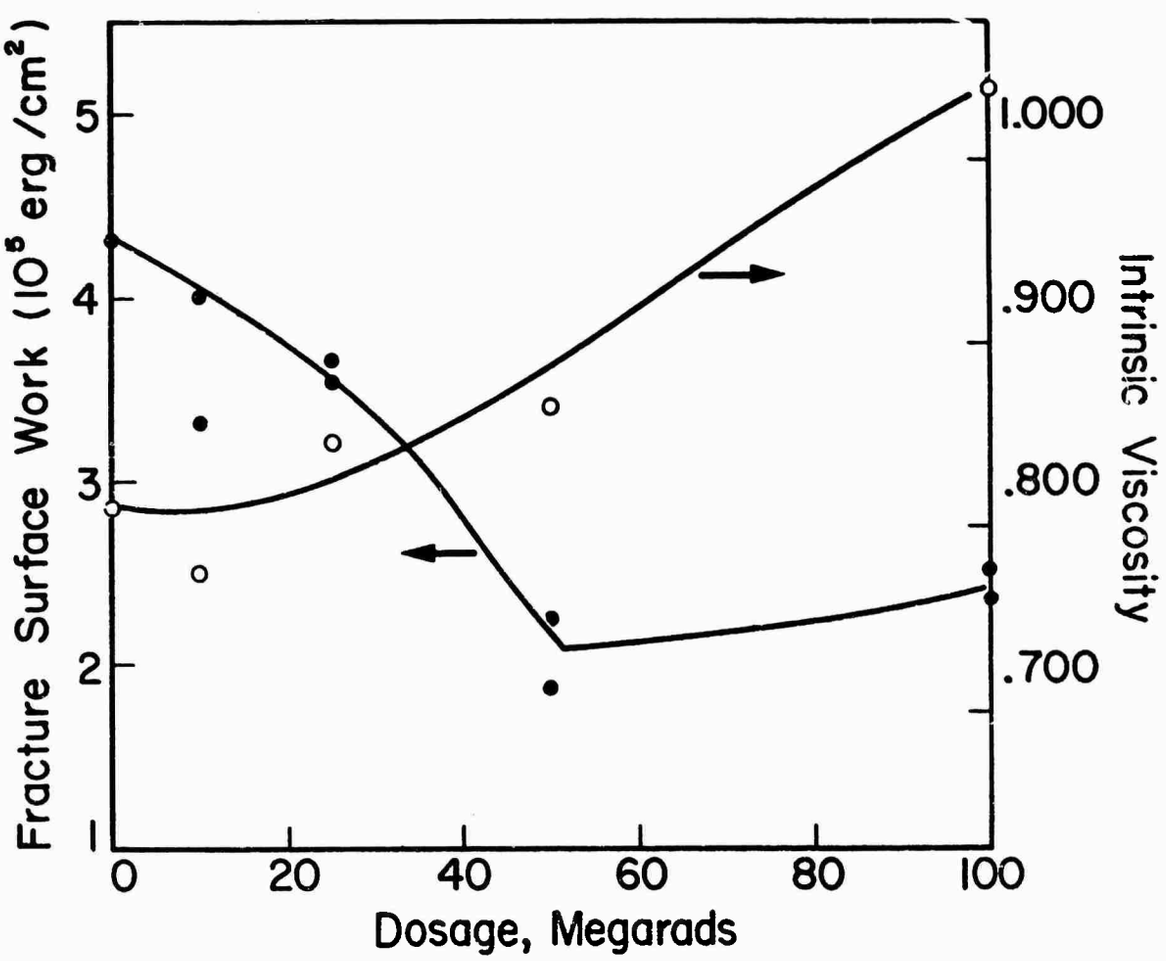

Figure 25. Intrinsic Viscosity and Fracture Surface Work Measurements for Irradiated Polystyrene (Commercially available Sheet)

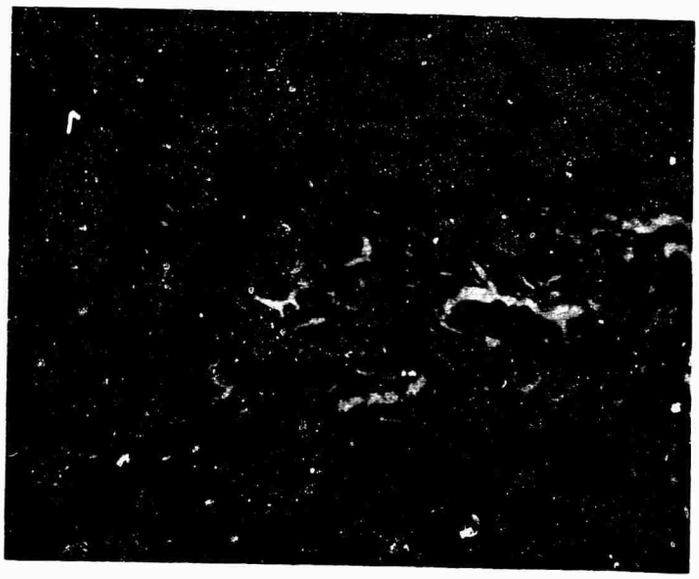

a) 100 Megarads (Mag. 50x)

b) 50 Megarads (Mag. 50x)

Figure 26 Cleavage Fracture Surfaces for Irradiated Polystyrene at Crack Initiation Regions. Crack propagated from left to right.

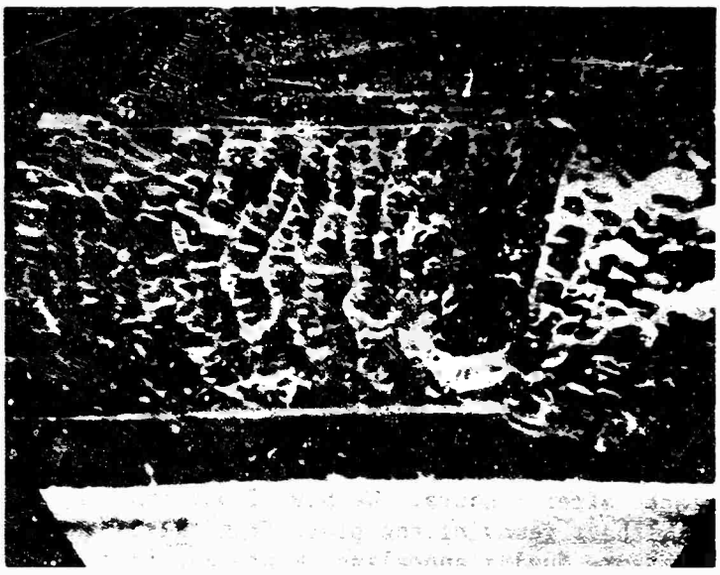

c) 25 Megarads (Mag. 50x)

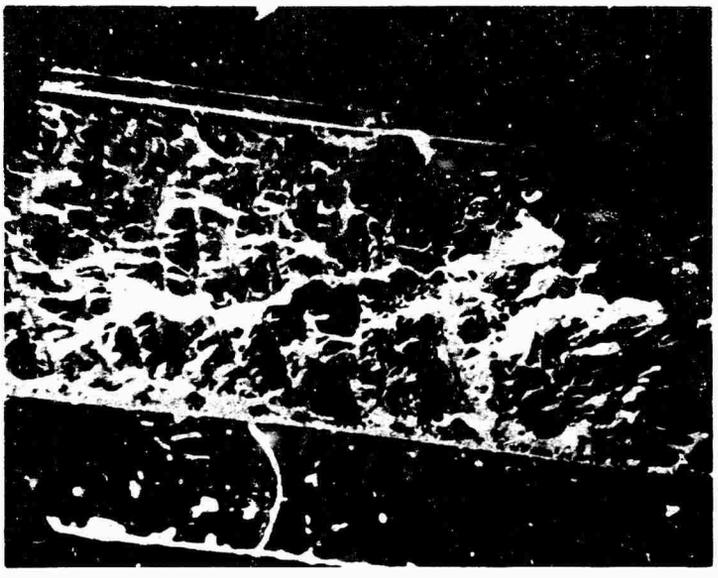

d) 10 Megarads (Mag. 50x)

Figure 26 (Continued)

Chapter VIII

INFLUENCE OF TACTICITY AND CRYSTALLINITY ON FRACTURE SURFACE WORK OF POLYSTYRENE

Quantities of isotactic polystyrene have been obtained from Monsanto Chemical Co. and the Dow Chemical Co. This material has been compression molded into 1/8" thick plates under conditions described in table 5. In order that we might study the effect of crystallinity on fracture, amorphous sheets were prepared (by quickly cooling from the molding temperature of 460°F) as well as several crystalline sheets. The crystalline sheets were prepared by annealing for various times at 180°C. For example, full cyrstallinity (40 percent by weight) can be developed after 4 hours. We have found that the annealing can best be accomplished without removing the plate from the compression mold and by maintaining the pressure during annealing to prevent formation of air bubbles. With this method we have produced plates with densities as great as 1.074 which corresponds to approximately 40 percent crystallinity. A comparison of the physical properties of a fully crystalline isotactic polystyrene with an atactic polystyrene material is presented in table 12. The molecular weight distribution of the isotactic polymer is shown in Fig. 27 compared to the previously discussed atactic polystyrene material. The following was determined for the isotactic polystyrene:

$\bar{A}_n$ = 4951A $\bar{M}_n$ = 202,991 MWD = 4.50

$\bar{A}_w$ = 22,275A $\bar{M}_w$ = 913,275

The molecular weights were determined using a Q value of 41.3 which is identical to that used for the atactic material. This may result in a small error in the results.

Studies were conducted to describe the micro structure of these crystalline isotactic polymers. In order to study the structure, polymer pellets were heated between glass slides on a hot plate and pressure applied in order to produce a thin film. This film was then annealed for various times at 180°C (temperature for maximum rate of crystallization) and 210°C. The microstructure has been studied in a transmission microscope using crossed polariods. The maltese cross patterns typical of spherulitic crystalline structures have been observed and hedrites can also be seen in the photomicrographs presented in Fig. 28. References to this hedrite type of morphological structure have been made by Geil.[40] The average diameters of the hedrites or spherulites ranged from 10 microns at 1 hour annealing (180°C) to 16 microns at 4 hours of annealing (180°C). After 1 hour of annealing at 210°C, spherulitic structures could not be detected, but after two hours crystalline structures having an average diameter of 10 microns were observed and after four hours the

TABLE 12

Comparison of Physical Properties of Isotactic Crystalline Polystyrene and Atactic Polystyrene (Dow Chemical Co.)

Property	Crystalline Polystyrene	Atactic Polystyrene
Tensile Strength, PSI		
23°C	6600	5500
55	6200	3800
85	5600	2800
Modulus-Tensile, PSI x 10^5		
23°C	5.3	4.9
55	6.3	5.3
85	3.5	2.9
Elongation-Percent		
23°C	1.2	1.4
55	1.0	1.1
85	1.0	1.6
Impact Strength-Izod ft. lbs/in. notch		
23°C	0.24	0.23
55	0.28	0.30
85	0.40	0.25
Melting Point, °C	235	-
Density at 25°C	1.07	1.05
Relative Crystallinity	25-40	0
Heat Distortion, °C		
Vicat	190	100
Tensile (100 PSI)	185	92
Abrasion Resistance		
Taber, wt. Loss 2000 Rev, g.	0.46	0.70
Dielectric Constant, 10^6 cps.	2.6	2.5
Dissipation Factor, 10^6 cps.	$2x10^{-4}$	$1x10^{-4}$
Appearance	Opaque-white	clear

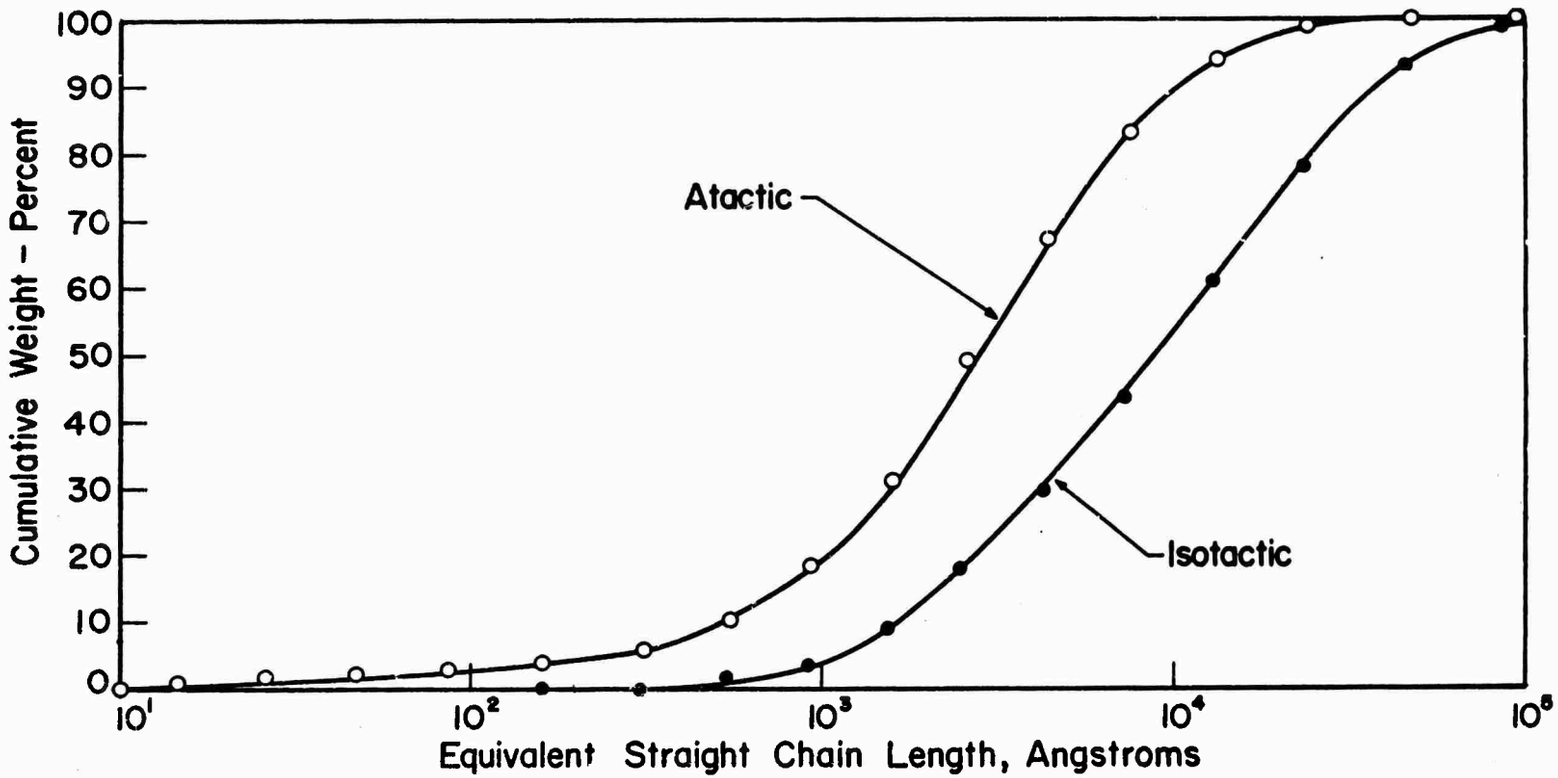

Figure 27. Comparison of Molecular Weight Distribution Curves for Isctactic and Atactic Polystyrene

a) Annealed for 4 hours at 180°C (Mag. 600x)

b) Annealed for 4 hours at 180°C (Mag. 600x)

Figure 28 Transmission Photomicrograph of Melt Crystallized Isotactic Polystyrene Films

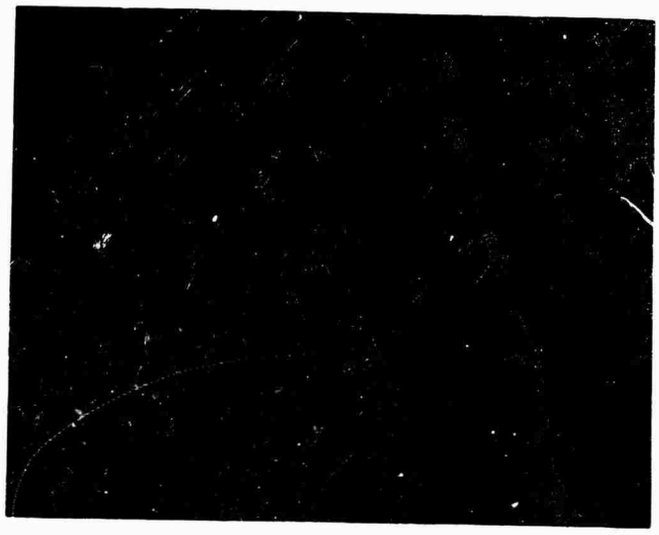

c) Annealed for 2 hours at 180°C (Mag. 600x)

d) Annealed for 2-1/2 hours at 210°C (Mag. 600x)

Figure 28 (Continued)

diameter increased to 20 microns. The distribution of crystallites is not uniform through a film and thus Fig. 28c appears to show a higher volume percent of crystallinity than in Fig. 28a or b for a shorter time of annealing. However, these photographs represent only a small area and the distribution of crystallites can vary greatly. Studies have also been conducted on thin films removed from the bulk crystallized specimens by a microtome. However, the crystalline structure cannot easily be determined due to distortions created by the microtome knife. The degree of crystallinity was determined by density measurement in a density gradient column and it was assumed that theoretical crystalline density was 1.11 and the amorphous density 1.055.

The fracture surface work of the isotactic amorphous polystyrene was determined using the uniform cantilever cleavage specimens. The results are presented in Table 13 for five different specimens. There appears to be a variation in fracture surface work with the cleavage specimen height attributed to more severe crazing as the specimen height is decreased. For similar specimen geometries (h=0.6 inches) the isotactic amorphous polystyrene has a fracture surface work at least twice as great as the atactic amorphous polystyrene. By comparison of the molecular weight distributions in Fig. 27, it appears that one explanation would be the increased molecular weight and narrower molecular weight distribution of the isotactic material. Because of this molecular weight difference, it is difficult to conclude whether the isotactic nature of the molecule itself influences the fracture processes. The isotactic molecules will have a different conformation from the atactic molecules but the glass transition temperature is only slightly different. Newman and Cox (41) have shown that T_g for an amorphous isotactic polystyrene is 93°C while the crystalline polymer (ρ = 1.074 g/cc) had a measured T_g of 99°C. This increase in T_g may be attributed to a loss in segmental mobility. The glass transition temperature of the atactic material used here was not determined but a quoted value of 95°C will certainly be quite close to the real value.

The isotactic amorphous polystyrene in all cases appears to craze considerably during the initiation of the crack which accounts for the high value of fracture surface work. In Fig. 29 the crazing which occurs during this initiation period is clearly shown.

The effect of crystallinity on the fracture surface work of isotactic polystyrene has been determined and the results are presented in table 13 and Fig. 30. The crystalline material was produced by annealing under pressure at 180°C for time periods from 2 to 6 hours. The densities were measured in a linear density gradient column prepared with demineralized water and a solution of calcium nitrate in demineralized water. Since the material becomes opaque as the crystallinity increases, crack length measurements were made from the appearance of the fracture surface after the specimen had been completely separated. The presence of crystals produces a rapid decreasc in the fracture surface work or toughness of the polymer which cannot be detected by simple

TABLE 13

Fracture Surface Work and Densities of Amorphous and Crystalline Isotactic Polystyrenes

Material	Density g/cc	Percent Crystalline Volume	Fracture Surface Work* (10^5 erg/cm^2)	Fracture Surface
Amorphous	1.052	0	9.85 (2)[a]	very rough, crazed
			11.9 (2)[a]	very rough, crazed
			11.3 (2)[b]	very rough, crazed
			15.2 (1)[b]	very rough, crazed
			16.8 (1)[c]	very rough, crazed
Annealed	1.064	20.3	3.16 (1)[a]	
			3.52 (3)[a]	
	1.067	25.4	2.07 (2)[a]	
			2.69 (2)[a]	
			2.24 (1)[a]	
	1.0738	37	.912(2)[a]	
			.734(3)[a]	
	1.074	37.4	.671(3)[a]	
			.850(3)[a]	

*Specimen Dimensions a: b=.120", h=0.6"
b: b=.120", h=0.5"
c: b=.120", h=0.4"

Numbers in parentheses refer to the number of data points per specimen

a) Crack Initiation Region (Mag. 50x)

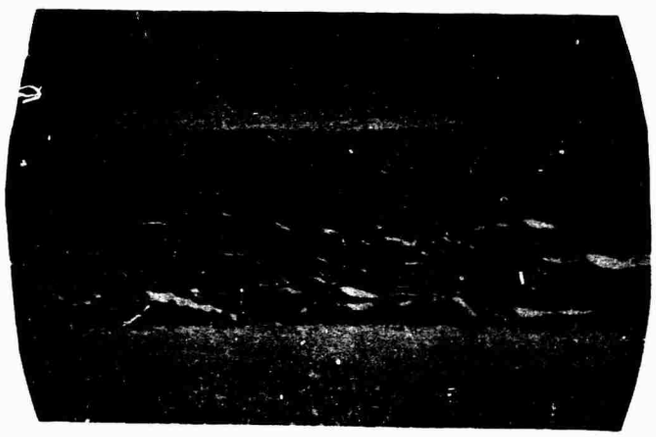

b) Rapid Crack Growth Region (Mag. 50x)

Figure 29 Fracture Surfaces of Isotactic Amorphous Polystyrene. Crack propagated from left to right.

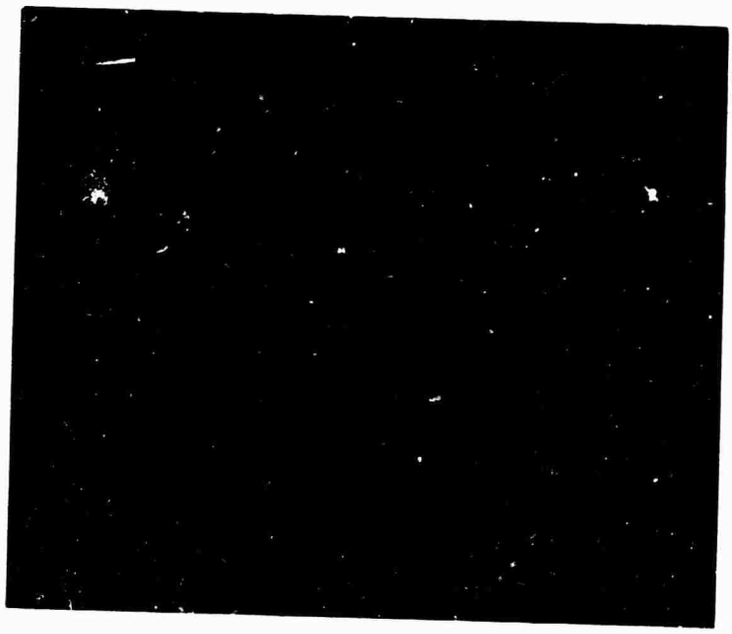

c) Crack Initiation Region Showing Craze Edges. Electron Scanning Microscope (Mag. 1000x)

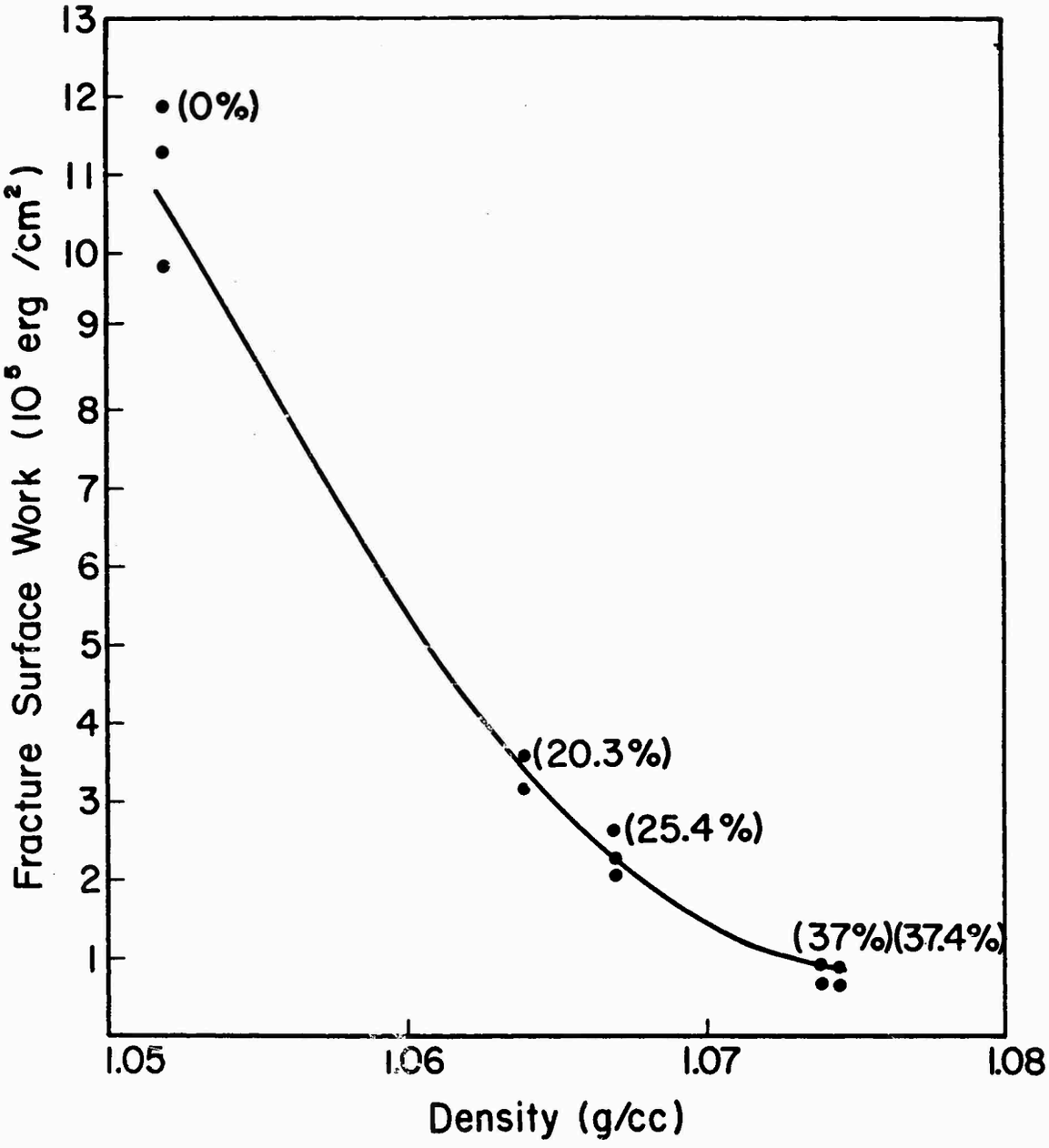

Figure 30. Fracture Surface Work for Isotactic Polystyrene as a Function of Polymer Density or Crystallinity

measurement of mechanical properties as shown reported in table 12. For example, ultimate strength or elongation measurements of these brittle materials are dependent also on the presence and size of flaws existing in the specimens prior to testing and thus the measurements can be misleading. The crystals apparently act to prevent realignment or orientation of the amorphous molecular chains which are below their glass transition temperature at room temperature and thus orientation and crazing at the fracture surface are inhibited relative to the wholly amorphous specimens.

A portion of a fracture surface for the crystalline polymer (ρ = 1.074 g/cc) is presented in Fig. 31. This particular specimen had a small fraction of air voids and a few of them can be seen on the fracture surface. The crystalline nature of the polymer can be detected by the grainy appearance of the fracture surface.

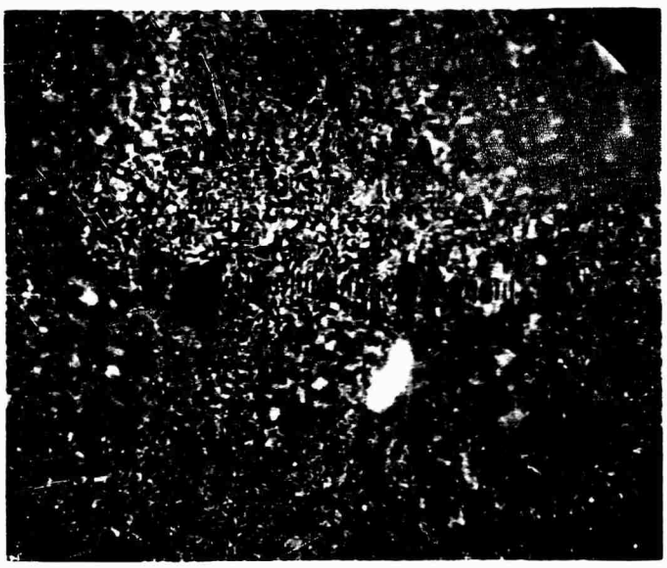

a) Optical Microscope (Mag. 600x)
Crack propagated from left to right.

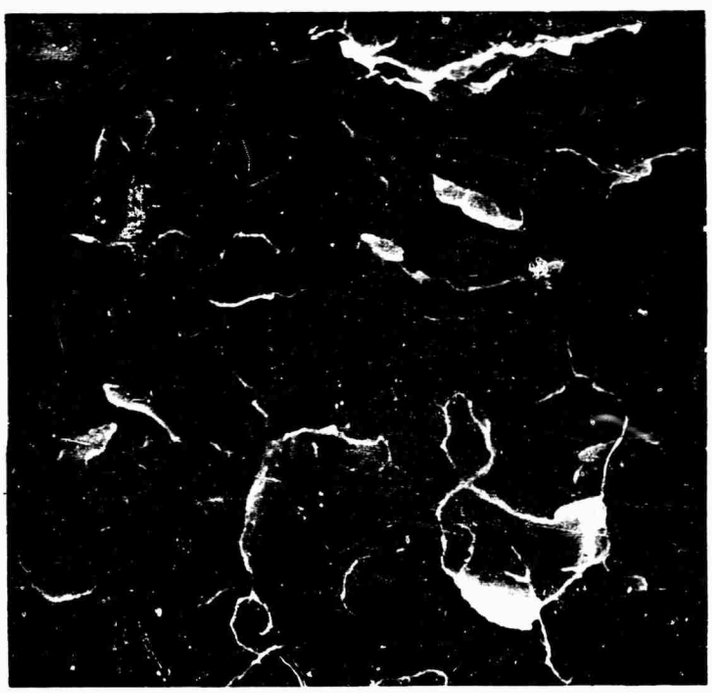

b) Electron Scanning Microscope (Mag. 600x)

Figure 31 Fracture Surfaces of Crystalline (37.4 percent by volume crystallinity) Isotactic Polystyrene

Chapter IX

INFLUENCE OF POLYMER MOLECULAR STRUCTURE AND TEMPERATURE ON FRACTURE SURFACE WORK

1. Background

In order to determine relationships between polymer molecular structure, temperature, and fracture surface work a series of polymers have been selected for study including those already discussed in previous sections. Of particular importance was a series of acrylate and methacrylate polymers since systematic changes in molecular structure can be achieved. For example, table 14 presents glass transition temperatures for several acrylate and methacrylate polymers which are influenced by the cohesive energy density of the polymer, and molecular chain stiffness or steric hindrance of the pendant groups. Glass transitions for the acrylate and methacrylate polymers have been studied by Rogers and Mandelkern (42) and Halden and Simha (43). Halden and Simha have also determined glass-glass transition temperatures or low temperature transitions due to the segmental motion of the pendant groups and these are reported in table 15. Some of these acrylate polymers have also been studied by Roetling (44) and Hoff et al (45). Roetling investigated the yield behavior of polyethylmethacrylate and Hoff studied the dynamic response (modulus and damping) of these polymers.

It was the purpose here to study the glassy state fracture surface work of some of the acrylate and methacrylate polymers as well as other selected polymers such as polyvinyl chloride and polyvinylacetate in order to determine the influence of molecular structure. The polymers investigated will be discussed individually in the remainder of this section.

2. Polymethyl methacrylate (PMMA)

A. Fracture Measurements at 25°C

Cleavage crack propagation in PMMA occurs in a continuous mode when the specimen ends are separated at a constant velocity providing that the rate of separation is less than 20 inches/minute. Thus the fracture surface work can be measured by a continuous separation of the specimen ends as shown by the load deflection curve of Fig. 15 for a tapered cleavage specimen. It can also be measured by a series of load-deflection measurements at various crack lengths. The load is removed between measurements and the sample is returned to a closed position. Force-deflection curves for a cast sheet of PMMA are shown for initial crack lengths of 6.58, 6.99, and 7.69 inches in Fig. 32 using a uniform cleavage specimen. These curves are characterized by a deviation from linearity which represents crack growth in the specimen. As the crack

TABLE 14 (Ref. 42)

Glass Transition Temperatures for Acrylate and Methacrylate Polymers

Acrylates

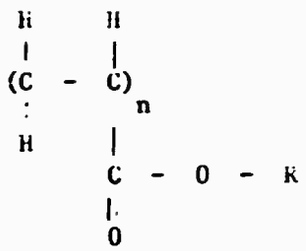

Methacrylates

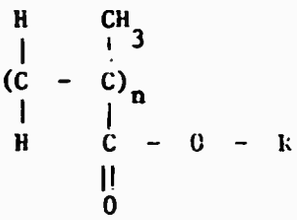

R	Tg(°C) of Acrylate	Tg(°C) of Methacrylate
methyl ($-CH_3$)	+ 3	+105
ethyl ($-CH_2-CH_3$)	-22	+ 65
n-propyl ($-CH_2-CH_2-CH_3$)	-44	+ 35
n-butyl ($-CH_2-CH_2-CH_2-CH_3$)	-56	+21
iso-butyl ($-CH_2-CH(CH_3)-CH_3$)		+54
n-hexyl $-(CH_2)_5-CH_3$		- 5
n-octyl $-(CH_2)_7-CH_3$		-20

TABLE 15 (Ref. 43)

Transition Temperatures for Acrylate and Methacrylate Polymers

Polymer	Length-Temperature Measurements (°C)				Torsion Pendulum (°C)	
	T_g	T_{gg}(1)	T_{gg}(2)	T_{gg}(3)	T_g	T_{gg}
Methyl methacrylate	103	--	15	-130	116	25
Ethyl methacrylate	64	25	-15	-115	73	15
n-Butyl methacrylate	18	-25	-51	- 95	24	
iso-Butyl methacrylate	54	25	-25	- 88	65	
Methyl acrylate	10	-40	-135			

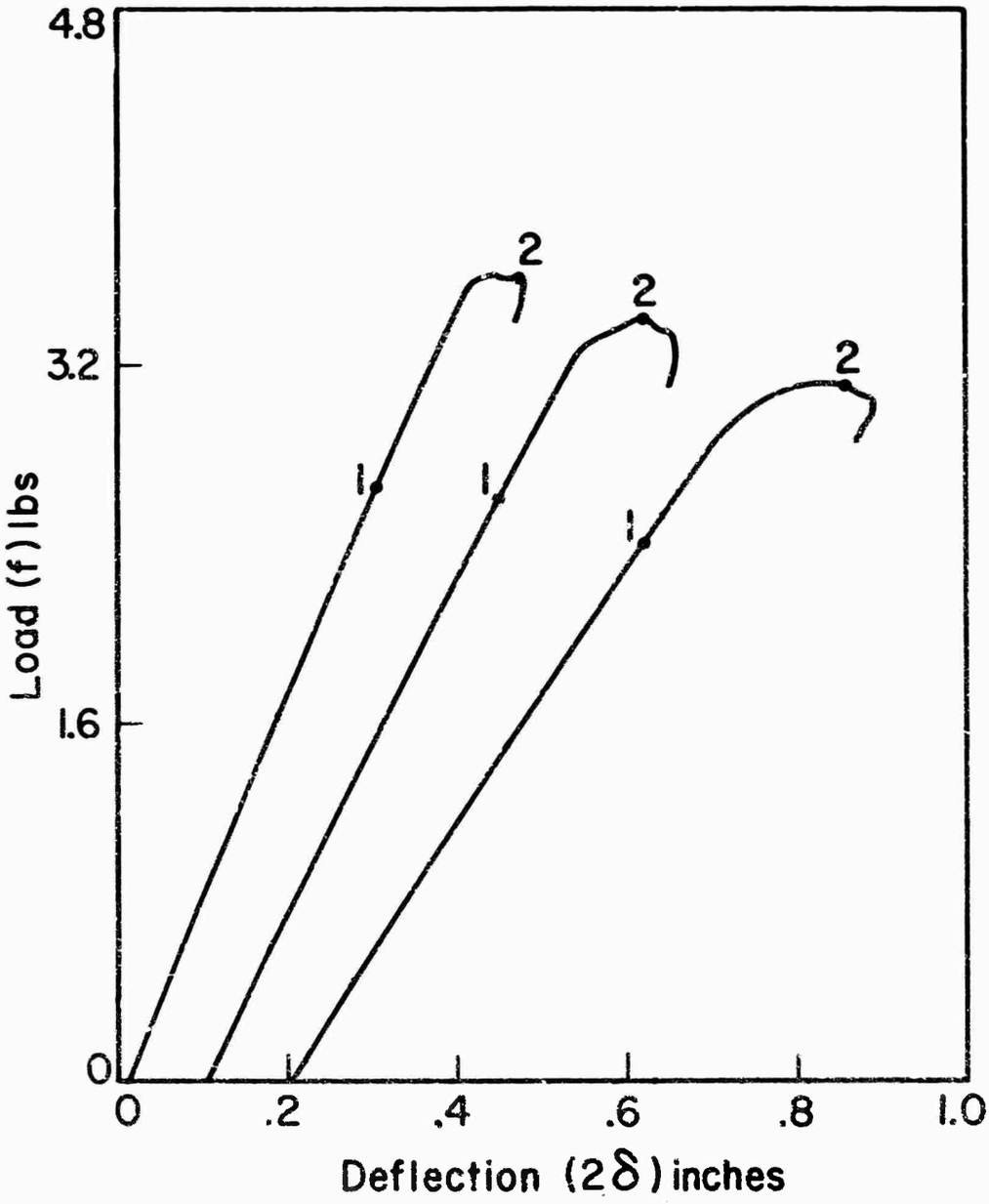

Figure 32. Experimental Force-Deflection for Plexiglas at +25°C

lengthens or the beam length increases the compliance ($2\delta/f$) of the cleavage sample decreases. A maximum in the force deflection curve occurs as the crack lengthens faster than the rate of separation of the specimen ends. The calculated value of fracture surface work will be dependent upon whether the force and deflection at crack initiation or unstable crack propagation are selected.

The crack length can be measured before the experiment and the crack is then observed with a telemicroscope to record the onset of propagation by making a pip in the force deflection curve corresponding to the visual observation. It was determined by inspection of the curves that the crack initiation and slow propagation corresponds to the beginning of non-linearity in the curve. The position of the crack or crack length can also be accurately measured after the conclusion of the experiment for each point since the crack front has a characteristic fingernail-like appearance. For PMMA, as many points as desired can be obtained from a single specimen since the growth of the crack to a new position can be accurately controlled. The points corresponding to crack initiation and unstable crack propagation have been noted by the numbers 1, 2 in Fig. 32. The value for fracture surface work using the force, deflection, and crack lengths corresponding to initiation (pts. 1) was calculated to be 1.10×10^5 erg/cm^2. The average value obtained by using the points corresponding to maximum force was calculated to be 2.11×10^5 erg/cm^2. This latter value agrees with those values obtained from both uniform and tapered cleavage specimens when the experiment is conducted by continuous crack propagation obtained from a constant rate of separation of specimen ends and thus corresponds to a value for crack propagation as opposed to crack initiation.

Two different types of PMMA have been considered in this investigation. One type is the cast sheet manufactured by Rohm and Haas Co. (Plexiglas) and the other is a molding grade of lower molecular weight. Molecular weights were measured and are compared in Fig. 33. It was reported by Arro Laboratories that the sample from the cast sheet was not well resolved because of its high molecular weight and their columns had a maximum porosity of 3×10^6 so were unable to resolve high molecular weight material. Realizing this limitation the following results were obtained:

	$\bar{A}_N$	$\bar{A}_W$	MWD
Cast PMMA	5827	28695	4.9
Molded PMMA	534	11292	21.1

Although an accurate comparison cannot be made, the molded PMMA is of lower molecular weight and greater molecular weight distribution. The fracture surface work values measured for these polymers at room temperature are shown in table 16. The cast sheet gives an average value of fracture surface work of 2.57×10^5 erg/cm^2 which is quite reproducible perhaps because of the low molecular weight distribution. The value for the molded polymer is nearly the same but the fracture

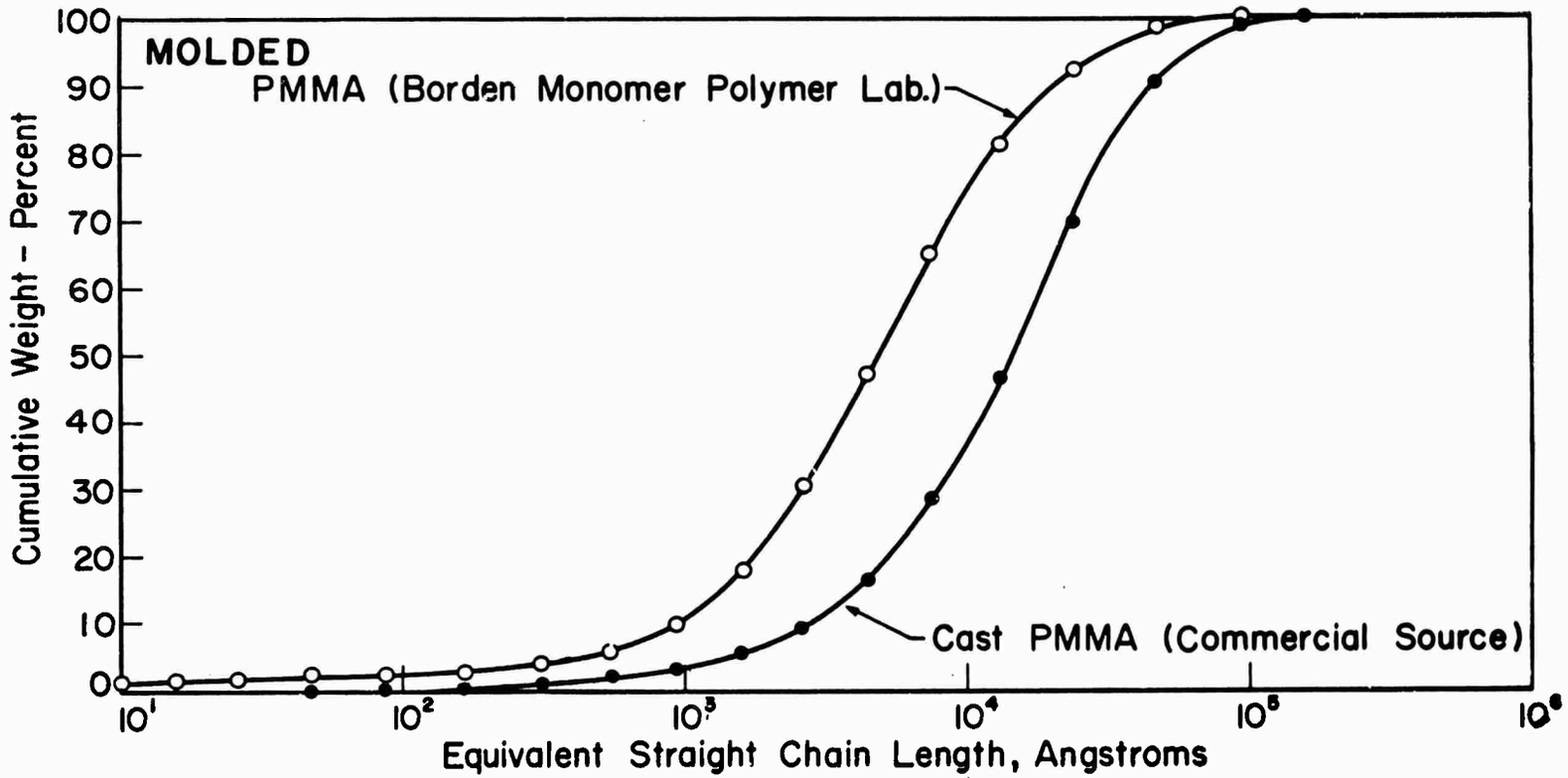

Figure 33. GPC Cummulative Distribution Curves for Methyl Methacrylate Polymers

TABLE 16

Fracture Surface Work Measurements for Methacrylate Polymers

Material	Specimen Type and Thickness	Test Temperature (°C)	Fracture Surface Work (10^5 erg/cm^2)	Fracture Surface
Cast Sheet	Tapered-1/4 in.	25	2.65	River Pattern, Color
	"	"	2.85	" "
	"	"	2.74	" "
	"	"	2.43	" "
	"	"	2.49	" "
	"	"	2.42	" "
	"	"	2.39	" "
			Ave 2.57x10^5 erg/cm^2	
	Uniform-1/4	-196	12.15 (Ave of 4 Specimens)	Smooth, no colors
	Tapered-1/4	-196	15.91	Smooth, no colors
Molded Sheet	Uniform-1/8 in.	25	2.65	Smooth, Colors
	Tapered-1/8 in.	25	2.87	" "
	"	25	2.79	" "
	"	-196	14.8	Smooth, no colors
	"	"	15.6	" "
	Tapered-1/4 in.	"	17.6	" "
	Tapered-1/4 in.	"	10	" "
	Tapered-1/8 in.	"	20.4	" "

surface appearances are quite dissimilar (Fig. 34). Within this molecular weight range, there does not appear to be a difference in fracture surface work for PMMA polymers which agrees with the results also reported by Berry (15). This is contrary to the results reported for polystyrene earlier in this report. Colors are very evident on the fracture surface of PMMA polymers and typical fracture surfaces are shown in Fig. 34. The lower molecular weight PMMA has almost a mirror smooth fracture surface which displays colors and it is unusual that these polymers have similar fracture surface works considering the difference in fracture surfaces.

B. Fracture Measurements at -196°C

In order to evaluate the fracture surface work of PMMA polymers at -196°C, cracks were introduced into the machined specimens by separation of the specimen ends at room temperature until desired crack lengths were obtained. The samples were then immersed in the liquid nitrogen and remained in the dewar for at least one hour. One of the samples was then placed in the loading grips and the force deflection curve measured while the other samples also still remained in the dewar. A typical force deflection curve is shown in Fig. 35. Crack lengths were measured after the experiment by examination of the characteristic markings of the fracture surface. The force-deflection curve shown in Fig. 35 is linear until fracture and was measured for a uniform cleavage specimen with h=o.6 inches, b=0.135 inches and ℓ=3.401 inches. The value of fracture surface work calculated from the curve in Fig. 35 was 13.65×10^5 erg/cm^2. A summary of results at liquid nitrogen temperatures is presented in table 16.

For the case of tapered cleavage bars at liquid nitrogen temperatures cracks of several lengths are grown at room temperature and the compliance of the specimen is then measured in liquid nitrogen for each crack length to establish $(dc/d\ell)_{exp}$; when a suitable number of points have been obtained the fracture surface work of the bar is measured. In these experiments, it is only possible to make one fracture surface work measurement per sample since the crack propagates completely through the sample after initiation and the specimen does not arrest the crack growth. The average fracture surface work value for the 5 cast PMMA specimens was 12.9×10^5 erg/cm^2 while the average value for the molded specimens was 15.7×10^5 erg/cm^2. This is five to six times greater than the values measured at 25°C. It is significant to note that this compares to a value of 10×10^5 erg/cm^2 determined by Berry (16) through the use of edge notched tensile specimens. It was observed that deviation in results from specimen to specimen could be partially attributed to differences in the shape and orientation of the initiating crack.

The appearance of the fracture surfaces after the specimens were returned to room temperature are shown in Fig. 36. These surfaces from the fast crack growth region are mirror smooth to the naked eye and also appear colorless. At the magnification shown in Fig. 36 it can be seen that the surface does have a structure and in one case the parabolic markings common to tensile fracture

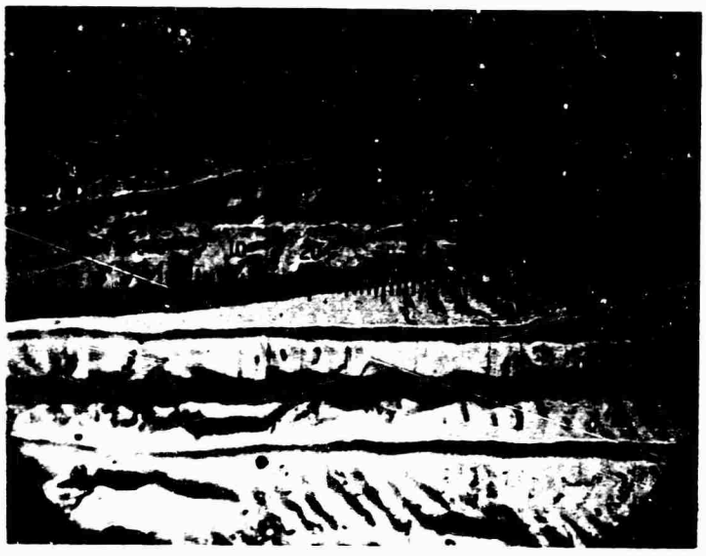

a) River pattern observed during continuous crack propagation of cast PMMA (Mag. 100x)

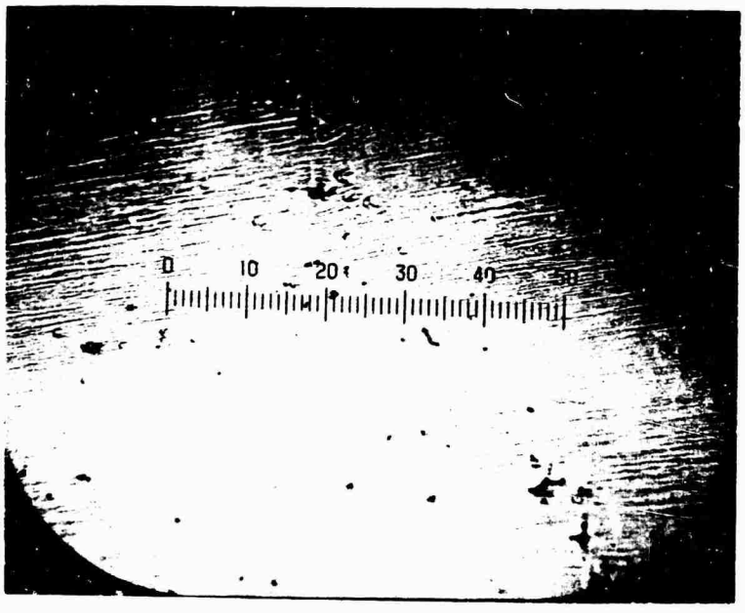

b) Smooth surface observed for molded PMMA during continuous crack propagation (Mag. 400x)

Figure 34 Cleavage Fracture Surfaces for Cast and Molded PMMA Polymers

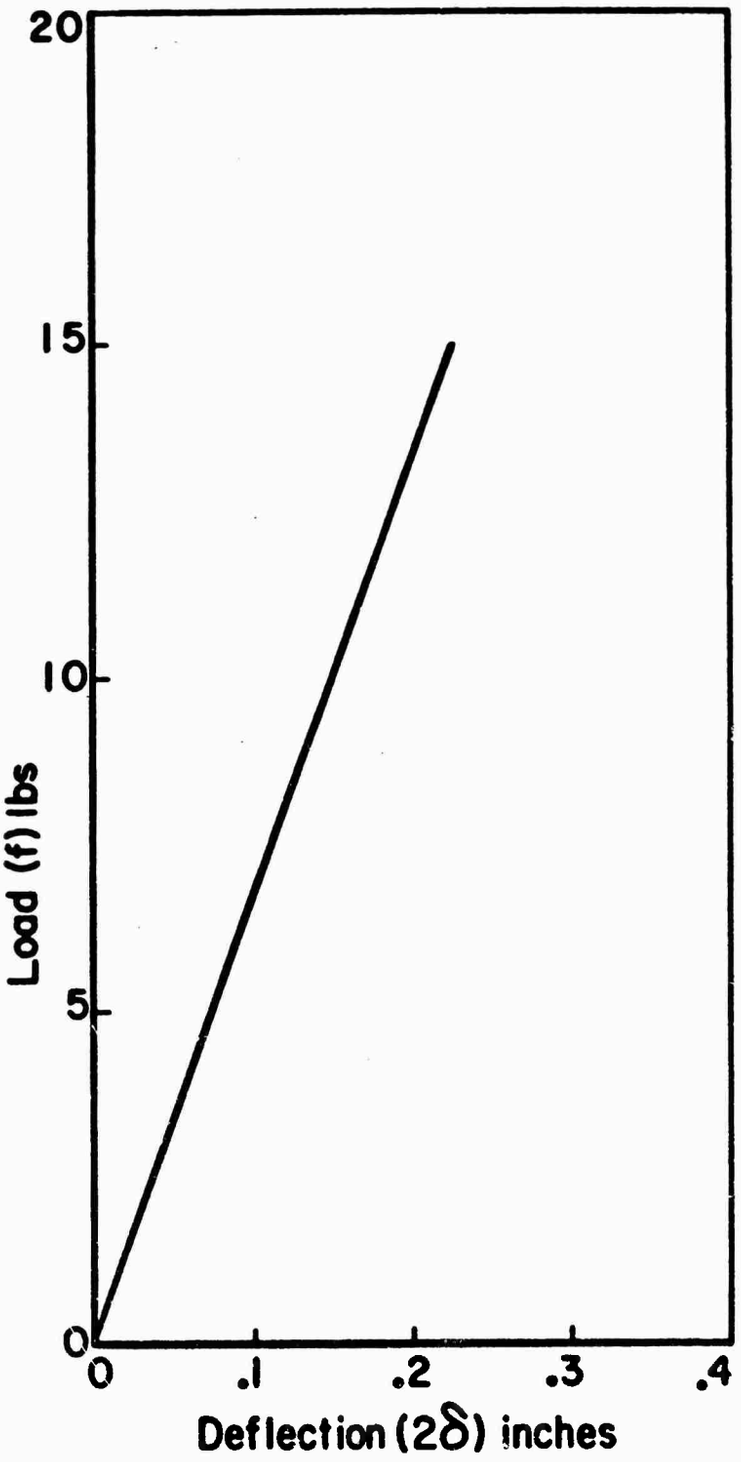

Figure 35. Experimental Force-Deflection for Plexiglas at -196°C

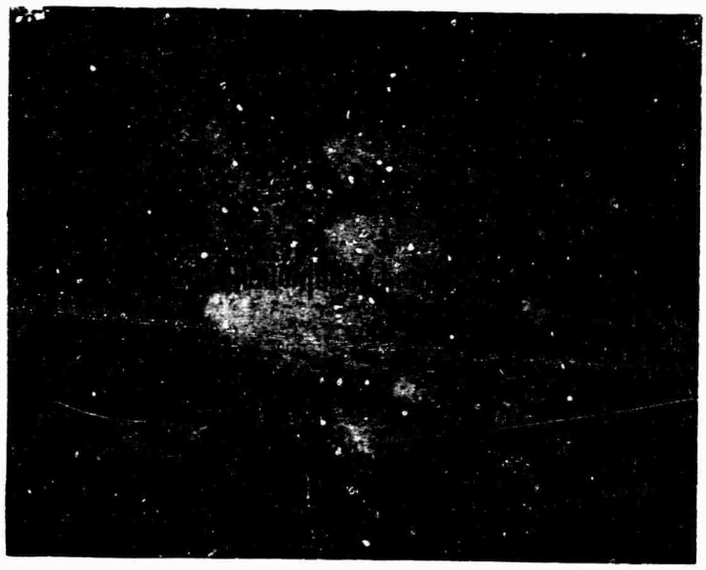

a) Parabolic Markings on Fracture Surface of Cast PMMA. Crack propagation direction from left to right. (Mag. 100x)

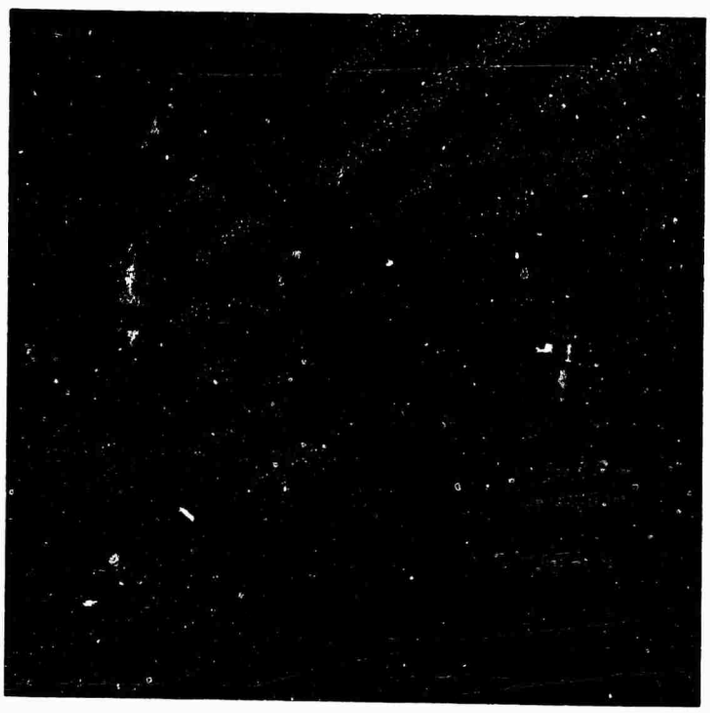

b) Detailed View of Parabolic Markings with Electron Scanning Microscope (Mag. 232x)

Figure 36 Cleavage Fracture Surfaces for Cast and Molded PMMA Polymers at -196°C

c) Characteristics of Smooth Fracture Surface of Molded PMMA. Crack propagation direction from left to right. (Mag. 400x)

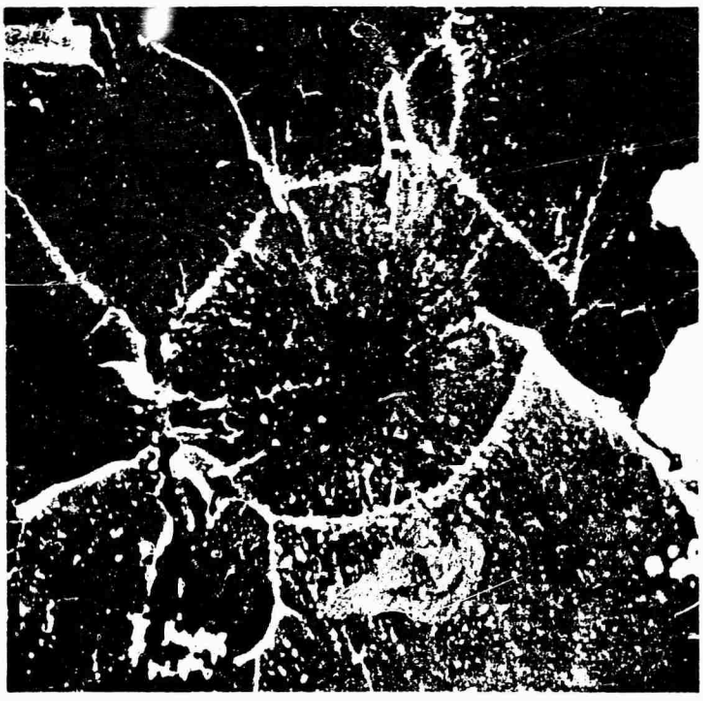

d) Detailed View of Molded PMMA Polymer Fracture Surface with Electron Scanning Micrcscope (Mag. 1000x)

Figure 36 (Continued)

surfaces could be seen. These markings are a result of fracture initiations ahead of the main crack front due to the high stresses at the crack tip.

It remains to be explained why the fracture surface work for crack initiation increases considerably as the polymer becomes more glassy and at -196°C the polymer is well below its glass transition temperature and all other glass-glass transition temperatures (table 15). One insight can be gained by considering cleavage experiments with polystyrene at liquid nitrogen temperatures. Ir this case, fractures could not be propagated and it was observed that an extensive amount of crazing occurred around the crack tip. From Kambour's studies (14) it is apparent that crazing is fundamental to the fracture process and occurs in advance of the crack front. The strength of the crazed or oriented material should be greatly increased at low temperatures. If this is the case, then the surrounding material can be raised to a stress level sufficient to induce crazing and a large region can become crazed. This has been observed during the loading of the specimen and the crazing is sufficient to resist the cleavage crack propagation. This crazing is reversible and when the specimen is warmed to room temperature the crazes disappear. A similar mechanism may account for the large value of fracture surface work measured for the PMMA polymers although the crazes could not be visually observed during the experiment. The fracture surface for PMMA polymers, although appearing mirror smooth in the fast crack growth region, is extremely rough in a small area where the crack initiates and becomes unstable. This is clearly shown in the combined photographs of Fig. 37 encompassing the initiation region. This extreme roughness and large surface area created is indicative of the large measured value of fracture surface work.

C. Influence of Crack Velocity on Fracture Surface Work

A limited number of experiments have been conducted on tapered cleavage specimens from cast PMMA sheets to observe the effect of crack velocity on fracture surface work. The technique utilized was to separate the ends of a cleavage specimen at varying constant rates in an Instron testing machine. This could be accomplished since it has been observed that for a constant separation rate using the tapered cleavage specimen a constant crack velocity could be achieved. Thus the separation rate can be varied within a given specimen to produce various crack velocities and measurement of the crack width and force are sufficient to determine fracture surface work. The data obtained from 3 specimens is shown in table 17. The crack velocities are only approximate since it takes a certain distance for the crack to reach a constant velocity after the separation rate has been changed. For both of the first two specimens shown in table 17 a small increase in fracture surface work was measured for increasing crack velocities. It is difficult to compare these specimens because of the approximate visual observation of crack velocity. Since there were reference marks on the specimen at 1/2 inch intervals, the crack position was marked on the load-deflection recording for each 1/2 inch of length to assist in the determination of crack velocity.

a) Measured Fracture Surface Work for Crack Initiation was 17.6×10^5 erg/cm^2

b) Measured Fracture Surface Work for Crack Initiation was 10×10^5 erg/cm^2

Figure 37. Initiation of a Crack in PMMA Polymers at -196°C. Crack propagated from left to right.

TABLE 17

Influence of Crack Velocity on Fracture Surface Work

Specimen	Separation Rate (in/min)	Approx. Crack Velocity (in/sec)	Crack Length (in)	Force (lb)	Crack Width (in)	$(dc/d\ell)_{exp}$	Average Fracture Surface Work (10^5 erg/cm^2)
1	.05	.0075	1.5	13.95	.218	6.30×10^{-3}	
			2.0	12.55	.216		2.42
			2.5	12.4	.174		
			3.0	13.6	.179		
	.1	.037	3.5	13.75	.177		
			4.0	13.8	.165		2.96
			4.5	13.35	.179		
	.2	.111	5	14.0	.177		
			5.5	14.0	.167		3.15
			6.0	13.5	.159		
2	.1	.018	4.5	12.6	.160	6.06×10^{-3}	2.60
			5.0	12.9	.171		
	.2	.060	5.5	13.5	.183		
			6.0	13.8	.170		
			6.5	13.5	.164		2.79
			7.0	13.1	.158		
			7.5	12.6	.165		
	.5	.167	8.5	13.8	.171		2.88
			9.0	13.5	.170		
3	20		7.8	11.7	.106	5.26×10^{-3}	
			11.2	11.6	.106		2.96

For a very high rate of separation of the specimen ends (20 inches/minute) the crack propagation is no longer continuous but occurs in steps or in stick-slip fashion. The data for such a specimen is also shown in table 17. The value of fracture surface work corresponds to that for unstable crack initiation. The crack propagated from an initial length of 7.8 inches to approximately 10.25 inches and then propagated in an unstable manner again at approximately 11.2 inches. The values of force were almost identical and a value of fracture surface work of 2.96×10^5 erg/cm^2 was measured. This value is compared to the average value of 2.57×10^5 erg/cm^2 recorded for cast PMMA at low rates of crosshead separation (.2"/min.). This increase in fracture surface work with increasing crack velocity agrees with measurements of other investigators but only spans a narrow range of crack velocities and is of a limited nature.

3. Polybutyl methacrylates

Two isomers of butyl methacrylate, n-butyl and iso-butyl have been studied and their structure and glass transition temperatures are shown in table 14. This slight difference in molecular structure results in n-butyl methacrylate polymer having a T_g of 24°C and iso-butyl methacrylate polymer having a T_g of 65°C as measured by damping modulus from a torsion pendulum. The materials studied were received from Borden Monomer-Polymer laboratory and were compression molded here into flat plates according to the conditions in table 5. The materials were very close in molecular weight and molecular weight distribution as can be seen from Fig. 38 and the following data:

	$\overline{A}_n$	$\overline{A}_w$	MWD
n-butyl	1198.3	5648	4.71
iso-butyl	1128.9	6090.1	5.40

Therefore, this factor can be eliminated in interpretation of the results.

The fracture surface work values are reported in table 18 for both room temperature and liquid nitrogen experiments. The n-butyl polymer was too tough to be cleaved at room temperature since T_g is approximately 24°C. However, it could be cleaved at -196°C and for two specimens the average value of fracture surface work was 1.75×10^5 erg/cm^2. The crack initiation is shown by a composite photograph in Fig. 39 and the rough region is clearly shown indicating considerable deformation at this temperature.

The iso-butyl methacrylate polymer can be cleaved at room temperature and crack propagation occurs in a stick-slip manner. The crack jumps are very small as can be seen by the fracture surface in Fig. 40. The average value of fracture surface work is 0.780×10^5 erg/cm^2 at room temperature. The fracture

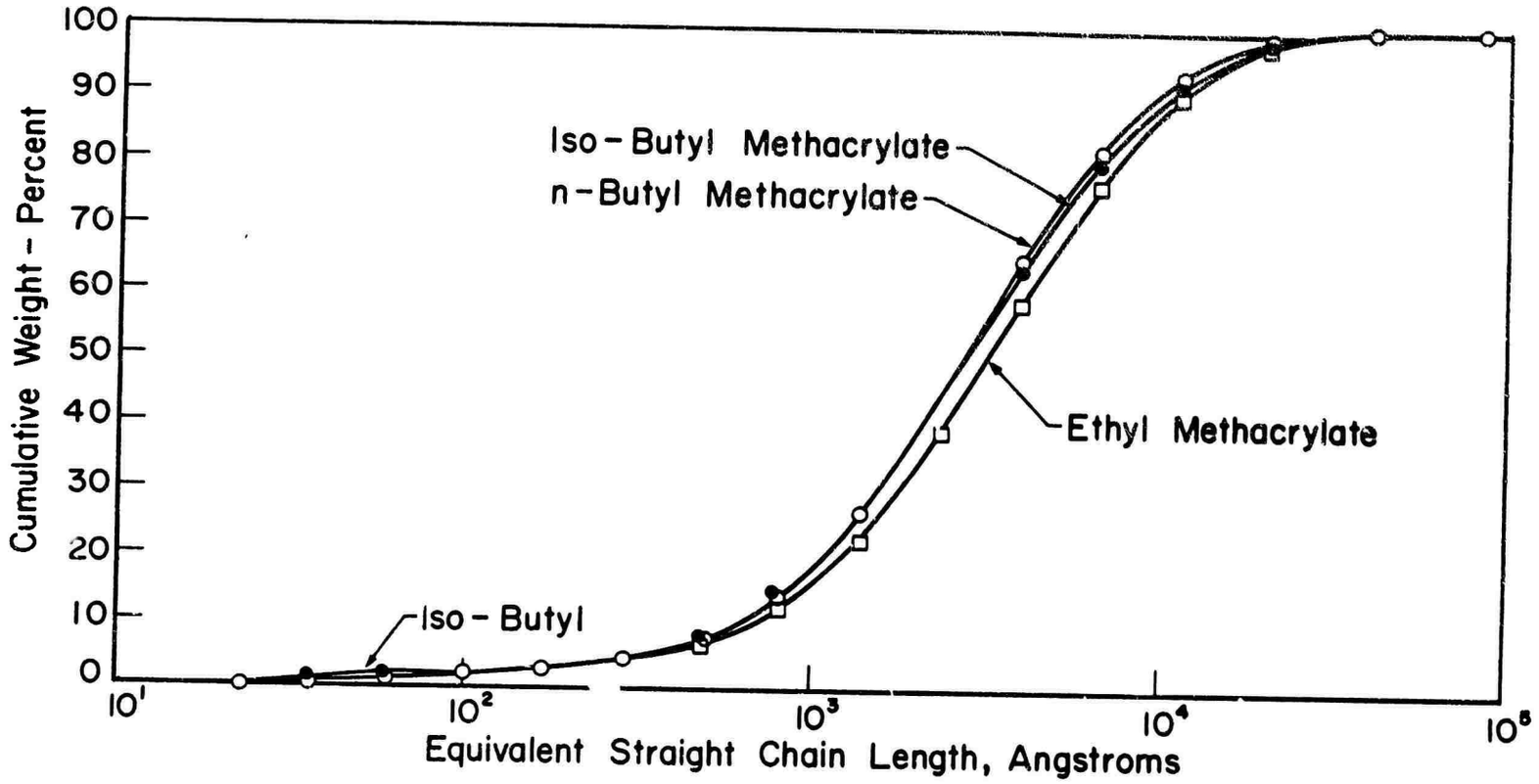

Figure 38. GPC Cummulative Distribution Curves for Three Methacrylate Polymers

TABLE 18

Fracture Surface Work Measurements for Butyl Methacrylate Polymers

Material	Specimen Type*	Temperature °C	Fracture Surface Work** (10^5 erg/cm^2)	Fracture Surface
n-butyl methacrylate	Uniform (h=1.2") (b=1/8")	-196	1.502(1)	rough
	" "	-196	2.02 (1)	"
iso-butyl methacrylate	tapered (b=1/8")	25	0.913(4)	rough
	tapered	25	0.621(3)	rough
	tapered	25	0.751(4)	rough
	tapered	25	0.827(5)	rough
	uniform (h=1.2")	25	0.790(14)	rough
	tapered	-196	0.315(1)	rough
	tapered	-196	0.273(1)	rough
	tapered	-196	0.317(2)	rough
	uniform (h=1.2")	-196	0.335(1)	rough

**Numbers in parentheses are data points per specimen

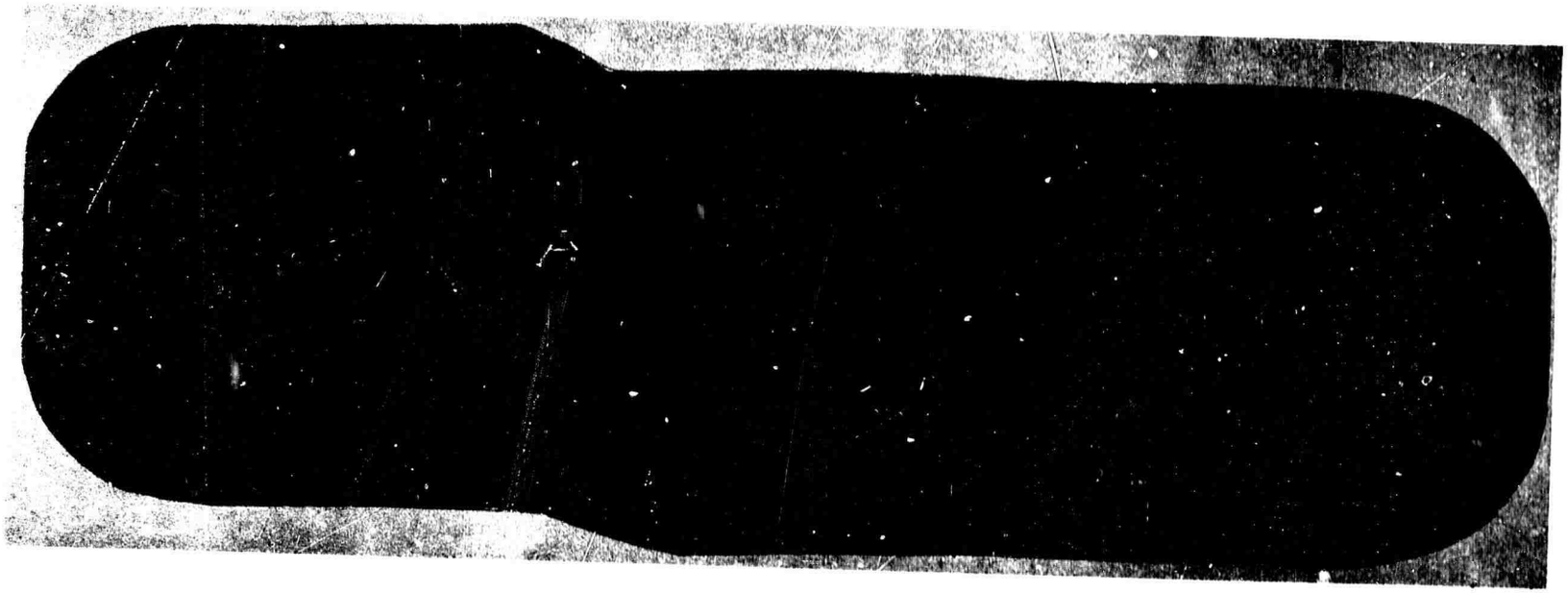

Figure 39 Initiation of Cleavage Fracture for n-butyl Methacrylate Polymer at -196°C. (Mag. 100x)

a) Cleavage at Room Temperature (Mag. 50x)

b) Cleavage at -196°C. Fast Crack Growth Region. (Mag. 50x)

Figure 40 Cleavage Fracture Surfaces for iso-butyl Methacrylate

surface work determined at -196°C was $.310 \times 10^5$ erg/cm^2 or a reduction from the room temperature value. This is opposite to the effect observed for PMMA and polystyrene but the same as observed for n-butyl methacrylate although the room temperature value for n-butyl methacrylate couldn't be measured because it was too great. The fracture surface for iso-butyl methacrylate at -196°C in a fast crack growth region is shown in Fig. 40. The initiation of a crack at -196°C is shown in Fig. 41 and has a relatively smooth appearance compared to PMMA or n-butyl methacrylate polymers.

4. Ethyl Methacrylate Polymer

The poly ethyl methacrylate investigated in this program was obtained from the Borden Monomer-Polymer Laboratory and was received as a powder. This material was compression molded into 1/8 and 1/4 inch sheets as described in table 5. The molecular weight has been characterized and is shown compared to the butyl methacrylates in Fig. 38. The averages for the equivalent straight chain lengths and molecular weight distribution are as follows:

$\bar{A}_n$	$\bar{A}_w$	MWD
1170.5	6653.7	5.68

Since this material is quite similar in molecular weight and distribution to the butyl methacrylate polymers, comparisons of fracture properties can be made independent of molecular weight. The glass transition temperature for this material is 73°C (torsion pendulum data) so that it is glassy or leathery at room temperature.

The measured values of fracture surface work at 25°C and -196°C are reported in table 19. As will be discussed, there is considerable variation in the results obtained for this material. The results using a tapered bar with a thickness of 1/4 inch gives a value of fracture surface work of 4.14×10^5 erg/cm^2 at room temperature and 4.61×10^5 erg/cm^2, at -196°C, equivalent considering the experimental scatter. Two other tapered bars gave values of 4.28 and 5.19×10^5 erg/cm^2 at -196°C. These results are lower than those reported for 1/8" thick plates using material received from an earlier date. By inspection of the fracture surfaces in Fig. 42 an explanation for these differences becomes more clear. It appears that the material producing the lower values of fracture surface work and resulting in a smoother fracture surface did not have well fused particles. Thus, the boundaries would cause the material to be weaker and more brittle. It is possible that the polymer, as received, may have a low degree of crosslinking which would have made

Figure 41 Initiation of Cleavage Fracture for Iso-butyl Methacrylate Polymer at -196°C. (Mag. 100x)

TABLE 19

Fracture Surface Work Measurements for Poly ethyl methacrylate

Specimen Type	Specimen Dimensions	Temperature (°C)	Fracture Surface Work (10^5 erg/cm^2)	Fracture Surface
Tapered*	b=0.25"	25	4.14(6)**	smooth
		-196	4.61(1)	smooth
Tapered	b=0.25"	-196	5.19(1)	smooth
Tapered	b=0.25"	-196	4.28(3)	smooth
Uniform	h=1.2", b=.125"	25	11.3(5)	very rough
Uniform	h=1.2", b=.125"	-196	7.55(2)	very rough
Uniform	h=1.2", b=.125"	-196	6.98(1)	very rough
Uniform	h=1.2", b=.125"	-196	8.00(2)	very rough
Uniform	h=1.2", b=.125"	-196	5.35(2)	very rough
Uniform	h=1.2", b=.125"	-196	12.5 (2)	very rough

* This specimen was used for 25°C and -196°C measurements. Six data points obtained at room temperature (range of values from 4.27 to 5.4x10^5 erg/cm^2) and one measurement at -196°C.

** Numbers in parentheses refer to number of data points per specimen.

fusion more difficult. The polymer producing higher values of fracture surface work is shown in Fig. 42b and c and the greatly increased surface roughness can be easily observed. The difference in fracture surface roughness can then be attributed to differences between different lots of material or differences in molding conditions.

5. Methyl Acrylate Polymer

Methyl acrylate is rubbery at room temperature (T_g=3°C) and thus has been studied at liquid nitrogen temperature since a fracture could not be propagated at room temperature. Two samples of methyl acrylate have been studied. One was from a cast sheet supplied by Rohm and Haas Co. and the other was compression molded from polymer purchased from Borden Monomer-Polymer Laboratories. The material from Rohm and Haas produced a fracture surface work of 110×10^5 erg/cm^2 (1 specimen) and the compression molded material yielded values of 59.7 and 63×10^5 erg/cm^2 at -196°C (Table 20). A uniform cantilever cleavage specimen was used for these measurements. In addition to the crack propagation along the grooved plane, a crack also grew normal to this plane from the point of initiation upon fracture of the specimen. Molecular weight distributions have not been determined for these polymers as they were not soluble in THF.

This polymer produced the largest measured value of fracture surface work at -196°C. Polystyrene, of course, which could not be failed by the cleavage technique is not considered in this comparison. The fracture surfaces for polymethyl acrylate during crack initiation and propagation are shown in Fig. 43.

6. Investigations with Polyvinyl Chloride and Polyvinyl Acetate

A polyvinyl chloride was obtained from Borden Monomer-Polymer Laboratories and molded in a press with the addition of 3pph of a tin stabilizer to prevent thermal degradation during the compression molding. The molding conditions are described in table 5. Polyvinyl acetate was also obtained from Borden and compression molded into flat plates. Molecular weight distributions for these materials are compared in Fig. 44. The average equivalent straight chain lengths are as follows:

	$\bar{A}_n$	$\bar{A}_w$	MWD
PVC	1135.2	4,090	3.60
PVAC	5717	25,248	4.42

A published value for the glass transition temperature of polyvinylchloride is 87°C and for polyvinyl acetate is 29°C. Uniform cleavage specimens were prepared in the standard manner using a 6 mil groove on each side of the sample. It was not possible to propagate a crack through these materials at 25°C due to yielding

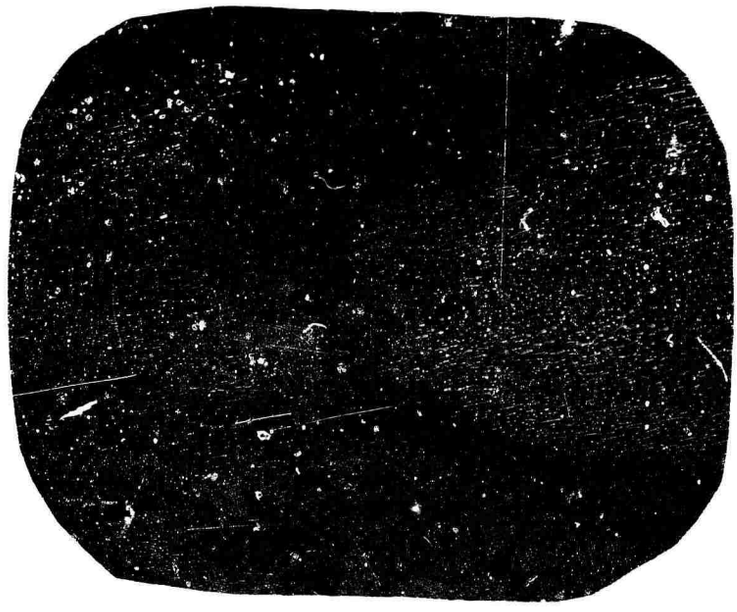

a) Crack Initiation at -196°C. Measured Fracture Surface Work = 4.61×10^5 erg/cm^2 for Crack Initiation. (Mag. 100x)

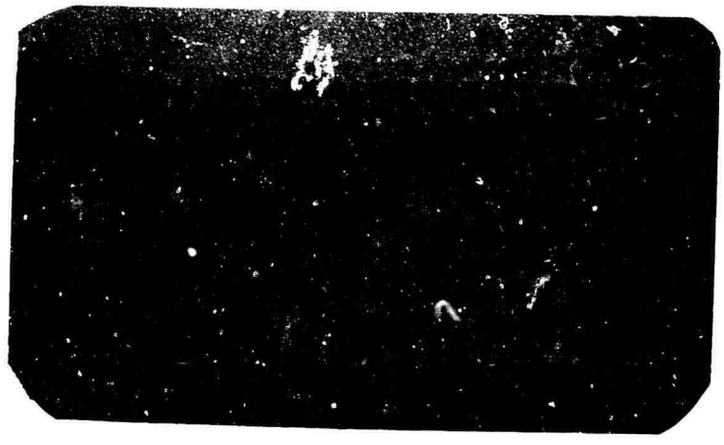

b' Crack Initiation at -196°C. Measured Fracture Surface Work = 8×10^5 erg/cm^2 (Mag. 35x)

Figure 42 Fracture Surfaces for Poly Ethyl Methacrylate. Crack propagated from left to right.

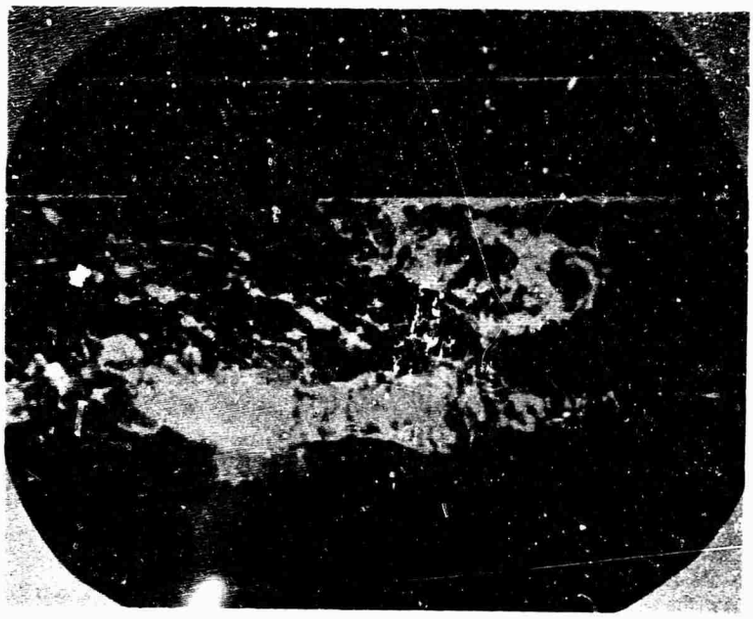

c) Crack Propagation Region at 25°C. Measured Fracture Surface Work = 11.3×10^5 erg/cm^2. (Mag. 35x)

a) Initiation

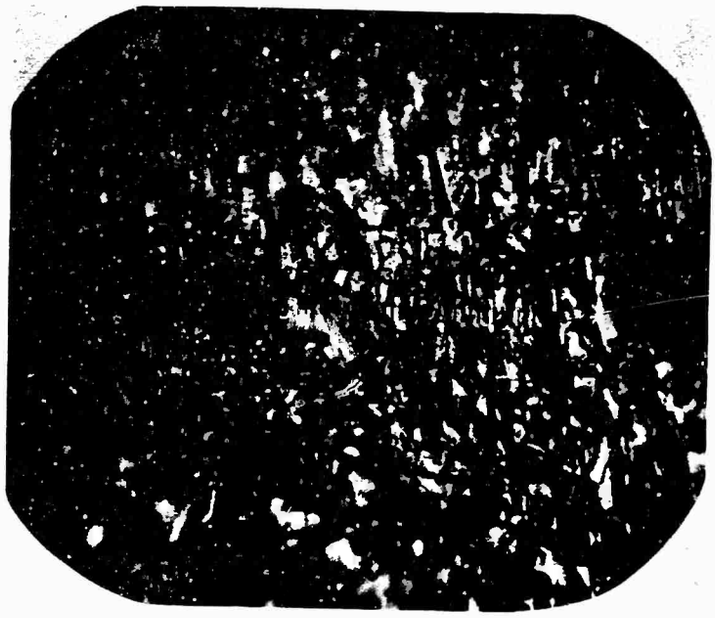

b) Slow Propagation

Figure 43 Fracture Surface for Polymethacrylate at -196°C (Mag. 100x)

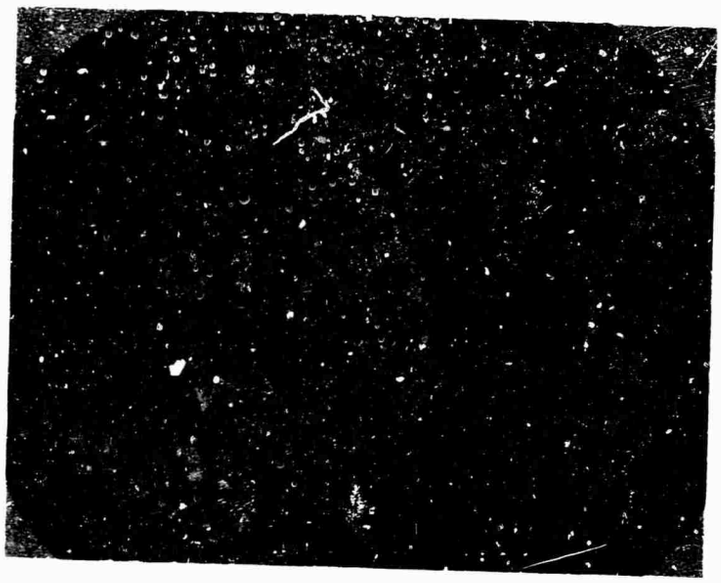

c) Rapid Propagation

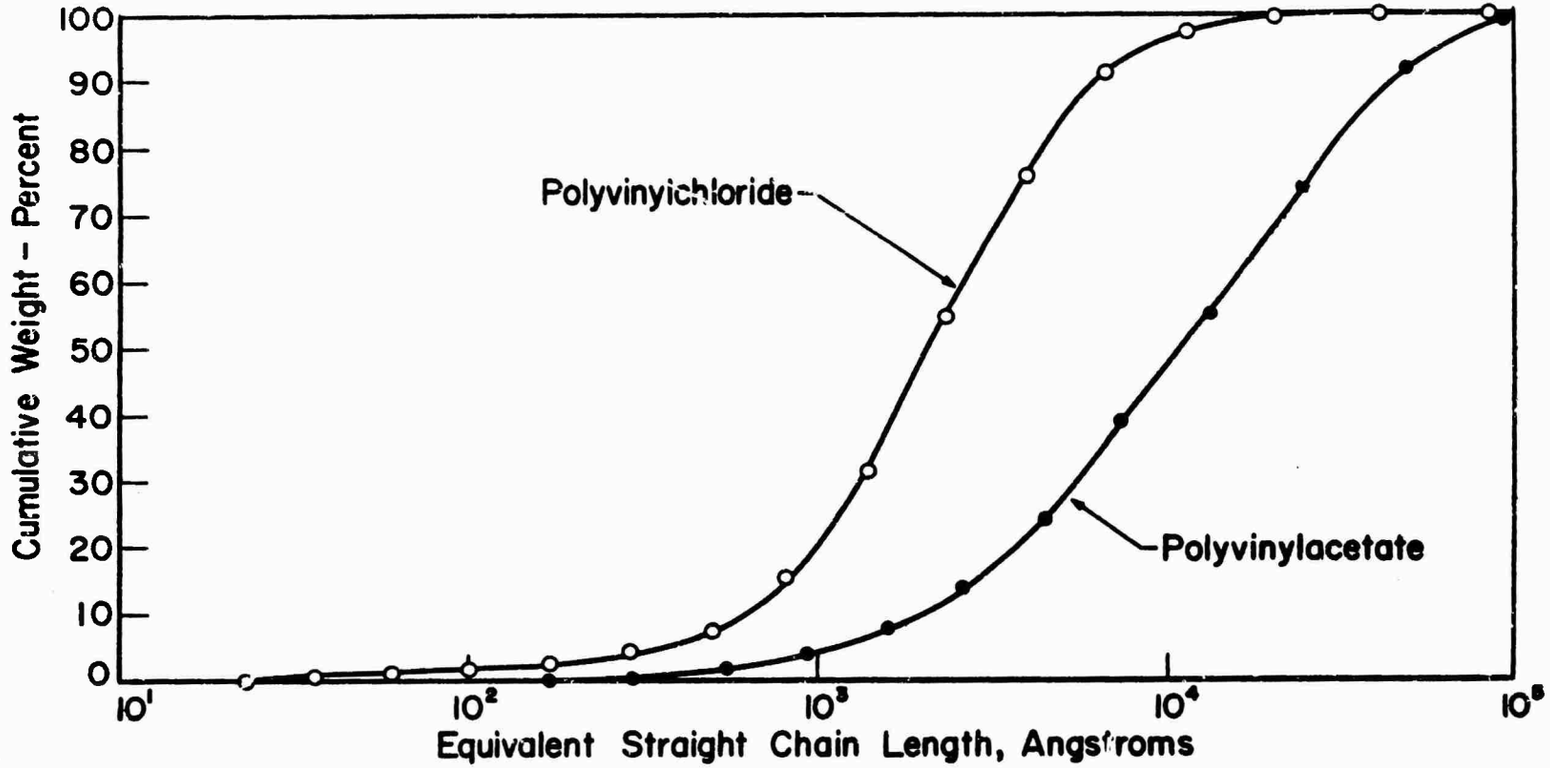

Figure 44. GPC Cummulative Distribution Curves for Polyvinyl Chloride and Polyvinyl Acetate

TABLE 20

Fracture Surface Work of Polymethyl acrylate

Material	Specimen Type	Force (lb)	Deflection (inches)	Crack Length (inches)	Crack Width (inches)	Fracture Surface Work γ(erg/cm^2)
Cast PMA	Uniform	45.58	.189	2.44	.072	110×10^5
Molded PMA	Uniform	30.66	.096	1.92	.055	59.7×10^5
Molded PMA	Uniform	25.97	.178	2.88	.058	63.05×10^5

of the material near the crack. Experiments were thus restricted to determinations of fracture surface work at liquid nitrogen temperatures. The results are presented in table 21 and it can be observed that polyvinyl acetate has a much greater value of fracture surface work than polyvinyl chloride. The crack initiation can be seen for polyvinyl chloride in Fig. 45. In the specimen shown in Fig. 45 the fracture surface work was calculated to be 21.2×10^5 erg/cm^2. The region of fracture surface to the left of the initiation area is a region of rapid crack growth. In this specimen an initial crack was propagated at the liquid nitrogen temperature and it arrested itself at the point shown. Thus the fracture surface where the velocity is high is still quite rough. This is also shown in Fig. 46 for polyvinyl acetate. The greater value of fracture surface work displayed by polyvinyl acetate may be a result of greater molecular weight as well as differences in the molecular structure which also result in differences in the glass transition temperature.

7. Summary Discussion

The understanding of the relation between polymer molecular structure and crack initiation or propagation energies would obviously be desirable. We have attempted to gain insight into this problem by this investigation. Certainly, a relation has been seen to exist between molecular weight and molecular weight distribution and fracture surface work, and crosslinking and crystallinity in glassy polymers and fracture surface work. Also the effect of molecular pre-orientation is by now quite well known. However, a more detailed understanding of molecular effects remains unclear. For example, the fracture surface work of polystyrene is almost twice as great as PMMA, but yet the molecular weight is considerably less than the cast PMMA polymer and the glass transition temperatures are quite near each other. The molar cohesion or cohesive energy density is not more than 10 percent different for these two polymers. However, we know that polystyrene crazes more obviously (since crazes are visible) than the PMMA polymers and this contributes greatly to the fracture surface work.

If one now considers only methacrylate polymers and compares them with respect to their glass transition temperatures as has been done in table 22, very little significance can be associated with glass transition temperatures. Even those polymers which are from 260°C to 300°C below their glass transition temperatures have significant differences in fracture surface work. Furthermore, iso-butyl methacrylate decreases in fracture surface work with decreasing temperature. Ethyl methacrylate has only a very small change in fracture surface work from room temperature to -196°C. The local conditions at the crack tip, particularly the large triaxial stresses govern the behavior of the material at the crack tip. The volume increase and temperature rise at the crack tip serve to locally decrease the difference between the real glass transition and actual temperature of the material. Thus glass transition temperatures, determined through measurements of expansion coefficients or damping peaks (from torsion pendulum data) on bulk polymers have no meaning with respect to polymer fracture.

Figure 45 Fracture Surface for Polyvinyl chloride Showing Crack Initiation at -196°C (Mag 100x). Crack propagated from left to right.

a) Slow crack growth

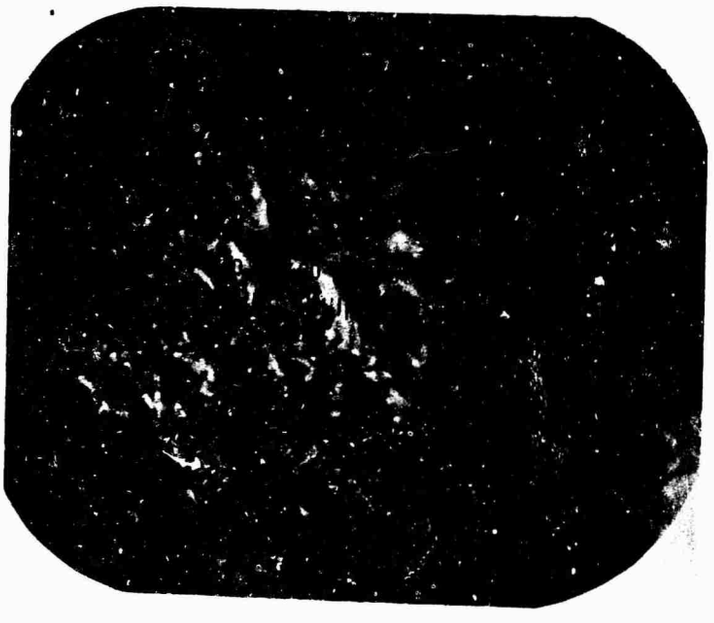

b) Rapid crack growth

Figure 46 Fracture Surfaces for Polyvinyl acetate at -196°C. (Mag. 100x) Crack propagated from left to right.

TABLE 21

Fracture Surface Work Measurements for Polyvinyl Chloride and Polyvinylacetate at -196°C

Material	Specimen Type*	Fracture Surface Work** (10^5 erg/cm^2)
Polyvinylchloride	Uniform Cantilever	21.22(1)
	Uniform Cantilever	17.47(1)
	Uniform Cantilever	20.09(1)
	Uniform Cantilever	22.52(1)
Polyvinylacetate	Uniform Cantilever	60.3 (1)
	Uniform Cantilever	52.8 (1)
	Uniform Cantilever	45.3 (1)
	Uniform Cantilever	49 (1)

*Dimensions b=.125"
h=1.2"

**Number of data points per specimen shown in parentheses.

TABLE 22

Relation Between Tg and Fracture Surface Work

Corresponding Temperature $(T_g - T_{exp})$ °C	Fracture Surface Work 10^5 erg/cm^2	Polymer
40	.6 to 9	iso-butyl methacrylate
48	4 (11)	ethyl methacrylate
80	2.57	PMMA
220	1.75	n-butyl methacrylate
261	.30	iso-butyl methacrylate
269	5.3 to 8.00 (12.5)	ethyl methacrylate
301	12 to 15	PMMA
199	60 to 100	methyl acrylate
283	17 to 22	vinyl chloride
225	45 to 60	vinyl acetate
75	4.5	polystyrene

One factor which has not been adequately treated is the effect of the environment on fracture surface work. Experiments are required in high vacuum as well as in atmospheres with controlled humidity or other controlled liquid environments. This will certainly influence the results and therefore the interpretation of the results. Another factor which will influence the fracture surface work at -196°C is the history of the material at the crack tip. For example, if a crack is formed at room temperature, as in our experiments, the material at the crack tip has been altered. For Plexiglas the polymer has been oriented and the measured fracture surface work at -196°C will reflect this pre-oriented structure. Future work should include measurements for cracks both initiated and propagated at -196°C so as to eliminate the material history at room temperature.

Chapter X

INFLUENCE OF MOLECULAR PRE-ORIENTATION BY COLD ROLLING ON POLYMER PHYSICAL PROPERTIES

Cold rolling of polymer sheets has been studied to determine structure and properties changes of a polymer when subjected to room temperature deformations. The influence of rolling on the stress-strain curve of polyethylene has been determined by Rothschild and Maxwell (46). Wilchinsky (47) showed that the brittleness temperature of polypropylene could be greatly reduced by cold rolling and also studied the changes in crystal orientation of polypropylene subjected to cold rolling (48). Gruenwald reported on changes in mechanical properties of a polycarbonate material after cold rolling (49).

In this study the rolling of plastic sheets was done on a laboratory 2 roll mill having 4.5" diameter rolls 6.3 inches in length. The reduction in thickness per pass through the rolls was dependent upon the material type but in general the sheet thickness was reduced .003 to .005 inches per pass. Greater reductions per pass can be made with more powerful rolling mills. A variety of polymers have thus far been studied including: Polycarbonate, ABS, hi-impact PVC, polyphenyleneoxide (Noryl), polysulfone, methylpentene (TPX polymer), Nylon, and polyethylene. The discussion here will primarily concern the studies on polycarbonates and ABS materials.

Although the rolling is performed at room temperature, a temperature increase occurs in the material during the rolling process as a result of the irreversible deformations. The surface temperature was measured for the polycarbonate (Lexan) sheet immediately after rolling by a surface pyrometer. This temperature increase is shown in Fig. 47 as the sheet was progressively rolled to 62 percent thickness reduction. The maximum temperature recorded was 115°F but this is not the maximum temperature of the sheet due to the delay time involved in the measurement.

Since all of the deformation is not permanent, there is some dimensional change in the rolled sheet after rolling. This dimensional change was measured for an ABS (Cycolac MS) sheet and a polycarbonate sheet and proved to be quite small. The sheets were reduced in thickness by 50 percent and the thickness was then measured as a function of time for 72 hours. After 7 hours the sheet thickness stabilized and remained constant and a total increase of 4 percent was measured for the ABS and an increase of 1.4 percent was measured for the polycarbonate sheet. The deformation of these sheets during rolling is 3-dimensional and, thus, as the thickness decreases there is an increase in length and width. For example, a Lexan sheet 0.248" thick, 3-7/8" wide and 5-5/8" long is changed to 0.124" thick, 4-1/2" wide and 10 1/2" long after rolling.

Stress-strain properties (elongation rate-0.2 in/min for all tests) have been measured for both uniaxially and biaxially rolled sheets. The biaxially rolled sheets were made by simply alternating the sheet direction 90 degrees for every pass through the rolling mill. Properties were measured both parallel and transverse to the rolling direction. Uniaxial stress-elongation curves for an ABS plastic are presented in Fig. 48 for various roll reductions. The measurements have been made parallel to the roll direction. The behavior of polycarbonates is almost identical and therefore the individual stress-strain curves are not presented. It can be observed that the yielding or necking and cold drawing become less evident as roll reduction increases and the curve at 27.6% shows an absence of the yield drop. This disappearance of the yield drop is shown in Fig. 49 for both polycarbonate, ABS and several other polymers.

In addition to the elimination of the formation of a neck prior to failure, stress whitening in the rubber modified polymers can be eliminated by prior roll reduction. For example, a series of ABS (Marbon GSE 1000) specimens are shown in Fig. 50 each having been uniaxially rolled to a different degree and then stressed in tension to fracture. It is obvious that the samples which have been reduced in thickness by 40 percent or more do not stress whiten prior to failure. This is most likely due to the high degree of molecular orientation occurring as a result of the rolling process.

The stress-elongation characteristics normal to the roll direction for uniaxially rolled sheets have been measured for ABS sheet and the results are presented in Fig. 51. The strength decreases very slightly and the elongation can be greater than for the virgin material. Thus, the transverse properties do not decrease as the properties in the roll direction are increasing and for this reason biaxial rolling can be easily performed. The results shown in Fig. 51 for ABS polymers are nearly identical for polycarbonates and other polymers exhibiting the same type of stress-strain curve in the virgin state.

The changes in strength for uniaxially and biaxially rolled ABS and polycarbonate materials are shown in Figs. 52 and 53 as a function of degree of rolling. The increase in strength for biaxially rolled material is less since approximately only one-half the orientation occurs in each direction for the same roll reduction. The reduction in transverse strength for Lexan at 20 percent roll reduction appears to be a real effect and correlates with a similar decrease in surface hardness as shown in Fig. 54. A suitable explanation is lacking at this time. The modulus of elasticity also changes for rolled materials. For example, the initial modulus for virgin Lexan (extruded sheet) was determined to by 3.43×10^5 psi and the value at 50 percent roll reduction was 4.5×10^5 psi.

Although the deformation produced by rolling appears permanent at room temperature, the deformation is recoverable at elevated temperatures. Polycarbonate rolled specimens were annealed for 5 hours at increasing temperatures as shown in Fig. 55. As the annealing temperature approaches the glass transition temperature the deformation is completely recovered.

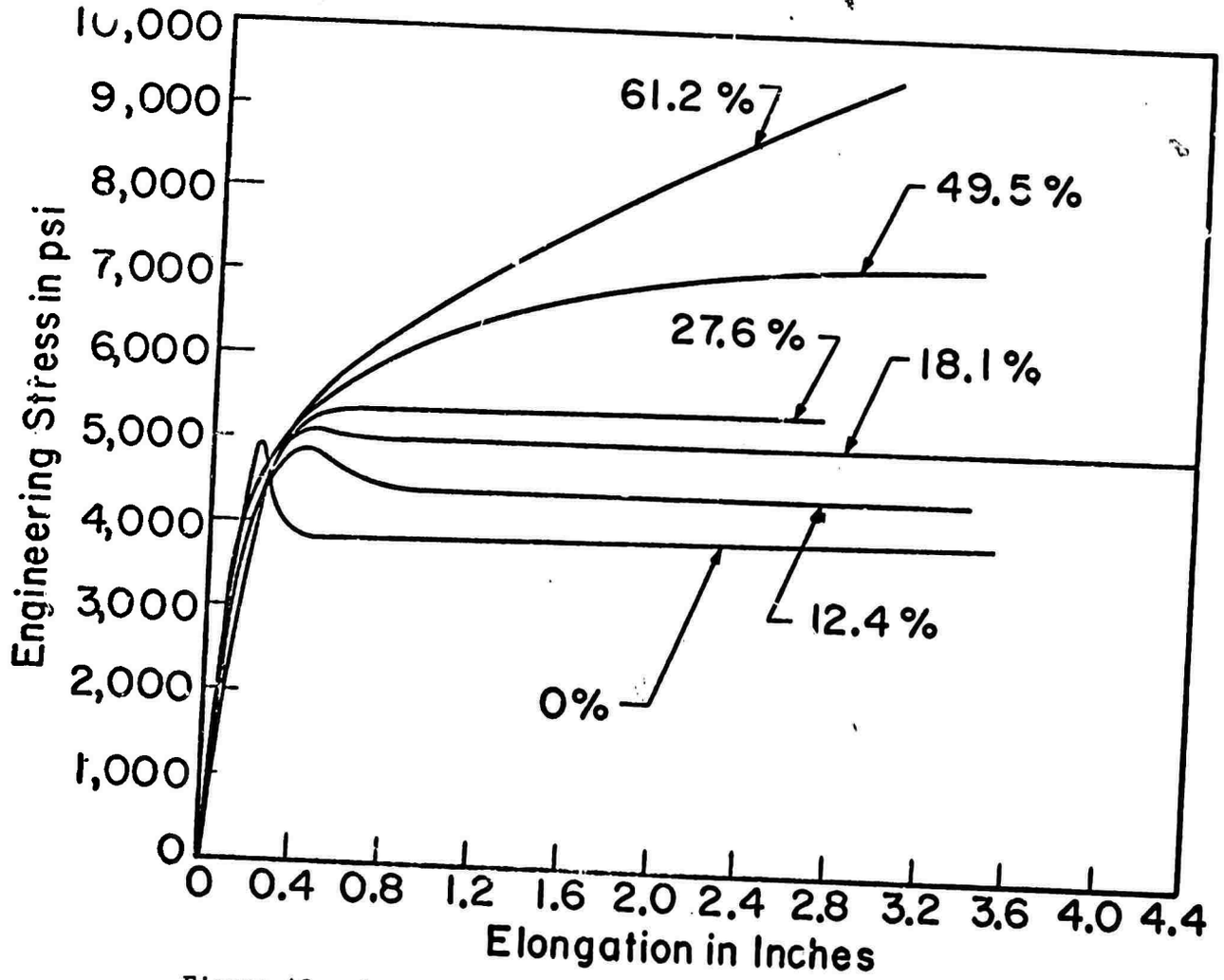

Figure 48. Stress-Elongation Curves for an ABS (Cycolac MS) polymer as a function of cold rolling thickness reduction, parallel to roll direction. (elongation rate = 0.2 in./min., gage length approximately 6 inches)

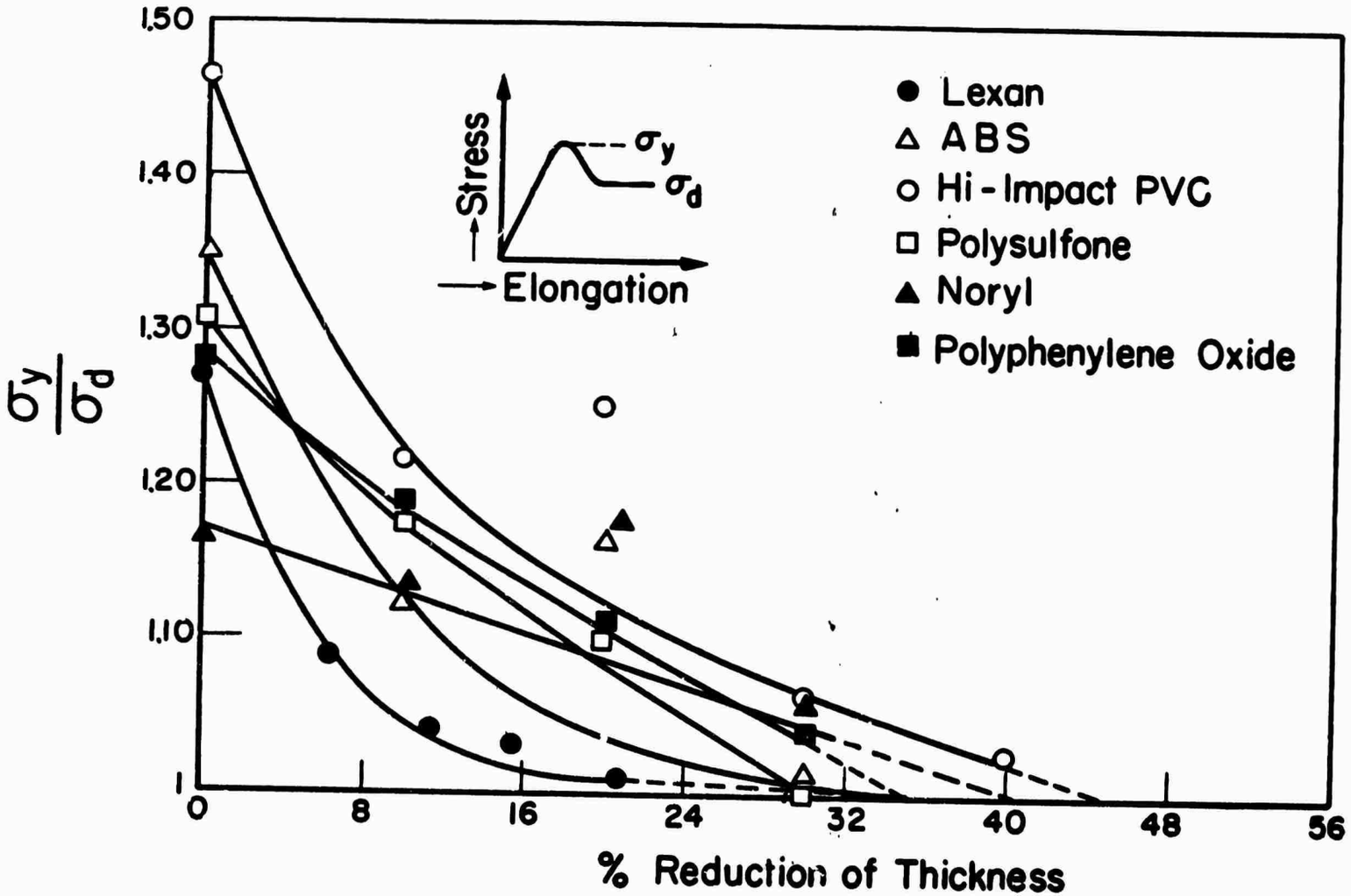

Figure 49. Relationship between the ratio of yield stress ($_y$) and draw stress ($_d$) and percent thickness reduction for several polymers.

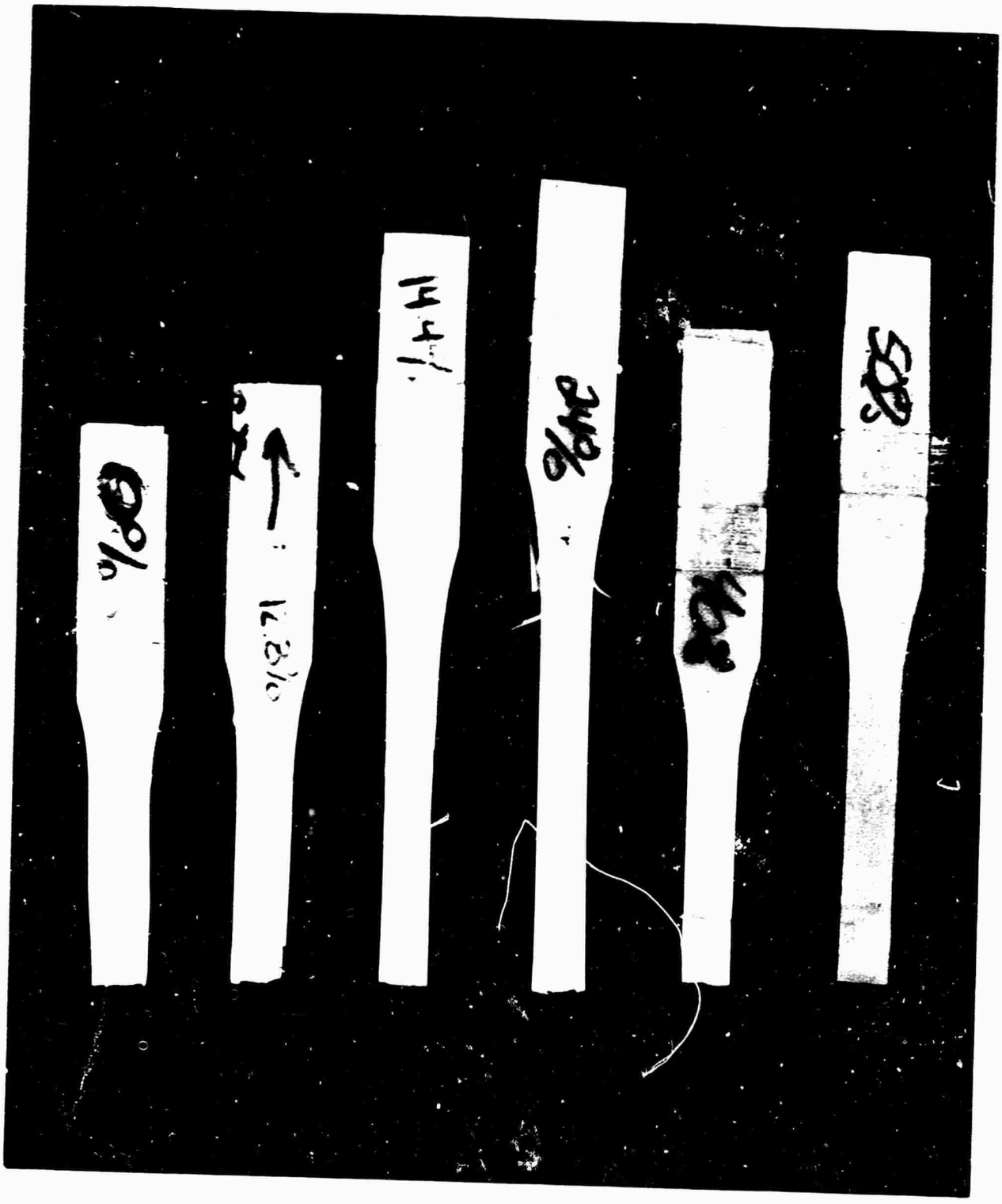

Figure 50 Cold Rolled ABS tensile bars showing reduction and elimination of stress whitening

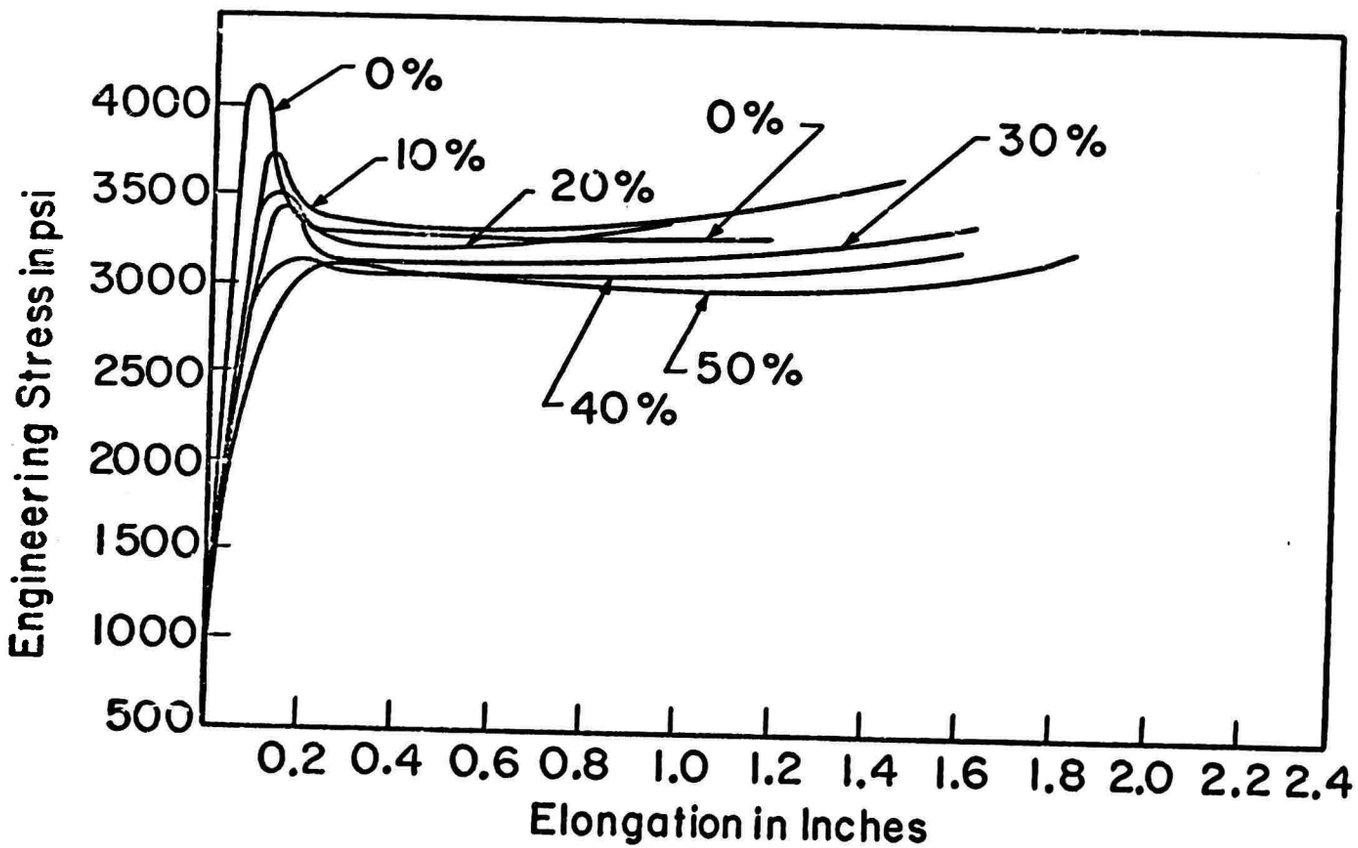

Figure 51. Stress-elongation curves for uniaxially rolled ABS polymers (Cycolac MS) tested at 90° to the roll direction (elongation rate = 0.2 ipm, gage length approximately 3 inches)

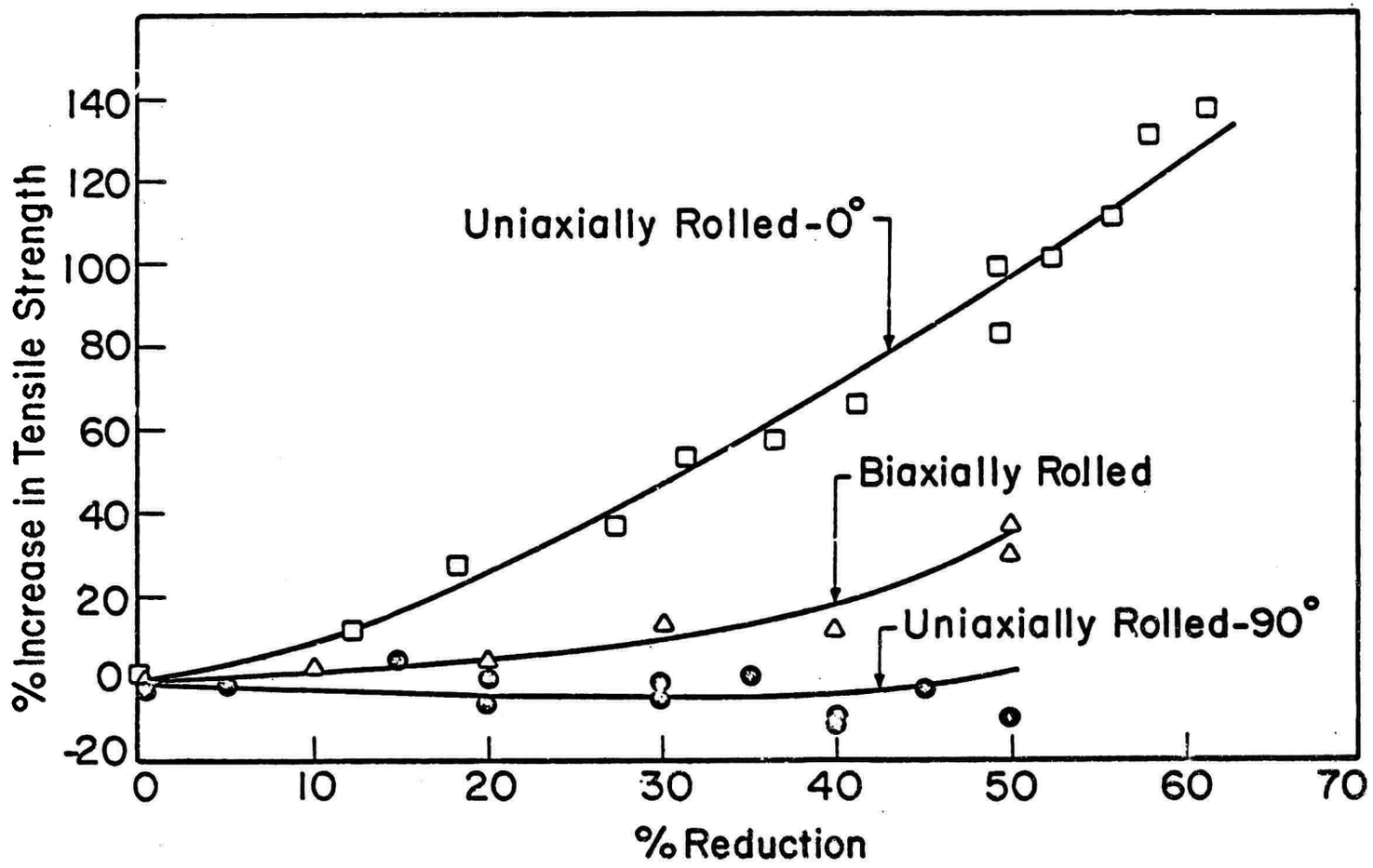

Figure 52. Change in tensile strength for uniaxially and biaxially rolled ABS (Cycolac MS)

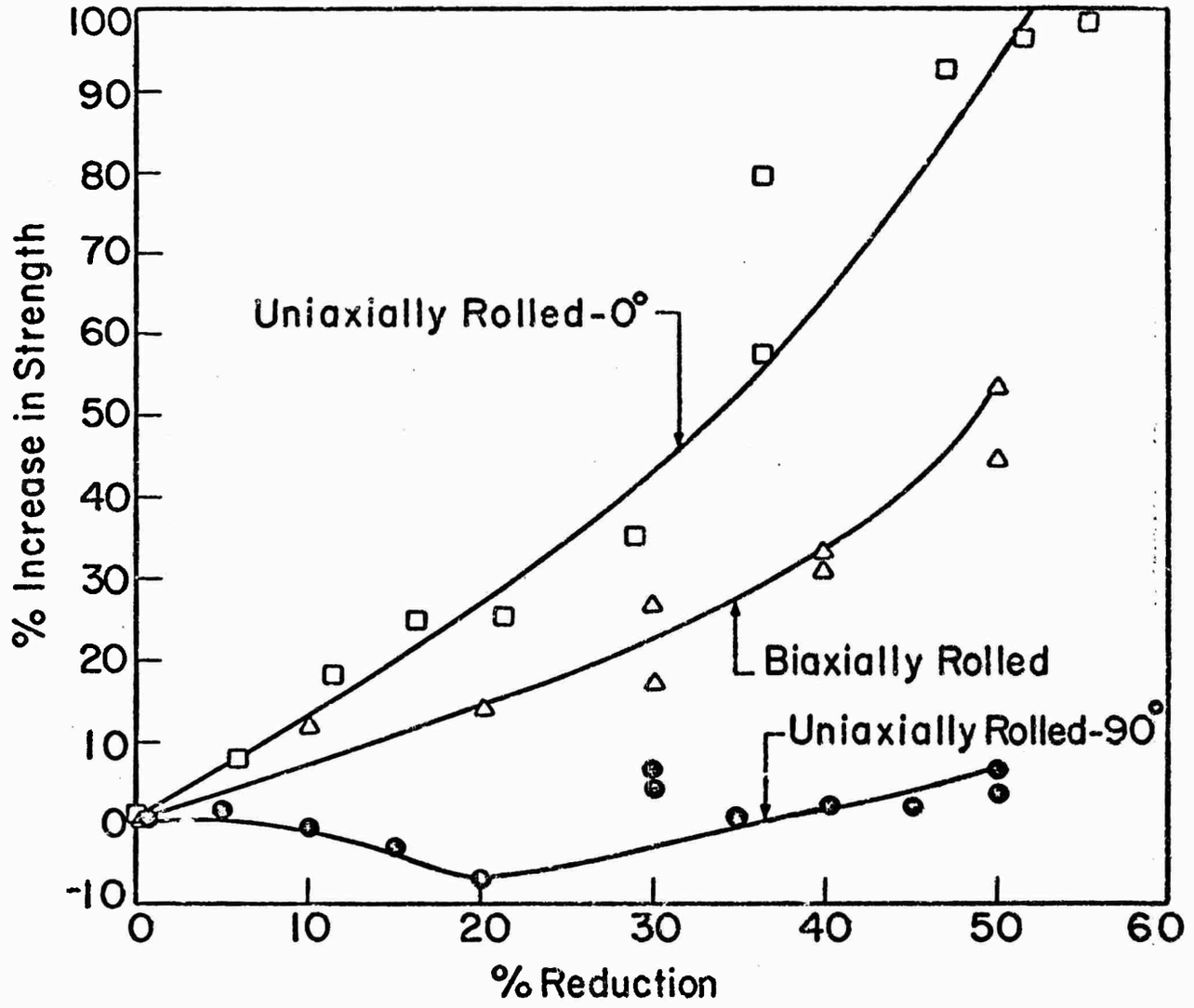

Figure 53. Change in tensile strength for uniaxially and biaxially rolled polycarbonate (Lexan)

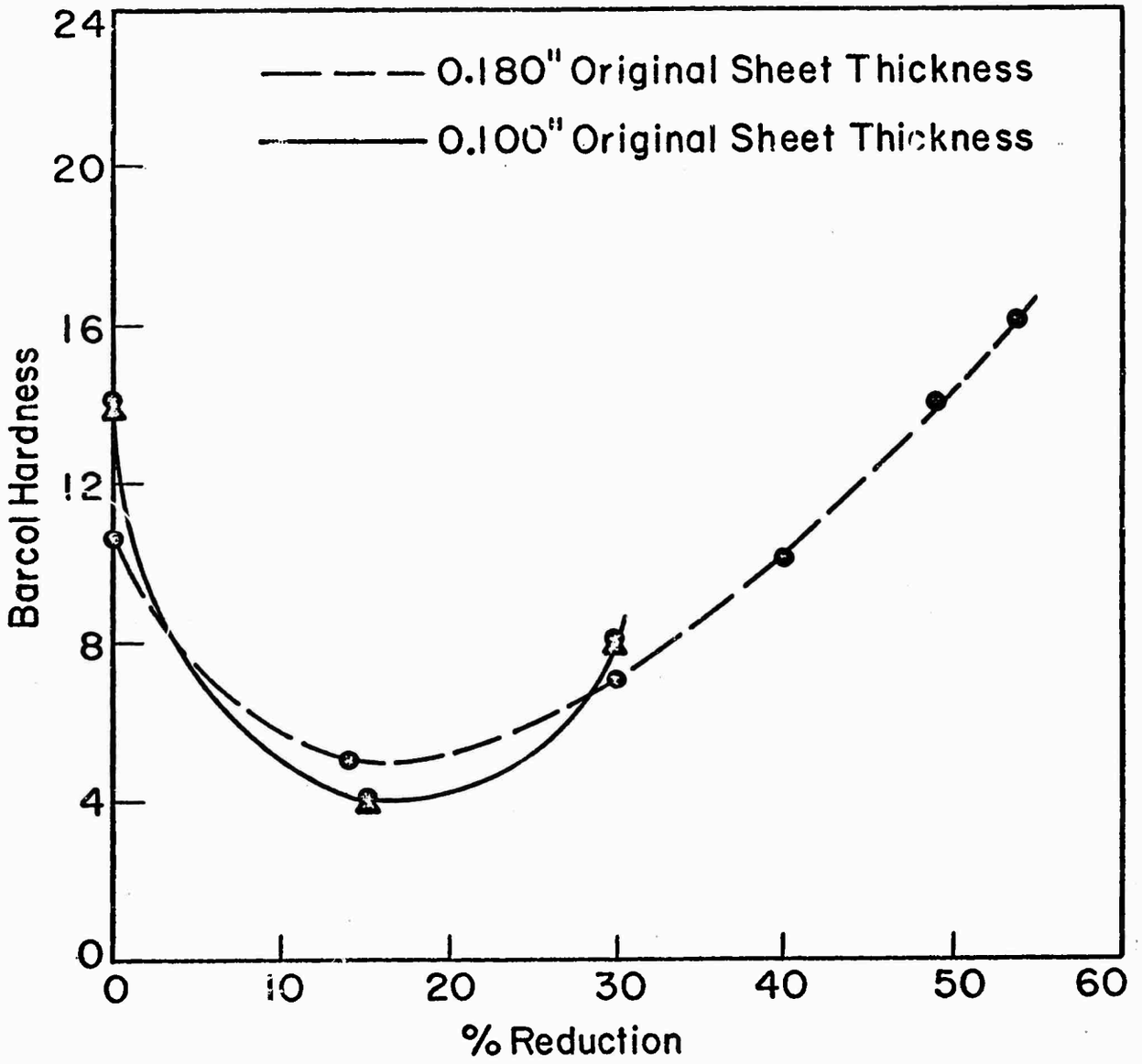

Figure 54. Barcol hardness as a function of roll reduction for a polycarbonate (Lexan) sheet

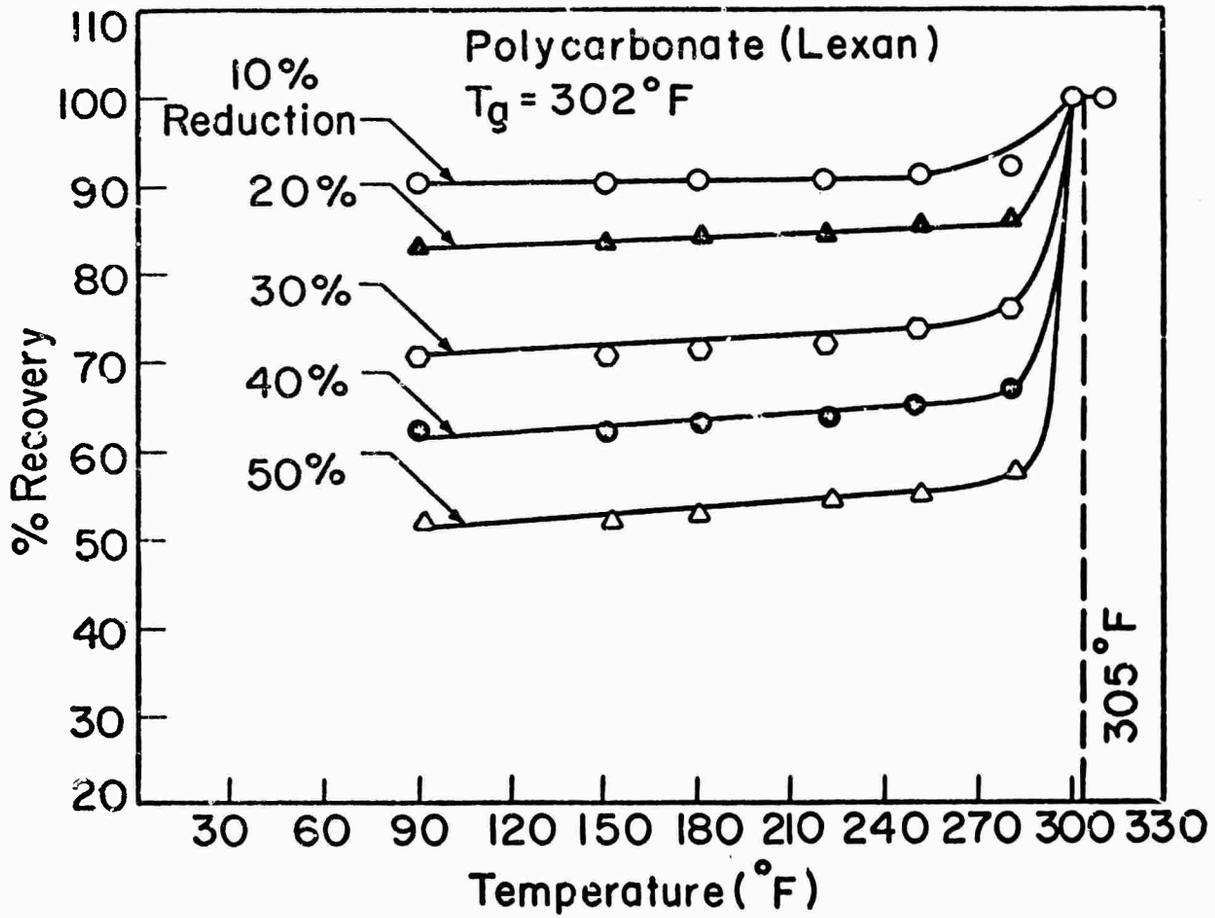

Figure 55. Percent recovery (thickness change) for cold rolled Lexan bars annealed for 5 hours at various temperatures

In conclusion, cold rolling of plastic sheets greatly increases the strength and impact resistance of the plastic sheet and allows for uniform extension rather than necking and cold drawing. The greatly increased values of Izod impact strength for uniaxially rolled Lexan are shown in Table 23. The impact strength appears to be a maximum at 10 percent roll reduction both parallel and perpendicular to the roll direction. Stress whitening can also be eliminated from rubber modified polymers by cold rolling.

TABLE 23

Izod Impact Strength Measurements

% Reduction of Thickness	Gage in Inch	Width in Inch	Energy in ft-lbs per Inch of Notch	Average Energy in ft-lbs per Inch of Notch
(A) Unidirectionally Rolled Polycarbonate (Lexan) Specimens Parallel to the Rolling Direction.				
0%	0.2425	0.403	1.485	1.505
0%	0.2425	0.405	1.525	
10%	0.227	0.396	19.450	19.22
10%	0.227	0.395	19.000	
20%	0.2025	0.401	18.550	18.705
20%	0.2028	0.397	18.860	
30%	0.1772	0.3978	16.300	16.62
30%	0.1774	0.394	16.950	
40%	0.1515	0.397	11.950	12.825
40%	0.1510	0.398	13.700	
50%	0.128	0.400	6.560	6.442
50%	0.128	0.402	6.326	
60%	0.105	0.397	5.325	5.277
60%	0.105	0.4035	5.230	
(B) Unidirectionally Rolled Polycarbonate (Lexan) Specimens Transverse to the Rolling Direction.				
10%	0.227	0.4055	17.900	18.175
10%	0.226	0.4020	18.450	
20%	0.203	0.4025	18.050	17.975
20%	0.2028	0.4022	17.950	
30%	0.177	0.3930	16.050	16.450
30%	0.177	0.3975	16.850	
40%	0.151	0.4040	15.500	14.875
40%	0.151	0.3945	14.250	
50%	0.128	0.4000	9.140	10.115
50%	0.128	0.3970	11.000	
60%	0.1045	0.3950	12.150	10.145
60%	0.1045	0.4040	8.140	

Chapter XI

TEMPERATURE MEASUREMENT AT A CRACK TIP

Heat generation and a temperature rise at the crack tip can play an important role on fracture surface work. R. P. Kambour and R. E. Barker (50) discussed the temperature rise at the crack tip theoretically with the expression

$$\Delta T = 212\left[1-4i^2\operatorname{erfc}\frac{\ell}{2(kt)^{1/2}}\right]$$

where ΔT: temperature rise (°C)

2ℓ: sheet thickness

k: thermal diffusivity

t: time interval between the initiation of the craze and its cleavage

i: $\sqrt{-1}$

This expression shows that no appreciable temperature rise can occur when crack velocities are below 1 cm/sec. Between 10 and 100 cm/sec ΔT begins to rise rapidly and approaches its maximum 212°C only in the range between 10^4 and 10^5 cm/sec.

In order to investigate heat generation and temperature change around the crack tip, liquid crystal coatings were applied to the surface of a tensile bar specimen. This specimen was used since the side slots of a double cantilever beam specimen made direct transmission of temperature rise around the crack tip to the liquid crystal coating difficult.

The liquid crystal in this experiment was a semi-solid mixture obtained from the Pressure Chemical Company and its temperature range and color response was 24.2°C (red), 24.7°C (yellow), 25.1°C (green), to 26°C (blue). This liquid crystal could be applied directly to the specimen surface; however, in order to improve contrast a black undercoat was applied. The application procedure was as follows: the specimen surface was washed with water, and the black water base paint was then uniformly applied by brush. After drying the black paint, a thin liquid crystal coating was applied uniformly with a soft brush. In coating the specimen a heat gun was used to decrease the viscosity of the liquid crystal. The width of the tensile specimen was 3 inches and the thickness approximately 1/4 inch. An edge crack was started to direct the fracture propagation.

Specimens were tested in the Instron Testing Machine. Room temperature was adjusted to 24.2°C so that the liquid crystal coating appeared a uniform red color. A PMMA polymer and polystyrene polymer were tested without detection of any color change during the crack initiation and propagation. A high density polyethylene and an ABS polymer were also investigated. Since these materials are ductile, the cross section area at the edge crack along the entire specimen width was grooved (on one side only) so the specimen thickness was reduced approximately 50 percent. Upon fracture of these materials a temperature increase was observed on either side of the crack. The color changed through the spectrum of the coating so that at least a 2°C increase was detected. The maximum value was not therefore obtained. Although this study has been very brief, the technique is feasible for measuring local temperature increases and should be further developed.

References

1. Orowan, E., "Report on Progress in Physics," Physical Society of London, 12, 12, 185 (1949).

2. Berry, J. P., SPE Transactions, 1, 3 (1961).

3. Broutman, L. J., and McGarry, F. J., J. App. Poly. Sci., 9, 585 (1965).

4. Broutman, L. J., and McGarry, F. J., J. App. Poly. Sci., 9, 609 (1965).

5. Griffith, A. A., Phil. Trans. Roy. Soc., A221, 163 (1920).

6. Berry, J. P., J. Poly. Sci., 50, 331 (1961); 50, 107 (1961).

7. Berry, J. P., J. Poly. Sci. A1, 993 (1963).

8. Berry, J. P., J. App. Phys. 33, 1741(1962); 34, 62 (1963).

9. Benbow, J. J., and Roesler, F. C., Proc. Phys. Soc., 70B, 201 (1957).

10. Ripling, E. J., and Mostovoy, S., J. App. Poly. Sci., 10, 1351 (1966).

11. Higuchi, M., Repts. of Res. Inst. for Appl. Mech., Kyushu Univ., 6, 173 (1958).

12. Berry, J. P., Nature, 185, 91 (1960).

13. Wolock, J., and Newman, S. B., "Fracture Topography," in Fracture Processes in Polymeric Solids, Interscience, New York, N. Y.

14. Kambour, R. P., "Mechanism of Fracture in Glassy Polymers," Part I, J. Poly. Sci., 3, 1713 (1965); Part II, J. Poly. Sci., 4, 17 (1966); Part III, J. Poly. Sci., 4, 349 (1966).

15. Berry, J. P., J. Poly. Sci., 2, 4069 (1964).

16. Benbow, J. J., Proc. Phys. Soc., 78, (1961).

17. "Study of Mechanisms of Armor Penetration Resistance," Contract DA-04-495-AMC-93(R), 30, Jan. 1964.

18. Svensson, N. L., Proc. Phys. Soc., 77, 876 (1961).

19. Vincent, P. I., and Gotham, K. V., Nature 210, 1254, 1966.

20. Cotterell, B., Applied Materials Research, Oct. 1965.

21. "Closed Loop," published by MTS Systems Corp. Vol. 1, No. 5, 1966.

22. Mostovoy, S. and Ripling, E. J., "Fracture Controlling the Strength of Composites," Final Report for the Naval Air Systems Command, Contract No. N00019-67-C-0493, Feb. 1968.

23. Flory, P. J., J. Am. Chem. Soc. 67, 2048, (1945).

24. McGarry, F. J., and Selfridge, G. C., Proceedings 19th Annual Technical and Management Conference, Reinforced Plastics Div., Society of the Plastics Industry, Inc., 1964.

25. Irwin, G. R., and Kies, J. A., Welding J. Res. Supp. 33, 1935, (1954).

26. A. S. Burhans et al, 21st Annual SPE Meeting, March, 1965.

27. Wilchinsky, Z. W., SPE Journal, March 1966.

28. Rothschild, P. H., and Maxwell, B., J. App. Poly. Sci. 5 S-11, (1961).

29. Gruenwald, G., Modern Plastics, Sept. 1960.

30. Wilchinsky, Z. W., J. App. Poly. Sci., 7 1963.

31. J. J. Gilman, "Direct Measurements of the Surface Energies of Crystals," J. App. Phys., 31, 2208 (1960).

32. A R. C. Westwood and T. T. Hitch, "Surface Energy of {100} Potassium Chloride," J. App. Phys., 34, 3085 (1963).

33. S. M. Wiederhorn, "Fracture Surface Energy of Soda-Lime Glass," in Materials Science Research, Vol. 3, Plenum Press, (1966).

34. Guernsey, R. and Gilman, J., Experimental Mechanics, August 1961.

35. Timoshenko, S., Strength of Materials, D. Van Nostrand Company, Inc., Third Edition, 1955, p. 318.

36. O'Donnell, W. J., "The Additional Deflection of a Cantilever Due to the Elasticity of the Support," Journal of Applied Mechanics, Sept. 1960.

37. S. Mostovoy, P. B. Crosley, and E. J. Ripling, "Use of Crack-Line Loaded Specimens for Measuring Plane-Strain Fracture Toughness," Journal of Materials, 2 661 (1967).

38. Srawley, J. E., and Gross, P., NASA TN D-3820 Feb. 1967.

39. Wall, L. A., and Brown, D. W., J. Phys. Chem., 61, 129, 1957.

40. Geil, P., Polymer Single Crystals, Interscience Publishers, New York, N. Y., 1963 (p. 209).

41. Newman, S. and Cox, W. P., J. Poly. Sci. 46, 29, (1960).

42. Rogers, S. and Mandelkern, J. Phys. Chem., 61, 935, (1957).

43. Halden, R. A., and Simha, R., J. App. Physics, 39, 3, 1890.

44. Roe'ling, J. A., Polymer, 7, 619, (1966).

45. Hoff, E., Robinson, R. W. and Wilbourr, H. A., J. Poly. Sci., 18, 161 (1955).

46. P. H. Rotschild and B. Maxwell, J. App. Poly. Sci., 5, S-11, 1961.

47. Z. W. Wilchinsky, "Orientation in Cold Rolled Propylene," J. App. Poly. Sic. 7 (1963).

48. Z. W. Wilchinsky, "Reduction of Brittleness in Polypropylene by Cold Rolling," SPE Journal, March 1966.

49. G. Gruenwald, "Cold-formed Polycarbonate Resin-Properties and Applications," Modern Plastics, Sept. 1960.

50. Kambour, R. P., and Barker, R. E., J. Poly. Sci., 4, 359 (1966).

APPENDIX I

Derivation of Fracture Toughness for both Fixed Load and Fixed Specimen Displacement

If for a given applied load f, the specimen end is displaced δ, the specimen compliance is defined as

$$\delta = cf \tag{I-1}$$

The elastic strain energy stored in the specimen is

$$U = \frac{1}{2} f\delta = \frac{1}{2} cf^2 \tag{I-2}$$

The increment of strain energy consumed in the crack extension $d\ell$ assuming fixed specimen ends is

$$\left.\frac{\partial U}{\partial \ell}\right|_{\delta \text{ fixed}} = \frac{1}{2} f^2 \frac{\partial c}{\partial \ell} + cf \frac{\partial f}{\partial \ell} \tag{I-3}$$

(I-4)

since δ=constant,

$$\frac{\partial \delta}{\partial \ell} = 0 = f \frac{\partial c}{\partial \ell} + c \frac{\partial f}{\partial \ell}$$

therefore

$$C \frac{\partial f}{\partial \ell} = -f \frac{\partial c}{\partial \ell} \tag{I-5}$$

substituting (5) into (3)

$$\left.\frac{\partial U}{\partial \ell}\right|_{\delta \text{ fixed}} = \frac{1}{2} f^2 \frac{\partial c}{\partial \ell} - f^2 \frac{\partial f}{\partial \ell} = -\frac{1}{2} f^2 \frac{\partial c}{\partial \ell} \tag{I-6}$$

the increment of surface energy in the crack extension $d\ell$ is

$$\frac{\partial s}{\partial \ell} = 2\gamma\omega \tag{I-7}$$

Applying the Griffith criterion - $\frac{\partial U}{\partial \ell} = \frac{\partial s}{\partial \ell}$ yields

$$2\gamma\omega = \frac{1}{2} f^2 \frac{\partial c}{\partial \ell}$$

$$G = 2\gamma = \frac{f^2}{2\omega} \frac{\partial c}{\partial \ell} \tag{I-8}$$

One can also arrive at this relationship by assuming that during crack extension the load rather than the specimen ends remain fixed. Thus

$$U = \frac{1}{2} f\delta = \frac{\delta^2}{2c} \tag{I-9}$$

$$\left.\frac{\partial U}{\partial \ell}\right|_f = \frac{\delta}{c} \frac{\partial \delta}{\partial \ell} - \frac{\delta^2}{2c^2} \frac{\partial c}{\partial \ell} \tag{I-10}$$

Since f=constant

$$\frac{\partial f}{\partial \ell} = 0 = \frac{1}{c} \frac{\partial \delta}{\partial \ell} - \frac{\delta}{c^2} \frac{\partial c}{\partial \ell} \tag{I-11}$$

$$\frac{\partial \delta}{\partial \ell} = \frac{\delta}{c} \frac{\partial c}{\partial \ell} \tag{I-12}$$

Substituting (12) into (10):

$$\left.\frac{\partial U}{\partial \ell}\right|_f = \frac{\delta^2}{c^2} \frac{\partial c}{\partial \ell} - \frac{\delta^2}{2c^2} \frac{\partial c}{\partial \ell} = \frac{\delta^2}{2c^2} \frac{\partial c}{\partial \ell} \tag{I-13}$$

However, at the same time, the force f does the work

$$dL = f\,d\delta = f^2 dc \tag{I-14}$$

From the Griffith criterion:

$$ds = dL - (dU)_f \tag{I-15}$$

$$ds = f^2 dc - \frac{f^2}{2}\, dc = \frac{f^2}{2}\, dc \tag{I-16}$$

$$\text{or} \quad \frac{\partial s}{\partial \ell} = \frac{f^2}{2}\,\frac{\partial c}{\partial \ell} \tag{I-17}$$

$$\text{thus} \quad 2\gamma\omega = \frac{f^2}{2}\,\frac{\partial c}{\partial \ell} \tag{I-18}$$

$$\text{or} \quad G = 2\gamma = \frac{f^2}{2\omega}\,\frac{\partial c}{\partial \ell} \tag{I-19}$$

APPENDIX II

Determination of Fracture Surface Work for Uniform Cleavage Specimen

The deflection of a cantilever beam is expressed as:

$$\delta_{exp} = \frac{f}{3EI} \left[\ell^3 + 1.8h\ell^2 + 2.08h^2\ell + 0.216h^3\right] \qquad \text{(II-1)}$$

The strain energy, U, for the cleavage specimen is thus

$$U = \frac{f}{2}(2\delta_{exp}) = f\delta_{exp} \qquad \text{(II-2)}$$

or

$$U = \frac{f^2}{3EI} \left[\ell^3 + 1.8h\ell + 2.08h^2\ell + .216h^3\right] \qquad \text{(II-3)}$$

$$\frac{\partial U}{\partial \ell} = \frac{f^2}{3EI} \left[3\ell^2 + 3.6h\ell + 2.08h^2\right] \qquad \text{(II-4)}$$

$$\frac{\partial s}{\partial \ell} = 2\gamma\omega \qquad \omega = \text{crack width} \qquad \text{(II-5)}$$

Using the Griffith criterion:

$$2\gamma\omega = \frac{f^2}{3EI} \left[3\ell^2 + 3.6h\ell + 2.08h^2\right] \qquad \text{(II-6)}$$

$$\gamma = \frac{3f\delta_{exp}}{6EI\omega\ell} \frac{f(\ell^3 + 1.2h\ell^2 + 0.693h^2\ell)}{\delta_{exp}} \qquad \text{(II-7)}$$

$$= \frac{3f\delta_{exp}}{2\omega\ell} \frac{f/3EI(\ell^3 + 1.2h\ell^2 + 0.693h^2\ell)}{\delta_{exp}} \qquad \text{(II-8)}$$

$$\gamma = \frac{3f\delta_{exp}}{2\omega\ell} \quad \frac{f/3EI[\ell^3 + 1.2h\ell^2 + .693h^2\ell]}{f/3EI[\ell^3 + 1.8h\ell^2 + 2.08h^2\ell + 2.16h^3]} \qquad \text{(II-9)}$$

$$\gamma = \frac{3f\delta_{exp}}{2\omega\ell} \quad \left[\frac{\ell^3 + 1.2h\ell^2 + 0.693h^2\ell}{\ell^3 + 1.8h\ell^2 + 2.08h^2\ell + .216h^3}\right] \qquad \text{(II-10)}$$

APPENDIX III

Comparison of Data Analysis Techniques for Uniform Cantilever Beam Specimens

In the method of data analysis represented by Eq. 10 of the report

$$\gamma = \frac{f\delta n}{2\ell\omega} \qquad (10)$$

two graphs are required. The first graph is to determine the value of n from

$$f = \frac{a\delta}{\ell^n} \qquad (6)$$

so $\log f/\delta = \log a - n \log \ell$

and $\log f/\delta$ is plotted versus $\log \ell$ to determine n. This is shown in Fig. III-1 for the data represented in table III-1. The value of n is determined to be 2.70. In Fig. III-2 $f\delta/\omega$ is plotted versus ℓ and the slope of this straight line is therefore $2\gamma/n$ and since n is known, γ can be determined. The value of γ is determined to be 2.05×10^5 erg/cm^2 by a least squares fit to the data.

The second method of analysis is based on Eq. 35.

$$\gamma = \frac{3f\delta_{exp}}{2\omega\ell} k \qquad (35)$$

where k is determined from Fig. 14. The results are shown tabulated in table III-1 and the average value of γ is 2.38×10^5 erg/cm^2.

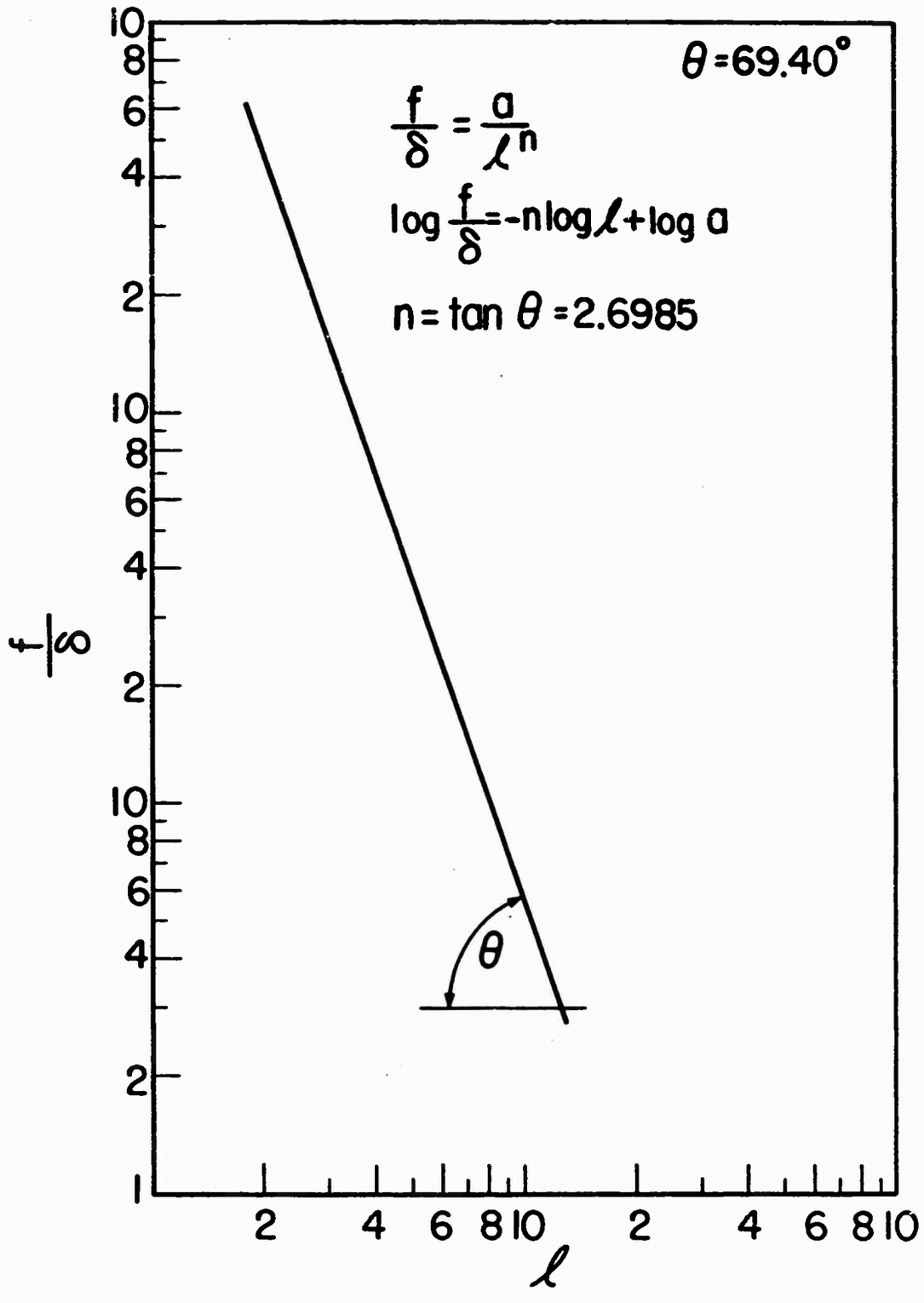

Figure III-1 Plot to Determine the Value n from $f=\frac{a\delta}{\ell^n}$

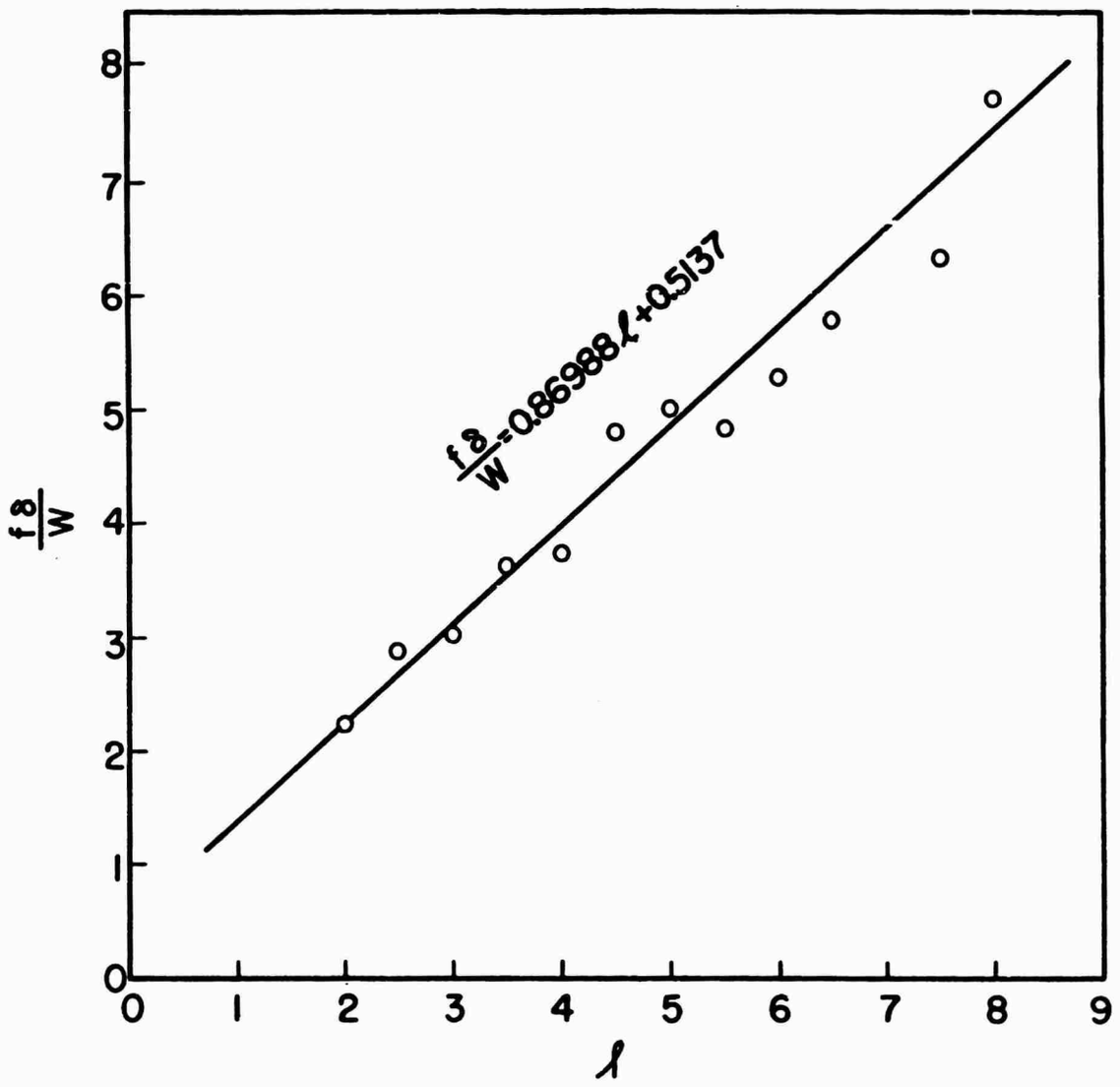

Figure III-2. Plot to determine the value of Fracture Surface Work

Table III-1

Data for Uniform Cantilever Beam Specimens

f lbs.	δ inches	ℓ inches	ω inches	3k	γ lb/in	γ erg/cm^2	f/δ	fδ/ω
10.8	0.026	2.0	0.1244	3x0.8297	1.4015	2.45×10^5	415.3846	2.2572
9.6	0.0395	2.5	0.1316	3x0.8595	1.4859	2.60×10^5	243.0379	2.8814
8.1	0.054	3.0	0.1442	3x0.8812	1.3364	2.34×10^5	150.00	3.0332
7.2	0.075	3.5	0.1446	3x0.8975	1.3980	2.45×10^5	98.6301	3.6348
6.15	0.0885	4.0	0.1458	3x0.9098	1.2737	2.23×0^5	68.9265	3.7331
5.7	0.1125	4.5	0.1336	3x0.9192	1.4708	2.57×0^5	50.6666	4.8001
4.7	0.1255	5.0	0.1176	3x0.9275	1.3956	2.44×10^5	38.3673	5.0161
4.2	0.1475	5.5	0.1280	3x0.9340	1.2327	2.16×10^5	28.4745	4.8378
3.95	0.1768	6.0	0.1326	3x0.9395	1.2389	2.17×10^5	22.3416	5.2709
3.75	0.2080	6.5	0.1350	3x0.9440	1.2585	2.20×10^5	18.0288	5.7777
4.00	0.269	7.0	0.1361	3x0.9480	1.6059	2.81×10^5	14.8698	7.9059
3.7	0.3058	7.5	0.1787	3x0.9515	1.2048	2.11×10^5	12.0994	6.3318
3.5	0.3465	8.0	0.1568	3x0.9565	1.3842	2.42×10^5	10.1010	7.7346
				Ave.	1.36053 lb/in	2.381×10^5 erg/cm^2		

APPENDIX IV

Load-deflection Curves and Fracture Surfaces

The load-deflection curves and the fracture surfaces are both very important experimental records in the study of fracture. By closely observing load-deflection curves and fracture surfaces and establishing a one-to-one relationship between them we can ascertain how cracks are propagated and thus have a better understanding of the fracture mechanisms. Some of the load-deflection curves and the fracture surface photographs are shown and correlations between them are discussed.

As mentioned in previous sections, there are two principal types of crack propagation: continuous and discontinuous. The first type of crack propagation can be observed in commercial cast Plexiglas or molded PMMA when tested at room temperature. The typical load-deflection curve of a tapered cast Plexiglas specimen is shown in Fig. 15, Chapter VI. The fracture surface picture can be seen in Fig. 34-a, Chapter IX. In this case the crack propagation was very stable. The applied load and the crack velocity were constant. The fracture surface appearance was constant over the entire length.

A typical example of discontinuous crack propagation is observed in polystyrene. The load-deflection curve and fracture surface picture are shown in Fig. IV-1. The specimen used here was a tapered cleavage specimen. As marked in the figure the initial crack tip position was "A-1". While the load and the deflection were increasing from "0" to "a-2" on the load-deflection curve, the crack tip slowly started to move from "A-1" to "A-2" in the picture. When the crack tip propagated to "A-2", instability took place and the crack jumped to "B-1" in the picture. The load decreased from "a-2" to "b-1". Between "A-2" and "B-1" the crack velocity was extremely high. Therefore, the cross head separation rate could not follow the crack length extension rate to keep the same load, and the load decreased. Again, while the load and the deflection were increasing from "b-1" to "b-2" the crack tip slowly moved from "B-1" to "B-2", and at "B-2" instability took place again and the crack jumped from "B-2" to "C-1". In the fracture surface photograph one also can see the finger nail marks between "B-2" and "C-1" or between "D" and "E". These marks show the places where the cracks were temporarily arrested. This temporary arrest is a result of local toughening or a material inhomogeneity but the stored energy is still sufficient to repropagate the crack. The crack propagated in similar mode from "C-2" to "D" and from "D" to "E" and so on until complete separation of the bar. The average measured fracture surface work value was 3.59×10^5 erg/cm^2.

Fig. IV-2 shows a very unusual crack propagation for a commercial molded polystyrene using a tapered cleavage specimen. Initial crack tip position was at "A" in the picture. While the load and the deflection were increasing from "0" to "b" on the load-deflection curve, at a point "a" on the curve the crack slowly started to propagage from "A" with gradually

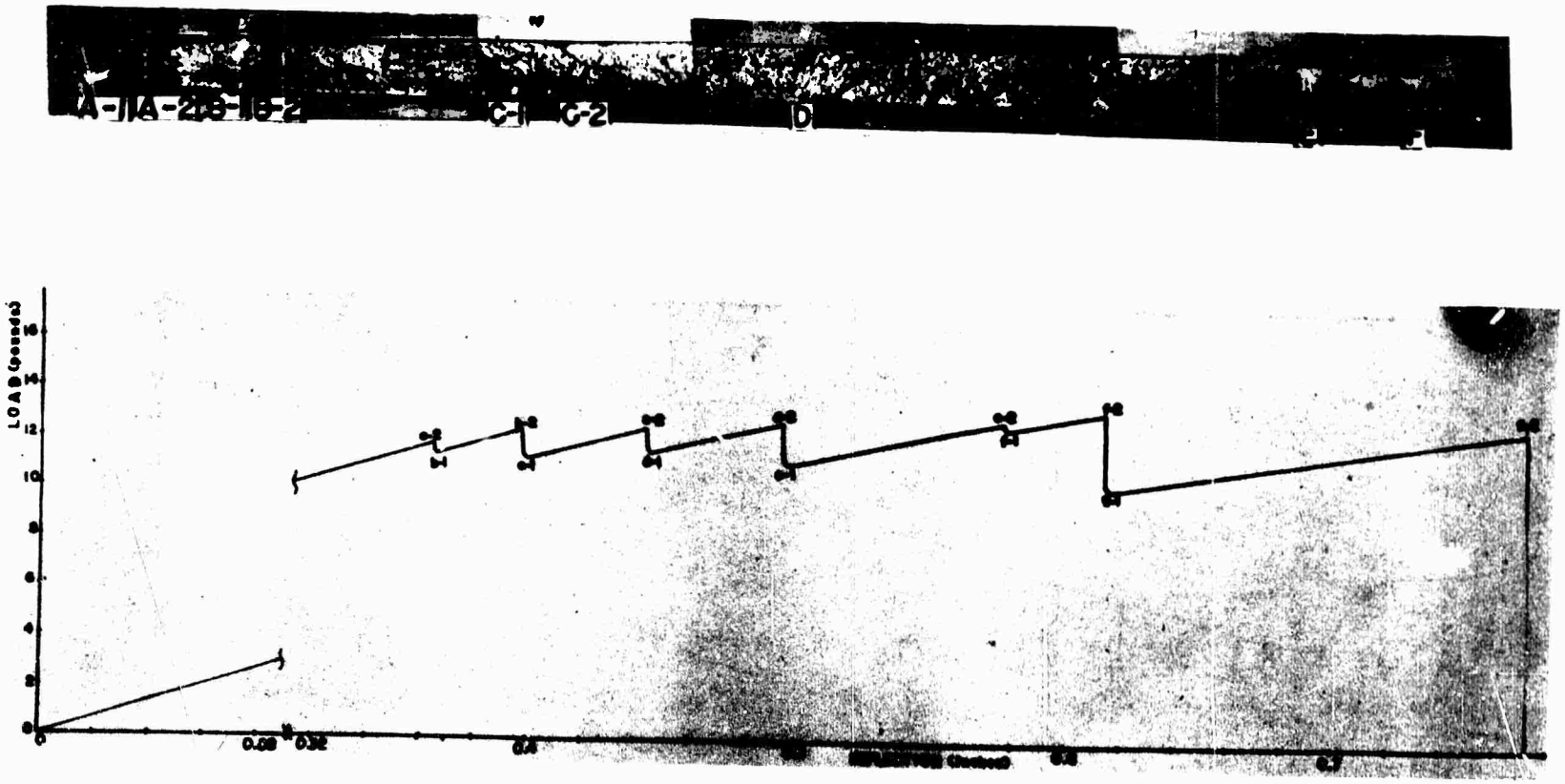

IV-1 Load-Deflection Curve and Fracture Surface of Commercial Polystyrene at Room Temperature. Specimen Type: Tapered Double Cantilever Beam Cleavage Specimen

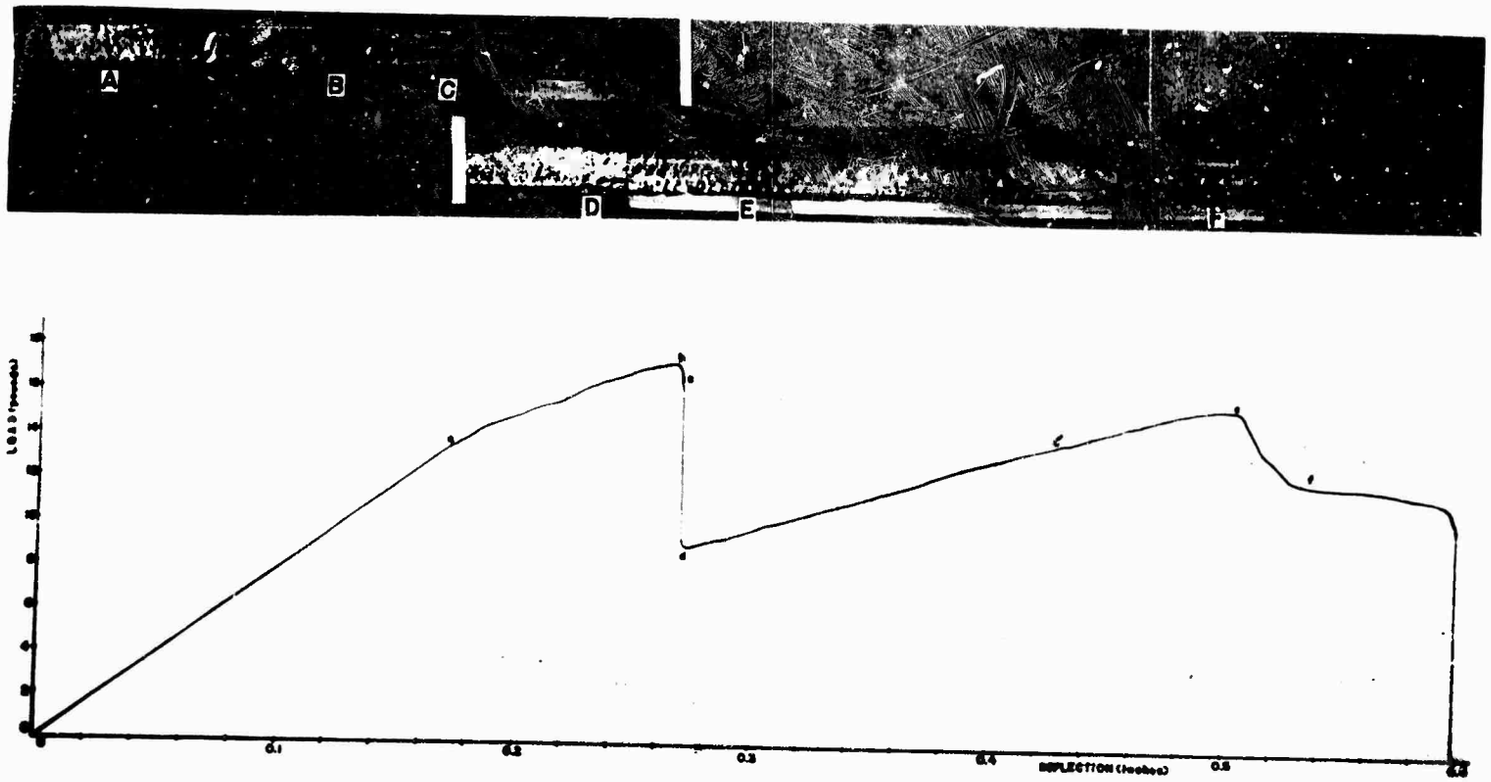

IV-2 Load-Deflection Curve and Unusual Fracture Surface of Commercial Polystyrene at Room Temperature. Specimen type: Tapered Double Cantilever Beam Cleavage Specimen

increasing crack velocity. At "b" on the curve the crack started to propagate rapidly. At "c" on the curve instability took place and the crack jumped from "C" to "D" on the fracture surface picture. Then the crack was arrested at "D". While the load and the deflection were increasing from "d" to 'd' on the load-deflection curve there was no crack propagation, and at 'd' the crack slowly started to propagate from "D" to "E" on the fracture surface. At "e" the crack started to propagate quickly but steadily. From "f" to the end of the specimen, the crack propagated in a steady continuous mode. The measured fracture surface work values were 6.32×10^5 erg/cm^2 at "b", 4.49×10^5 erg/cm^2 from "f" to the end of the bar. A detailed fracture surface picture of the smooth surface after "f" was shown in Fig. 21, b.

Fig. IV-3 is the case of polystyrene ($\bar{M}_w$=53,211) with a tapered cleavage specimen. Initial crack tip position was at "A". One can see the crack arrested line on the fracture surface. When the load and the deflection were increased to "a-2" on the load-deflection curve, instability took place and the crack propagated to "B". In this specimen the crack tip ran out of the median plane and perhaps the machined groove was not sufficient to contain the crack. The crack width increased causing the resistance to crack propagation to increase, and the crack was arrested at "B". While the load and the deflection were increased again from "b-1" to "b-2", the crack propagation direction returned to the median plane. At "b-2" instability took place and the crack propagated again from "B" to "C". This repeated itself along the fracture surface. The average measured surface work value was 3.71×10^3 erg/cm^2.

The load-deflection curve and the fracture surface picture of the isotactic amorphous polystyrene tested at room temperature are shown in Fig. IV-4. The type of specimen was the uniform double cantilever beam cleavage specimen. The initial crack tip position is marked "A" in the picture. While loading, the crack started to propagate at "a" with extensive amount of crazing and at "B" the crack jumped slightly to "C". At "C" instability took place, and the crack started to propagate rapidly with crazing accompanying the crack propagation. At "D" the resistance to crack propagation increased and the crack propagation velocity slowed down but the crack was not arrested. The crack continuously and slowly propagated from "D" to "E". At "E" instability again took place and the crack jumped with very high speed to the end of the specimen. When crazing is involved in fracture, the crack propagation becomes very complex. It is necessary to study further the role of crazing in fracture. The measured fracture surface work was 7.92×10^5 erg/cm^2 at "b".

The load-deflection curve and the fracture surface appearance of polyethyl methacrylate tested at room temperature are shown in Fig. IV-5. The crack propagation mode is classified as the continuous mode. The marks "A", "B" and "C" show the crack tip position while the crack was continuously

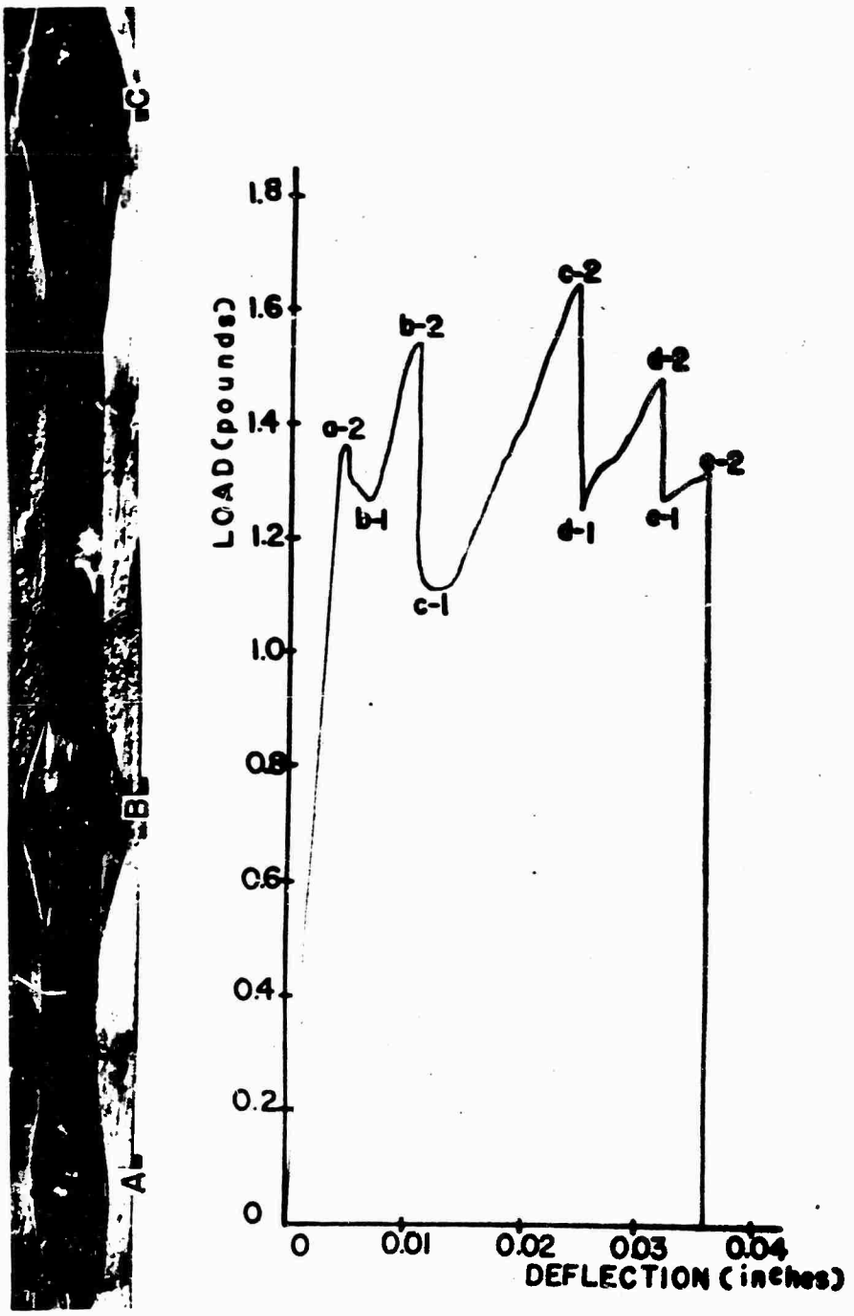

IV-3 Load-Deflection Curve and Fracture Surface of Low Molecular Weight Polystyrene ($\bar{M}_w$=53,211) at Room Temperature. Specimen Type: Tapered Double Cantilever Beam Cleavage Specimen

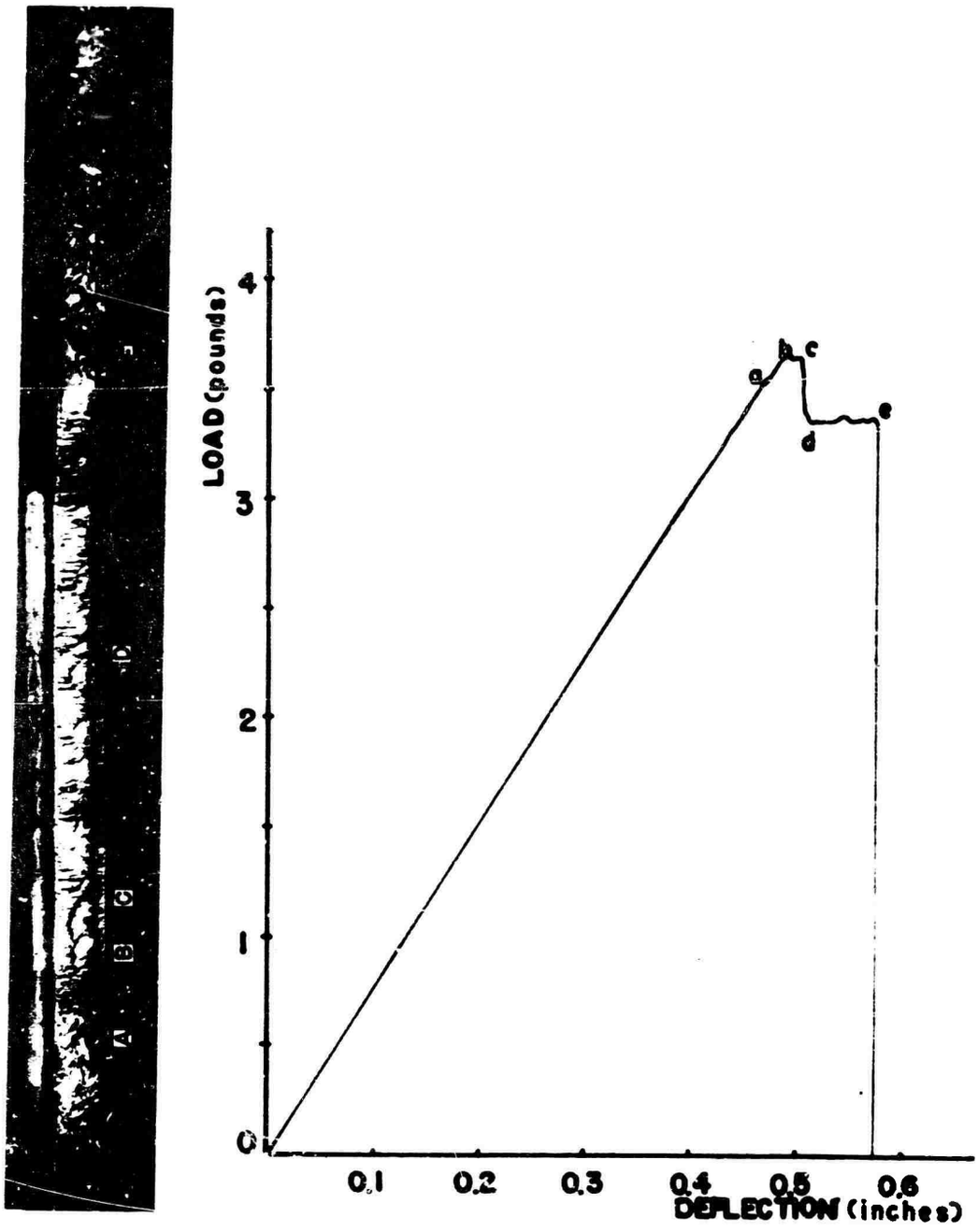

IV-4 Load-Deflection Curve and Fracture Surface of Isotactic Amorphous Polystyrene at Room Temperature. Specimen Type: Uniform Double Cantilever Beam Cleavage Specimen

ropagated. The variation of the load was due to the variation of the crack velocity, the crack width, and the variation of the local property of the material. In the picture one can see a lot of voids on the fracture surface, and these voids were not observed elsewhere in the specimen. It is thought that air compressed in the molding was expanded due to volume expansion at the crack tip caused by the high stress at the crack tip. The average measured fracture surface work value was 4.14×10^5 erg/cm^2.

Fig. IV-6 shows the load-deflection curve and the fracture surface of iso-butyl methacrylate polymer tested at room temperature using a tapered cleavage specimen. The crack propagation mode is classified as discontinuous type. As the deflection continuously increased from "0" to "a" the crack propagated discontinuously and repeatedly in short spurts. A detailed picture of this kind of fracture surface is shown in Fig. 40-a. At "a" instability took place and the crack jumped from "A" to "B"; however, the energy released by this jump was not sufficient, so the crack jumped again from "B" to "C". At "C" the crack propagated in two planes; therefore, the resistance to crack propagation was high. This can be seen on the load-deflection curve. When the load and the deflection were increased to "c" on the curve, instability took place and the crack jumped from "C" to "D". At the terminus of the crack jump between "C" and "D" on the fracture surface picture the crack again propagated into two planes. The resistance to crack propagation increased, and the crack was arrested at "D". This also can be seen on the load-deflection curve. The position of the elbow between "c" and "d" on the load-deflection curve is higher than that between "b" and "c" or "d" and further points; however, as one can see on the fracture surface, there is not much plastic deformation at each crack arrested line. The measured fracture surface work value was 0.913×10^5 erg/cm^2.

Fig. IV-7 shows the load-deflection curve and the fracture surface of a molded PMMA tapered cleavage specimen tested at liquid nitrogen temperature (-196°C). The crack tip position was initially at "A-1" in the picture. While loading from "0" to "a-2", the crack moved from "A-1" to "A-2", then instability took place and the crack jumped. As one can see in the picture a large amount of plastic deformation occurred at the crack tip. This plastic deformation is an important part of the measured fracture toughness. Detailed pictures of the crack tip can be seen in Fig. 37-a and b. The measured fracture surface work value was 17.62×10^5 erg/cm^2.

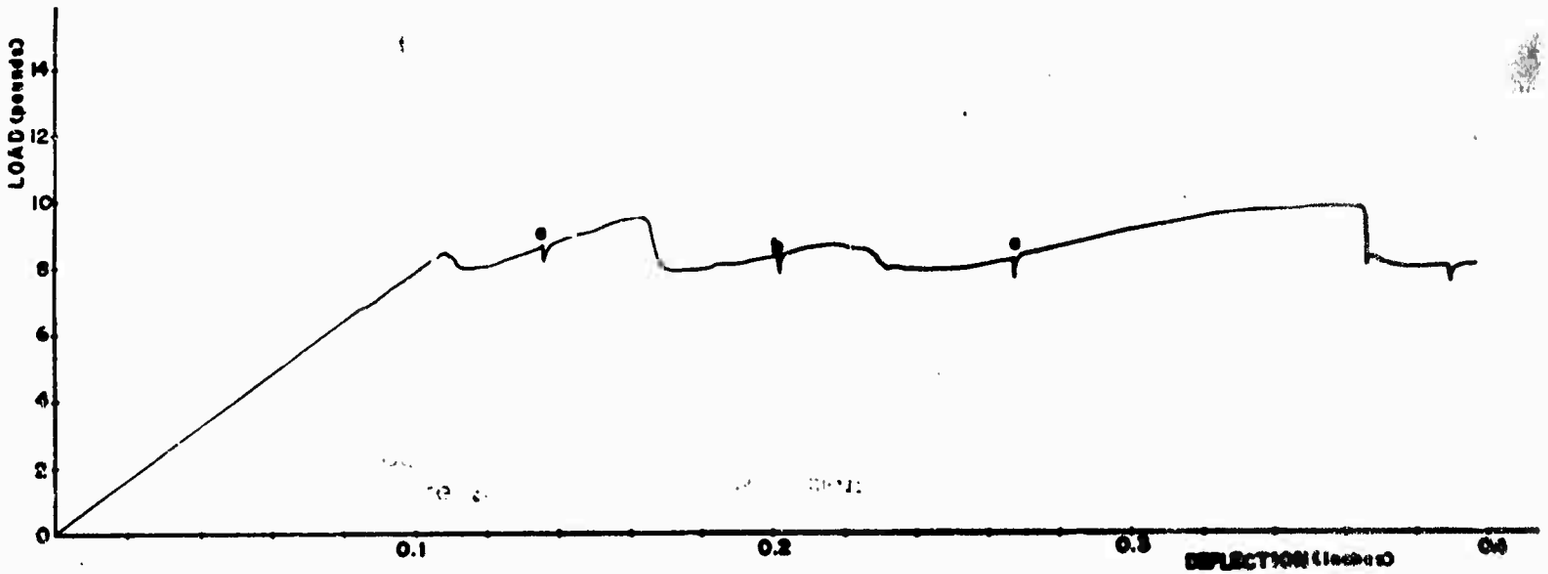

IV-5 Load-Deflection Curve and Fracture Surface of Polyethyl Methacrylate at Room Temperature. Specimen Type: Tapered Double Cantilever Beam Cleavage Specimen

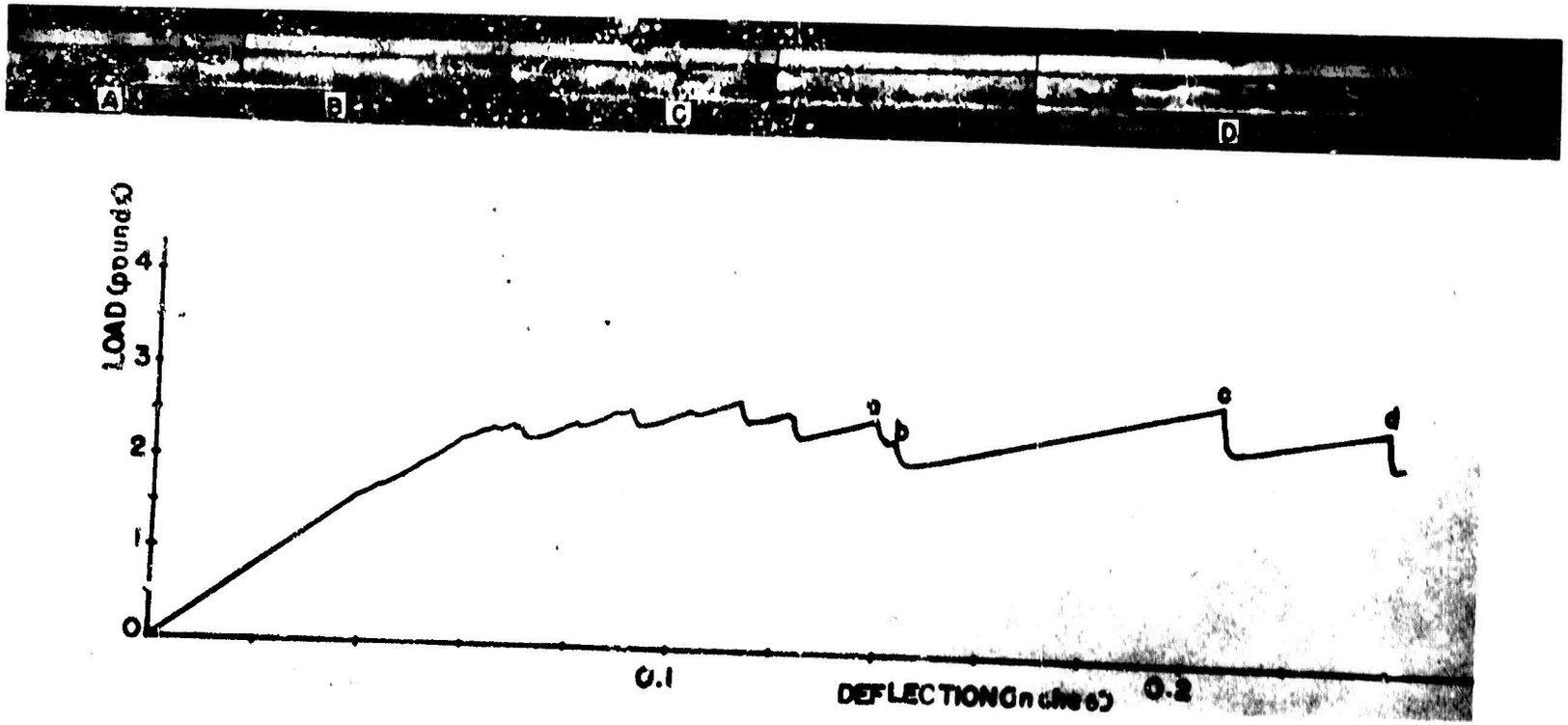

IV-6 Load-Deflection Curve and Fracture Surface of Iso Butyl Methacrylate at Room Temperature. Specimen Type: Tapered Double Cantilever Beam Cleavage Specimen

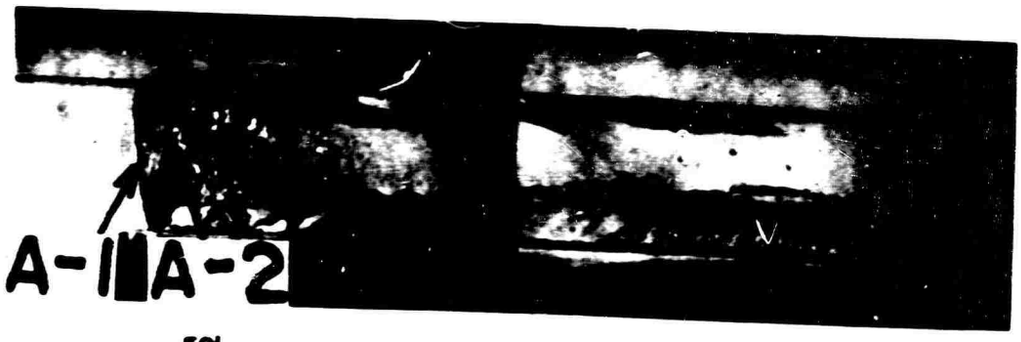

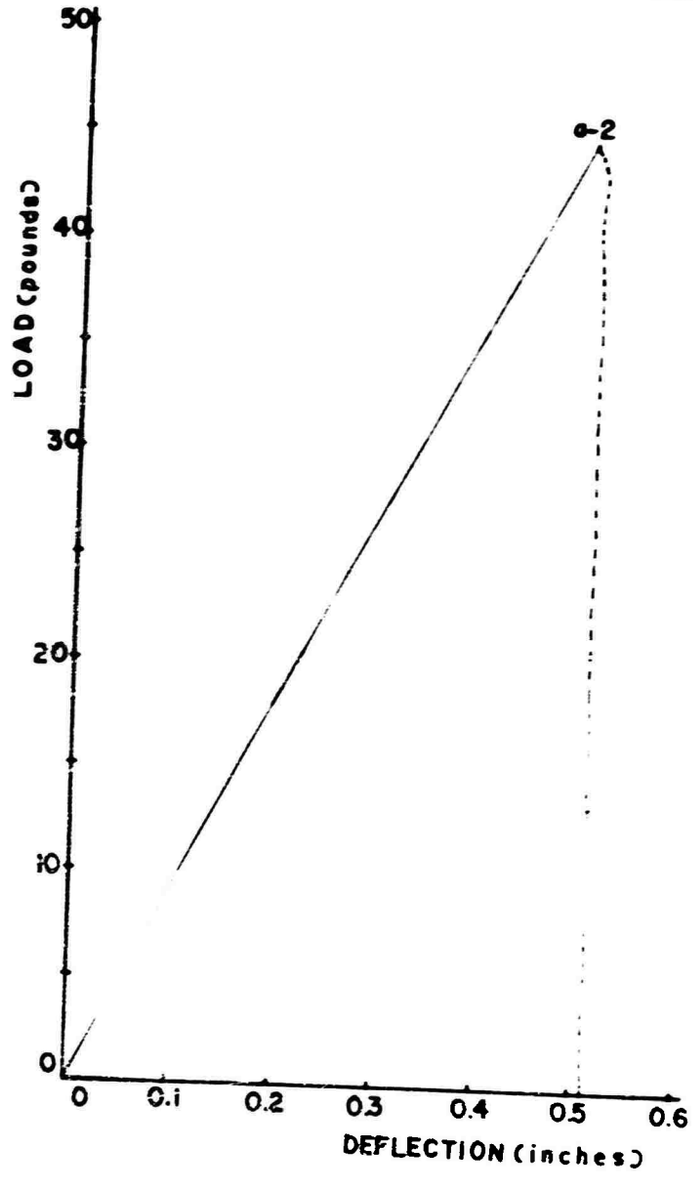

IV-7 Load-Deflection Curve and Fracture Surface of Molded PMMA at -196°C. Specimen Type: Tapered Double Cantilever Beam Cleavage Specimen

UNCLASSIFIED

Security Classification

DOCUMENT CONTROL DATA - R&D

(Security classification of title, body of abstract and indexing annotation must be entered when the overall report is classified)

1. ORIGINATING ACTIVITY (Corporate author) Illinois Institute of Technology Chicago, Illinois 60616	2a. REPORT SECURITY CLASSIFICATION Unclassified 2b GROUP

3. REPORT TITLE

FRACTURE STUDIES IN GLASSY POLYMERS

4. DESCRIPTIVE NOTES (Type of report and inclusive dates)

Final Report - 8 May 1967 through 8 November 1968

5. AUTHOR(S) (Last name, first name, initial)

Broutman, Lawrence J., and
Kobayashi, Takao

6. REPORT DATE August 1969	7a. TOTAL NO. OF PAGES 176	7b. NO. OF REFS 50
8a. CONTRACT OR GRANT NO. DAAG 17-67-C-0133 b. PROJECT NO. D/A 1C024401A329 (FY-68) D/A 1F121401A150 (FY-69) c. AMCMS Code 5025.11.295 d. Subtask 37301	9a. ORIGINATOR'S REPORT NUMBER(S) AMMRC CR 69-13 9b. OTHER REPORT NO(S) (Any other numbers that may be assigned this report)	

10. AVAILABILITY/LIMITATION NOTICES

This document has been approved for public release and sale; its distribution is unlimited.

11. SUPPLEMENTARY NOTES	12. SPONSORING MILITARY ACTIVITY U. S. Army Natick Laboratories (FY-68) Army Materials & Mechanics Research Center (FY-69)

13. ABSTRACT

An investigation has been made of the fracture behavior of organic polymers to develop correlations with polymer structural features. Equipment was designed and built and test specimens were developed for the determination of fracture surface work (FSW) of polymers from room temperature to liquid nitrogen temperature.

For polystyrene a decrease in molecular weight and an increase in molecular weight distribution reduced the value of FSW. With polystyrene cross-linked by gamma radiation, the FSW decreased with increasing degree of crosslinking. For isotactic polystyrene the FSW decreased as the degree of crystallinity was increased.

With a series of acrylate and methacrylate polymers, as well as polyvinyl chloride and polyvinyl acetate, and for measurements made both at room temperature and liquid nitrogen temperature, correlations could not be established between the FSW and the polymer molecular structure or the glass transition temperature. Uniaxial and biaxial cold rolling of sheets of various polymers greatly increased the strength and impact resistance of these materials.

With polymethyl methacrylate an increase in the crack velocity along the cleavage bar caused a small increase in the FSW. A preliminary study with liquid crystal coatings has shown a temperature rise at the crack tip for certain polymers. (Authors)

DD FORM 1 JAN 64 1473

UNCLASSIFIED

Security Classification

14. KEY WORDS	LINK A		LINK B		LINK C	
	ROLE	WT	ROLE	WT	ROLE	WT
Fracture (materials)						
Organic polymers						
Glassy state						
Fracture surface work						
Polymer structure						
Molecular weight						
Crosslinking						
Tacticity						
Crystallinity						
Temperature						
Cleavage specimens						
Crack propagation						
Fracture morphology						
Cold rolling						
Molecular orientation						
Stress-strain diagrams						

INSTRUCTIONS

1. ORIGINATING ACTIVITY: Enter the name and address of the contractor, subcontractor, grantee, Department of Defense activity or other organization *(corporate author)* issuing the report.

2a. REPORT SECURITY CLASSIFICATION: Enter the overall security classification of the report. Indicate whether "Restricted Data" is included. Marking is to be in accordance with appropriate security regulations.

2b. GROUP: Automatic downgrading is specified in DoD Directive 5200.10 and Armed Forces Industrial Manual. Enter the group number. Also, when applicable, show that optional markings have been used for Group 3 and Group 4 as authorized.

3. REPORT TITLE: Enter the complete report title in all capital letters. Titles in all cases should be unclassified. If a meaningful title cannot be selected without classification, show title classification in all capitals in parenthesis immediately following the title.

4. DESCRIPTIVE NOTES: If appropriate, enter the type of report, e.g., interim, progress, summary, annual, or final. Give the inclusive dates when a specific reporting period is covered.

5. AUTHOR(S): Enter the name(s) of author(s) as shown on or in the report. Enter last name, first name, middle initial. If military, show rank and branch of service. The name of the principal author is an absolute minimum requirement.

6. REPORT DATE: Enter the date of the report as day, month, year, or month, year. If more than one date appears on the report, use date of publication.

7a. TOTAL NUMBER OF PAGES: The total page count should follow normal pagination procedures, i.e., enter the number of pages containing information.

7b. NUMBER OF REFERENCES: Enter the total number of references cited in the report.

8a. CONTRACT OR GRANT NUMBER: If appropriate, enter the applicable number of the contract or grant under which the report was written.

8b, 8c, & 8d. PROJECT NUMBER: Enter the appropriate military department identification, such as project number, subproject number, system numbers, task number, etc.

9a. ORIGINATOR'S REPORT NUMBER(S): Enter the official report number by which the document will be identified and controlled by the originating activity. This number must be unique to this report.

9b. OTHER REPORT NUMBER(S): If the report has been assigned any other report numbers *(either by the originator or by the sponsor)*, also enter this number(s).

10. AVAILABILITY/LIMITATION NOTICES: Enter any limitations on further dissemination of the report, other than those imposed by security classification, using standard statements such as:

(1) "Qualified requesters may obtain copies of this report from DDC."

(2) "Foreign announcement and dissemination of this report by DDC is not authorized."

(3) "U. S. Government agencies may obtain copies of this report directly from DDC. Other qualified DDC users shall request through _____."

(4) "U. S. military agencies may obtain copies of this report directly from DDC. Other qualified users shall request through _____."

(5) "All distribution of this report is controlled. Qualified DDC users shall request through _____."

If the report has been furnished to the Office of Technical Services, Department of Commerce, for sale to the public, indicate this fact and enter the price, if known.

11. SUPPLEMENTARY NOTES: Use for additional explanatory notes.

12. SPONSORING MILITARY ACTIVITY: Enter the name of the departmental project office or laboratory sponsoring *(paying for)* the research and development. Include address.

13. ABSTRACT: Enter an abstract giving a brief and factual summary of the document indicative of the report, even though it may also appear elsewhere in the body of the technical report. If additional space is required, a continuation sheet shall be attached.

It is highly desirable that the abstract of classified reports be unclassified. Each paragraph of the abstract shall end with an indication of the military security classification of the information in the paragraph, represented as *(TS)*, *(S)*, *(C)*, or *(U)*.

There is no limitation on the length of the abstract. However, the suggested length is from 150 to 225 words.

14. KEY WORDS: Key words are technically meaningful terms or short phrases that characterize a report and may be used as index entries for cataloging the report. Key words must be selected so that no security classification is required. Identifiers, such as equipment model designation, trade name, military project code name, geographic location, may be used as key words but will be followed by an indication of technical context. The assignment of links, rules, and weights is optional.